Master's thesis

NTNU
Norwegian University of Science and Technology
Faculty of Engineering
Department of Structural Engineering

Josefine Dawes

Investigating the Effects of High Strength Concrete Properties on Capillary Absorption and Adhesion in Offshore Concrete Rehabilitation

Master's thesis in Civil and Environmental Engineering (IBM)
Supervisor: Jan Arve Øverli (NTNU)
Co-supervisor: Ragnar Aarstein (RaKon AS)
June 2023

NTNU
Norwegian University of
Science and Technology

Josefine Dawes

Investigating the Effects of High Strength Concrete Properties on Capillary Absorption and Adhesion in Offshore Concrete Rehabilitation

Master's thesis in Civil and Environmental Engineering (IBM)
Supervisor: Jan Arve Øverli (NTNU)
Co-supervisor: Ragnar Aarstein (RaKon AS)
June 2023

Norwegian University of Science and Technology
Faculty of Engineering
Department of Structural Engineering

NTNU
Norwegian University of
Science and Technology

Department of Structural Engineering
Faculty of Engineering
NTNU - Norwegian University of Science and Technology

ACCESSIBILITY
Open

MASTER THESIS 2023

SUBJECT AREA: Concrete	DATE: 11.06.2023	NO. OF PAGES: 95 + Appendix: 33

TITLE:

Investigating the Effects of High Strength Concrete Properties on Capillary Absorption and Adhesion in Offshore Concrete Rehabilitation

Undersøkelse av Effektene av Høyfast Betongs Egenskaper på Kapillær Absorpsjon og Heft i Rehabilitering av Offshore Betongkonstruksjoner

BY:

Josefine Dawes

Josefine Dawes

SUMMARY:
Delving into the realm of offshore concrete structures, this research investigation is dedicated to unraveling the intricacies of adhesion between repaired concrete and repair materials. With a particular focus on high strength concrete properties, including the use of silica fume, the study embarks on an exploration of their impact on capillary absorption and adhesion during concrete rehabilitation. Through a thorough examination of the correlation between different levels of capillary absorption and the requirement for precise pre-wetting techniques during repairs, the primary objective is to establish a foundation for enhancing techniques and guidelines, ultimately achieving optimal adhesion in high strength concrete repairs.

A comprehensive methodology is implemented, including a literature study and laboratory testing. The literature study establishes a theoretical framework by evaluating concrete technology, rehabilitation techniques, and existing facts on the effect of high strength concrete properties on capillary absorption. Laboratory testing involves bond strength tests performed on high strength concrete specimens casted specifically for this purpose, and capillary absorption tests conducted on core specimens from existing offshore structures. The results are analyzed and compared with a previous study on capillary absorption, conducted by SINTEF in 1988.

The conclusion highlights the importance of considering capillary absorption properties in determining repair and rehabilitation approaches. The findings from the literature study, the SINTEF study, and the bond strength tests indicate that concrete with silica fume and lower water-to-cement ratios demonstrates reduced capillary absorption and increased sensitivity to pre-wetting. However, the capillary absorption tests reveal disparities, emphasizing the influence of variables in existing offshore structures. Thus, it is concluded that real-world offshore factors significantly impact capillary absorption, complicating the assessment of optimal moisture conditions for adhesion during concrete rehabilitation. Further research is recommended, including field tests on offshore structures and the development of capillary absorption tests for initial in-field moisture levels.

RESPONSIBLE TEACHER: Jan Arve Øverli

SUPERVISOR(S): Jan Arve Øverli (NTNU), Ragnar Aarstein (RaKon AS)

CARRIED OUT AT: Department of Structural Engineering, NTNU Trondheim

Preface

I am pleased to present this master's thesis, which was conducted at the Department of Structural Engineering (KT) at the Norwegian University of Science and Technology (NTNU) in Trondheim. It serves as the finalizing assignment of my master's degree program in Civil and Environmental Engineering (IBM), with main profile in Structural Engineering.

I want to take this opportunity to thank all the individuals who have helped me through the process of this research. Firstly, I extend my sincere gratitude to Ragnar Aarstein and Per Christian Grønstein from RaKon AS for their invaluable assistance throughout the literature study. Their extensive knowledge and expertise in the field provided valuable insights and facilitated essential contacts. Moreover, their wise counsel and guidance greatly influenced the direction and execution of this thesis. I am also grateful to Jelena Zivkovic from Equinor, whose expertise and suggestions greatly enhanced the literature study phase of this research. Her valuable input contributed to the depth and quality of the study.

Special recognition goes to Tom Gefle and Jan Øyvind Christensen from Weber Norway for their exceptional support during the laboratory testing. Their dedicated involvement, provision of materials, equipment, and extensive assistance throughout the entire process were instrumental in the successful execution of the experiments. Their expertise and generosity are deeply appreciated. I would also like to thank Svein Løken from RaKon AS for his contribution to the execution of dry shotcrete repair during the laboratory work and Jo Kjetil Ruud from RaKon AS for delivering materials when we faced shortages.

Finally, I would like to extend my sincere appreciation to my supervisor, Jan Arve Øverli, for his support and guidance throughout this semester. His valuable mentorship has been instrumental in shaping this research, and I am truly grateful for the opportunity provided to me to undertake this study.

Abstract

Delving into the realm of offshore concrete structures, this research investigation is dedicated to unraveling the intricacies of adhesion between repaired concrete and repair materials. With a particular focus on high strength concrete properties, including the use of silica fume, the study embarks on an exploration of their impact on capillary absorption and adhesion during concrete rehabilitation. Through a thorough examination of the correlation between different levels of capillary absorption and the requirement for precise pre-wetting techniques during repairs, the primary objective is to establish a foundation for enhancing techniques and guidelines, ultimately achieving optimal adhesion in high strength concrete repairs.

A comprehensive methodology is implemented, including a literature study and laboratory testing. The literature study establishes a theoretical framework by evaluating concrete technology, rehabilitation techniques, and existing facts on the effect of high strength concrete properties on capillary absorption. Laboratory testing involves bond strength tests performed on high strength concrete specimens casted specifically for this purpose, and capillary absorption tests conducted on core specimens from existing offshore structures. The results are analyzed and compared with a previous study on capillary absorption, conducted by SINTEF in 1988.

The conclusion highlights the importance of considering capillary absorption properties in determining repair and rehabilitation approaches. The findings from the literature study, the SINTEF study, and the bond strength tests indicate that concrete with silica fume and lower water-to-cement ratios demonstrates reduced capillary absorption and increased sensitivity to pre-wetting. However, the capillary absorption tests reveal disparities, emphasizing the influence of variables in existing offshore structures. Thus, it is concluded that real-world offshore factors significantly impact capillary absorption, complicating the assessment of optimal moisture conditions for adhesion during concrete rehabilitation. Further research is recommended, including field tests on existing offshore structures and the development of capillary absorption tests for initial in-field moisture levels.

Sammendrag

Ved å utforske offshore betongstrukturer, er denne masteroppgaven viet til å avdekke kompleksiteten knyttet til heft mellom reparert betong og reparasjonsmaterialer. Med spesielt fokus på egenskapene til høyfast betong, inkludert bruk av silika støv, tar studiet sikte på å undersøke deres innvirkning på kapillærabsorpsjon og adhesjon under rehabilitering av betong. Gjennom en omfattende undersøkelse av sammenhengen mellom ulike nivåer av kapillærabsorpsjon og behovet for presise forvanningsmetoder under reparasjoner, er hovedmålet å legge grunnlaget for forbedrede teknikker og retningslinjer, med det ultimate målet om å oppnå optimal heft i reparasjon av høyfast betong.

En omfattende metodikk implementeres, inkludert en litteraturstudie og laboratorietesting. Litteraturstudiet etablerer en teoretisk ramme ved å evaluere betongteknologi, rehabiliteringsteknikker og eksisterende fakta om effekten av høyfast betongs egenskaper på kapillærabsorpsjon. Laboratorietesting innebærer heftprøver utført på høyfast betong prøver støpt spesifikt for dette formålet, samt kapillærabsorpsjonstester utført på kjerneprøver fra eksisterende offshore konstruksjoner. Resultatene analyseres og sammenlignes med en tidligere studie på kapillærabsorpsjon utført av SINTEF i 1988.

Konklusjonen fremhever viktigheten av å vurdere kapillærabsorpsjonsegenskaper ved bestemmelse av reparasjons- og rehabiliteringsmetoder. Funnene fra litteraturstudiet, SINTEF-studiet og heftprøvene indikerer at betong med silikastøv og lavere vann-til-sement-forhold har redusert kapillærabsorpsjon og økt sensitivitet for forvanning. Imidlertid avdekker kapillærabsorpsjonstestene ulikheter, noe som understreker påvirkningen av variabler i eksisterende offshore konstruksjoner. Det konkluderes dermed med at faktorer til stede i virkelige offshore konstruksjoner betydelig påvirker kapillærabsorpsjon og kompliserer vurderingen av gunstige fuktighetsforhold for adhesjon under rehabilitering av betong. Videre forskning anbefales, inkludert felttester på offshore konstruksjoner og utvikling av kapillærabsorpsjonstester for initiale fuktighetsnivåer tilsvarende i felt.

Table of contents

List of Figures

List of Tables

List of Symbols and Abbreviations

Symbols / Abbreviations	**Meaning**
P_w	Water pressure [Pa]
h	Height of water rise
σ	Surface tension [N/m]
α	Contact angle [°]
r	Tube radius [m]
ρ	Water density [kg/m^3]
g	Gravitational acceleration [m/s^2]
d_{max}	Max diameter of coarse aggregate
g_x	Weight of test specimen after x days
Q	Measured absorption values [kg/m^2]
t	Time
k	Capillarity coefficient [kg/m^2√s]
m	Resistance coefficient [s/m^2]
w	Water
c	Cement
b	Binder in concrete mix
s	Weight of silica fume
k	Action factor
UHP	Ultra-high pressure
SP	Superplasticizers
SSD	Saturated surface dry
CSH	Calcium silicate hydrate
GBS	Gravity-based structure
FWT	Foundations for wind turbines

1. Introduction

1.1 Background

The topic of this thesis is centered around the important area of concrete rehabilitation, specifically in the context of offshore concrete structures. When concrete is exposed to harsh environmental conditions over time, concrete platforms may suffer from various forms of degradation, such as corrosion, mechanical damage, and chemical attacks. Degradation of concrete can compromise the performance and lifespan of the structure if not repaired. Concrete rehabilitation techniques, including repair and protection measures, are therefore performed to tackle these issues and extend the service life of the structures.

This research aims to contribute to SINTEF's research program, Excon [1], which focuses on extending the service life of concrete structures through sustainable management practices. By exploring effective rehabilitation techniques, this thesis aligns with Excon's vision of finding optimal solutions for infrastructure durability.

1.2 Problem Statement

The main focus of this thesis is the adhesion achieved between the repaired concrete and the repair material applied to the offshore concrete platforms during rehabilitation. Adhesion is a critical factor in ensuring the durability of the repair. To ensure the durability and strength of the repair, enabling it to withstand the same environmental conditions that caused the degradation of the original concrete, optimal adhesion between the repaired concrete and the repair material is crucial.

In particular, this thesis presents an investigation on how the properties of high strength concrete, including the use of silica fume as an additive, can affect the adhesion and capillary suction between the repaired concrete and the repair material. High strength concrete, which is characterized by its enhanced compressive strength, is increasingly being used in offshore concrete platforms due to its superior mechanical properties and durability. However, the higher strength and reduced porosity of high strength concrete may lead to challenges in achieving optimal capillary suction for good adhesion with the repair materials. Therefore, this thesis aims to investigate the impact of the properties of high strength concrete, including the use of silica fume, on the capillary suction and adhesion in concrete rehabilitation. A specific focus will be held on the pre-wetting techniques used to achieve the optimal state of capillary suction between the concrete and the repair material.

In conclusion, the aim of this thesis is to determine if the capillary absorption characteristics of the concrete should be considered when determining the appropriate approach for repairing and rehabilitating the structure, and if tailored requirements should be established accordingly. The findings of this research are expected to provide valuable insights into the challenges and opportunities associated with concrete rehabilitation of offshore concrete platforms and may contribute to the development of improved techniques and guidelines for achieving optimal adhesion and durability in high strength concrete repair projects.

1.3 Delimitation

It is important to acknowledge that the adhesion between repaired concrete and repair materials can be influenced by various factors, including surface preparation, curing conditions, and type of repair material. Although these subjects will be discussed to some extent, this thesis primarily focuses on investigating the effect of capillary suction and pre-wetting techniques in the context of high strength concrete and the use of silica fume as an additive. Other factors that may affect adhesion, such as chemical compatibility, temperature, and application techniques, are also not the main focus of this study.

Additionally, this research is limited to laboratory testing and does not include field or long-term performance evaluations of repaired concrete on offshore concrete platforms. The scope of this thesis is limited to the specific research objectives outlined in the introduction, and any generalization or extrapolation of the findings should be done with caution.

1.4 Methodology

In order to accomplish the objectives of this thesis, a comprehensive methodology will be implemented, encompassing a literature study and laboratory testing. The literature study will involve an extensive examination and evaluation of existing literature pertaining to various aspects of concrete technology, concrete rehabilitation techniques, concrete material properties (including high strength concrete and the utilization of silica fume), capillary suction theory, and pre-wetting methods in the context of concrete rehabilitation. Furthermore, a review of SINTEF's capillary absorption study conducted in 1988 will be executed, serving as a fundamental basis for further investigation. This thorough literature review will establish a robust foundation for the research and assist in constructing the theoretical framework for the study.

Laboratory testing will be conducted to investigate the capillary suction of high strength concrete and the adhesion achieved by different pre-wetting techniques. Bond strength tests, by execution of the pull-off method, will be used to evaluate the adhesion between the repaired high strength concrete and the repair material. In addition, capillary absorption tests will be performed to measure the capillary absorption of high strength concrete and assess the effect of low water-to-cement ratio and silica fume on capillary suction. The results of these laboratory tests will be analyzed and discussed in the results and discussion chapter.

Lastly, a comprehensive analysis of the results will be performed, followed by an evaluation of the relationship between the findings obtained from the literature study and the outcomes of the laboratory tests. This evaluation aims to address the issues presented in the introduction and provide answers to the research questions posed.

2. The Fundamentals of Concrete Technology

A solid understanding of concrete technology is vital for comprehending the complexities of concrete rehabilitation. This chapter establishes the foundation by exploring key aspects of concrete composition and properties. It discusses the role of cement, aggregates, admixtures, and additives in the concrete mix and their influence on its behavior. The chapter also covers the significance of pores, their formation, and their effects on concrete properties. It examines post-treatment processes like curing and their impact on concrete properties over time. Additionally, common degradation mechanisms of concrete structures are discussed to highlight the challenges and the need for rehabilitation.

By providing a comprehensive understanding of these fundamental aspects of concrete technology, this chapter lays the groundwork for subsequent discussions on concrete rehabilitation methods and strategies in later chapters of this thesis. A strong grasp of these fundamentals is vital for comprehending the complexities of concrete rehabilitation and developing effective strategies to address challenges in the context of the thesis topic.

2.1 The Concrete Mix

Concrete is mainly a composition of cement, water, and aggregates, in addition to additives and admixtures. Cement and water are first mixed to form a cement paste, where the ratio between the two components is defined as the w/c-ratio. If the w/c-ratio exceeds 0.32, the volume of water is greater than the volume of cement in the mix, and the cement grains are surrounded by water.

The concrete mix is in the mixing phase a relatively fluid mass, but when the cement, which is a hydraulic binder, reacts in contact with the water it will begin to hydrate. Hydration initiates the CSH phase, where calcium-silicon-hydrate bonds are formed, and the fluid concrete mass begins to stiffen. In addition, loose crystals of calcium hydroxide are also formed, giving the concrete a very high pH value. This is a great advantage for reinforced concrete structures, as the basic concrete provides a protective oxide layer around the reinforcement and therefore acts as a protection against reinforcement corrosion. [2]

2.2 Pores in Concrete

When the concrete hardens, pores are also formed in the concrete. The formation of the pores is mainly due to the water/cement reaction. When cement reacts with water, the water is consumed in two different ways. The chemical reaction belonging to the CSH phase requires a water volume corresponding to a w/c-ratio of 0.25. In addition, a water volume corresponding to a w/c-ratio of 0.15 is bound as gel water in so-called gel pores. Therefore, a w/c-ratio of greater than or equal to 0.4 is required to achieve total hydration of the cement.

If the w/c-ratio in the concrete mix is greater than 0.4, we get excess water that does not react with the cement in the mix. When the cement hydrates, the chemical reaction will cause a temperature increase which will result in the evaporation of the excess water in the concrete, and this leaves so-called capillary pores. These are 1000 times larger than a gel pore.

In addition to gel pores and capillary pores, concrete also consists of shrinkage pores. These pores are formed because the volume of the reaction product between water and cement is less than the volume of the starting materials. The cement paste hardens when only 0.5% of the water is chemically bound, and the outer volume therefore remains unchanged while the total volume continues to decrease. This results in evenly distributed pores in the cement paste.

As described, it is the w/c-ratio that controls the volume of pores, and with an increased w/c-ratio we get an increased volume of pores. This results in a reduction of the concrete's strength and density. If, on the other hand, the w/c-ratio is less than 0.4 and the amount of water is not sufficient for all the cement to hydrate, we get a smaller pore volume and the unreacted cement acts as a strong aggregate in the concrete. [2]

2.3 The Components of Concrete

2.3.1 Cement

Portland cement is a term that originated from the early cement industry, and now serves as a collective term for most of the cements used in the construction industry. Cement consists of clay and calcareous materials that are first ground down and fired into clinkers, and then ground down again together with gypsum. The gypsum is added with the purpose of regulating the cement's hardening properties. When producing blended cement, fly ash may also be added. Cement also contains the element chromium, a substance which can be hazardous to health and the environment. Therefore, iron sulfate is added in the final stage of cement production to bind chromium and dechrome the cement mix. [2]

2.3.2 Aggregates

The aggregates consisting of sand and stone usually accounts for about 60-70% of the total concrete volume and is of great importance for the properties of the concrete. There are several requirements for what is suitable as aggregate, and we generally find good rocks for concrete around Norway. The composition of sand and stone in the aggregate is determined by grain grading, grain shape, and surface structure.

Sand and stone used in concrete production is taken from the Norwegian nature and will therefore have different moisture contents depending on the conditions from which it is taken. When the aggregate is mixed into the concrete mix, the moisture level of the aggregate can affect the w/c-ratio. If the aggregate is dry, it will absorb water from the concrete mix and result in a reduction of the w/c-ratio. On the other hand, if the aggregate is moist, the concrete mix will have a higher w/c-ratio. The moisture condition of the aggregate can therefore give unexpected changes in the properties of the concrete, and it is therefore very important to consider when producing concrete. [2]

2.3.3 Admixtures

To achieve desired properties in concrete, admixtures are a very necessary component in the concrete mixture. Admixtures account for less than 5% of the concrete mixture but play a very important role in achieving or improving special properties in the product. Admixtures are classified by function as follows:

Class P: Water-reducing agents.

Class R: Retarding.

Class L: Air entraining.

Class A: Hardening accelerators.

In addition to this, there are also other admixtures suitable for special purposes. These include auxiliaries for injection, underwater pouring or pumping, as well as adhesion enhancers, corrosion inhibitors and frost protection agents. [2]

2.3.4 Additives

Silica fume is an additive that, together with cement and water, is part of the chemical reaction that binds the concrete mixture and makes it harder. The additive does not have hydraulic properties itself, but still forms chemical bonds with calcium hydroxide in the cement paste. Materials with this property are called pozzolans. As silica fume makes the concrete harder, more energy is required for the pouring process, but in return the concrete has a reduced risk of separation. [3]

If silica fume is added to the concrete mixture, the risk of surface evaporation will be high. Evaporation of surface water creates a hydraulic pressure in the outer layer of the concrete. In silica-free concrete, this results in water being drawn out from the inner concrete mass, and thus the chance of drying is not as great. For concrete mixtures with silica, however, the water inside the concrete is very tightly bound, and the concrete is therefore much more prone to drying in its fresh state. Drying causes the concrete surface to crack and plastic shrinkage is generated.

When water and cement react, calcium hydroxide is produced which forms a weak layer around the reinforcing steel. If silica is added to the concrete mixture, this layer is replaced by a strong reaction mass which increases the adhesion between the reinforcement and the concrete in addition to reducing the concrete's pore volume. The reaction mass will also replace coarse pores evenly distributed in the concrete, resulting in a more homogeneous concrete and a reduction in the concrete's permeability. The compressive strength of the concrete will thus be significantly increased.

For concrete mixtures with silica fume, the term mass ratio, w/(c+ks), may be used instead of the w/c-ratio. This describes the weight ratio between water and the sum of cement and the converted amount of silica fume. The converted amount of silica fume is the weight of the silica fume multiplied by the action factor k. NS 3420 defines this factor as how many parts of cement can be replaced with silica fume without changing the properties. [2] For simplicity, the term w/c-ratio will be used for both concrete with and without silica fume in this thesis.

2.4 Post-treatment of Fresh and Hardened Concrete

The composition of the concrete is not the only factor that affects the properties of the finished concrete. The execution of transportation, pouring and post-treatment of the concrete also has a great impact on the quality. When pouring the concrete, it is essential to compress the mass with the help of a vibrator to get unwanted air bubbles out of the concrete. In addition, the concrete should be poured in such a way that it ensures the least amount of separation and avoids cold joints. Different methods of pouring and vibrating are determined depending on the type of construction and formwork.

Once the pouring process is completed, post-treatment is required to prevent plastic shrinkage cracks that occur due to the drying of the concrete surface. To avoid this, it is desired that the concrete's capillary suction ability is low. The capillarity coefficient describes the concrete's ability to absorb water and gives an expression of the permeability. A tight, non-porous concrete that absorbs water slowly to a low level has a low capillarity coefficient. This reduces the chance of the concrete surface drying out, and the risk of infiltration of degrading chemicals is reduced. To achieve a low capillarity coefficient, post-treatment methods such as the application of membrane or plastic film, or water storage for a certain number of days have been developed. Water storage is the method with the greatest effect. [2]

2.5 Degradation Mechanisms

Concrete has long been regarded as a durable and low-maintenance material, favored in construction for its strength and longevity. However, it is now widely acknowledged that concrete structures are not impervious to degradation over time. Environmental, chemical, and physical mechanisms can inflict wounds and damage upon concrete, compromising its performance and structural integrity. Consequently, the maintenance and rehabilitation of concrete structures have become imperative to ensure their long-term functionality and safety.

Through the examination of various degradation mechanisms that impact concrete structures, a comprehensive understanding of the importance of concrete rehabilitation is developed. This knowledge establishes the basis for recognizing the significance of maintenance and rehabilitation in ensuring the long-term performance and durability of concrete structures. It provides a foundation for the subsequent chapters of this thesis.

2.5.1 Reinforcement Corrosion

Reinforcement corrosion is the most widespread degradation mechanism in concrete structures. The mechanism occurs when the concrete around the reinforcement is broken down and the protective oxide film from the concrete on the steel surface disappears. The rate of degradation depends on pollutants, oxygen supply, relative humidity, and the conductivity of the concrete. It is mainly the w/c-ratio in addition to the silica addition in the concrete mixture that is decisive for the structure's corrosion risk.

Reinforcement corrosion generally occurs either by carbonation or chloride penetration, but for offshore concrete structures, only corrosion caused by the latter is seen. Chlorides can be present already from production due to the use of seawater, chloride-containing accelerator or aggregates that are chloride-contaminated, or it can penetrate after production through de-icing salts or through exposure to seawater. Reinforcement corrosion can lead to a reduced reinforcement cross-section and, in the worst case, a loss of structural capacity, and is therefore very important to consider. [2]

2.5.2 Mechanical Degradation

Mechanical breakdown occurs due to external forces and can lead to cracks and fissures in the concrete. Cracks and fissures are not necessarily a problem for the structure's load bearing capacity but can lead to increased infiltration of aggressive substances which can result in reinforcement corrosion. Generally, therefore, cracks with a width of more than 0.2 mm must be repaired. [2]

2.5.3 Chemical Degradation

Chemical degradation in concrete structures occurs when chemical reactions lead to a reduction of the concrete's functional properties. This can happen either in the form of dissolution of the concrete's binder or by the formation of reaction products which create pressure and act explosively on the concrete. Several factors determine the rate of degradation, and the most important ones are the pH of the chemicals, the rate of exchange, and the moisture condition, as well as environmental factors such as temperature and drying conditions. [2]

2.5.4 Frost

Frost in concrete structures occurs when the water in the capillary pores freeze and thus expand. The expansion of pore water can lead to a hydraulic pressure which creates tensile stresses in the concrete, which in turn can lead to cracks and scaling if the stresses exceed the tensile strength. To achieve concrete with satisfactory frost resistance, air entraining admixtures are required. [2]

2.5.5 Alkali Reactions

Alkali reactions can occur if there are reactive aggregates in the concrete, enough alkalis in the cement, and a relatively high degree of water saturation. If this is the case, the reaction between the minerals in the aggregate will form a reaction product which will absorb water and expand. The forces generated from the expansion will result in cracks and scaling in the concrete. [2]

2.5.6 Acid Attack

Concrete structures with high quality concrete can withstand weak acids, but if the acids are too strong, the binders in the concrete will be converted and become soluble in water. If there is flowing water present, the binders will be washed out of the concrete, and the structure will break down. [2]

2.5.7 Sulfate and Nitrate Attack

Water containing sulfates and nitrates will react with concrete by forming compounds that bind water and swell. The swelling will cause a pressure which can result in cracks and scaling in the concrete. [2]

3. Concrete Rehabilitation

The primary objective of this chapter is to provide an extensive understanding of the conventional methods used for rehabilitating concrete in offshore structures. These methods encompass mechanical, chemical, and thermal pre-treatment, mechanical repair, repair of cracks, and electrochemical repair techniques. By delving into the principles, applications, advantages, and limitations of each method, this chapter aims to provide a comprehensive insight into how concrete rehabilitation is performed.

By presenting an overview of these common methods, this chapter establishes the groundwork for comprehending the challenges and considerations involved in concrete rehabilitation for offshore structures. This will provide a foundation for further analysis and discussion of potential modifications or enhancements to the concrete rehabilitation methods in subsequent chapters of this thesis. A comprehensive understanding of these common methods is crucial for thoroughly evaluating their applicability and effectiveness in the unique context of offshore structures, and identifying areas where improvements or innovations may be needed.

3.1 Pre-treatment

To ensure good adhesion where surface treatment or topping is to be carried out, it is very important that the concrete is pre-treated. This can be done mechanically, chemically, or thermally, however, when it comes to offshore concrete structures, mechanical pre-treatment is the most appropriate and preferred method.

3.1.1 Mechanical Pre-treatment

Mechanical pre-treatment can be carried out in various ways, with the most relevant methods related to pre-treatment of offshore concrete structures being dry sand and vacuum blasting, high pressure washing, dot punching and needle scabbling.

Dry sandblasting is a method where dry sand is blasted with high pressure against the concrete surface, causing the material on the surface to be abraded away. The method is effective in removing scale layers and brittle paint, as well as removing corrosion from steel, and it leaves the surface rough and thus favorable for good adhesion. The drawbacks of this method are that it is not as effective at removing elastic paints and membranes, as well as the fact that it produces a lot of dust and environmental emissions. As an alternative to this method, vacuum sandblasting has been developed, where the blasting medium and abraded material is sucked up into a container. [4]

High-pressure washing is a method that utilizes water at a high pressure to effectively cleanse the concrete surface by eliminating dirt and debris. This treatment typically involves the use of fresh water, although additional cleaning agents or fat solvents may be incorporated to achieve the desired level of surface cleanliness. The method is well suited for removal of surface dirt but is not very effective at removing membranes and corrosion from steel. As an alternative, a method using ultra-high-pressure (UHP) water jetting has been developed, where the working pressure is relatively higher. This method is often called hydro blasting and is better suited for the removal of concrete and coatings. [4]

Dot punching and needle scabbling are methods where a machine equipped with hard metal needles breaks away material in the concrete surface. The methods are especially well suited for removing contaminated concrete on horizontal surfaces such as at the shaft tops, as well as for removing thick membrane coatings. The methods result in a rough surface optimal for good adhesion. The limitations of dot punching and needle scabbling are capacity and the ability to remove elastic materials. [4]

3.1.2 Chemical Pre-treatment

Chemical pre-treatment can be carried out in three different ways, by cleaning in an open or closed system, or by acid washing. These methods are carried out using chemicals that dissolve paint on the concrete surface, which is then rinsed away. The biggest drawback of this method is the use of chemicals and the environmental burden this entails. [4]

3.1.3 Thermal Pre-treatment

Thermal pre-treatment methods are generally not used on concrete structures and are therefore only briefly mentioned here. The most common method of thermal pre-treatment is flame-cleaning. This involves removing the outermost layer of the concrete surface by exposing it to a temperature shock. The method is developed with the aim of improving the surface's adhesion ability but is very limited by explosion risk in addition to leaving an uneven surface. [4]

3.2 Mechanical Repair

Mechanical repair is the most used method for concrete rehabilitation. In this method, damaged concrete is removed from existing structures, and we therefore distinguish between bearing and non-bearing repairs. When it comes to offshore concrete structures in the North Sea, it is commonly believed that the structural capacity remains unaffected by the removal of concrete during the rehabilitation process. This is due to the relatively negligible volume of material that is removed compared to the total volume of the structure.

There are several methods for the removal of damaged concrete, but the most common methods used on Norwegian offshore concrete structures are various forms of chiseling or water jetting. For the repair of minor damage, it is most common to prepare the surface either with an electric chisel machine or pneumatic hammer, while for larger repairs, hydro blasting is the method of choice. This method is very useful for selective removal of concrete and is well suited for removal at specified depths. Fresh water is blasted into the concrete's pores and cracks, creating an inner pressure that breaks up the concrete and dissolves the aggregate. The advantages of hydro blasting are that it is easy to distinguish between good and bad concrete, it ensures good adhesion, and is also well suited for highly reinforced structures as it does not damage the reinforcement. [4]

Furthermore, after the damaged concrete has been removed, the next important step is the cleaning of the reinforcement and the wound surfaces. To achieve the best possible adhesion, the wound surfaces must be cleaned of dust, cement slurry, oil, and other foreign substances. The concrete surface is therefore cleaned either by high-pressure washing or compressed air blasting. For chloride-infected concrete, the reinforcement is cleaned to a cleaning grade Sa 2.5, which means that all rust, scale, and other foreign particles are removed, and the surface is left smooth. Immediately after cleaning, any corrosion protection should be applied. The corrosion protection not only helps to protect against corrosion, but also ensures better adhesion between the reinforcement and the new concrete. [4]

A very important step in concrete rehabilitation is pre-wetting. To achieve the desired adhesion between the bond coat or new topping, the concrete must be saturated surface-dry (SSD), and therefore the concrete substrate should be pre-wetted at least one day before pouring. If the concrete is not sufficiently pre-wetted, it will absorb water from the bond coat or topping and prevent complete hardening. Assuming that no mortar or concrete spraying is to be used later, the bond coat is applied after pre-wetting. The bond coat is a layer of either cement-based or epoxy-based adhesive that is applied to ensure good adhesion between the new and old concrete. [4]

When the concrete has been pre-wetted and prepared, it is ready for reconstruction with new mortar/concrete. This can be done by hand mortaring, casting, pumping, dry spraying, or wet spraying. The mortar/concrete should ideally have the same material properties as the existing concrete to ensure good interaction between the new and old concrete. The application should generally be done wet-in-wet with the adhesive bridge and be leveled with the existing surface. After casting, it is very important to have sufficient aftercare of the surface to avoid drying out. [4]

3.3 Repair of Cracks

If the size of the cracks and fissures exceeds a certain limit, corrosion of the reinforcing steel, water penetration and reduced capacity of the concrete may occur. Therefore, crack repair is a very important part of concrete rehabilitation and is carried out either by brushing, re-casting, injecting, sealing, or jointing.

Generally, epoxies or polyurethane products are used for crack repair. Epoxy is a two-component system consisting of resin and hardener and has a high adhesion to concrete. The material is well suited for watertightness and for gluing to restore strength. Polyurethane is a versatile and flexible material widely employed for various applications, primarily for corrosion protection and achieving watertightness. When polyurethane comes into contact with water, it expands and transforms into foam, effectively sealing cracks. Conversely, in dry cracks, a two-component variant of polyurethane can be injected, which cures without water and creates a bonding effect with the concrete. [4]

3.4 Electrochemical Repair

Corrosion of reinforcing steel can also be repaired by electrochemical repair methods in addition to mechanical repair. This involves alkali-realization, chloride extraction, cathodic protection and drying. The methods are carried out by establishing an electric field on the structure and serve as an alternative or supplement to mechanical repair. Since the methods are not particularly related to adhesion, the methods will not be further elaborated. [4]

4. Capillary Absorption and Adhesion in Concrete Rehabilitation: A Literature Review

Before executing laboratory testing on capillary absorption and adhesion, we must assess what is already known about the subject. This chapter is therefore a literature review that provides a foundation for the subsequent experimental work by examining the theoretical and practical aspects as well as the relation between capillary suction, pre-wetting methods and adhesion in concrete rehabilitation.

The evolution of the concrete industry has exerted a notable influence on the material properties of concrete, especially in the realm of high strength concrete production. By investigating these advancements, we can enhance our comprehension of the characteristics of high strength concrete and their correlation with capillary absorption and adhesion. Before going into the theory behind this relation, establishing the theory behind capillary suction is crucial. This fundamental concept is key to understanding how to achieve good adhesion between the repair material and the substrate. Additionally, pre-wetting of the substrate is a significant aspect of concrete rehabilitation. By examining the theory and the effects of pre-wetting, we can gain a comprehensive understanding of how pre-wetting affects capillary suction and, consequently, adhesion in concrete rehabilitation.

Finally, the known effects of higher strength concrete properties on the capillary pore system needs to be determined, especially with regards to the use of silica fume as a component in the concrete composition. In a prior investigation carried out by SINTEF in 1988 [5], the capillary absorption of concrete was examined, considering different water-to-cement ratios and the presence or absence of silica fume. The method, results, and conclusion of this study will be reviewed to understand the implications of the properties of high strength concrete on the capillary pore system and its effect on capillary absorption in the context of concrete rehabilitation.

The aim of this literature review is to establish an understanding of how the properties of high strength concrete may affect capillary suction and adhesion in concrete rehabilitation, laying a foundation for further testing regarding capillary absorption of modern high strength concrete and adhesion by execution of different pre-wetting methods.

4.1 High Strength Concrete

At the beginning of the 1970's a very important development in the Norwegian concrete industry started. The discovery of the now well-known Ekofisk oilfield led to the initiation of significant ideation and concept development for concrete structures in the North Sea. Unique challenges regarding dimensions and field conditions called for great technical development in concrete production, which lead to substantial progress on a global level. It was during this time the concept of high strength concrete was created. [6]

4.1.1 Compressive Strength Development

When the oilfield Ekofisk was initially designed, the applicable standard was NS 427 A, which was released in 1962. This standard defined concrete qualities up to a characteristic cube strength of 450 kg/cm2, which is similar to today's C45. However, as the industry underwent significant advancements, this standard became outdated and no longer suitable. Subsequently, new rules were developed to define higher compressive strengths. In 1973, NS 3473 replaced NS 427 A, setting an upper limit of 65 MPa. This version remained in effect until 1989 when a new edition was published, introducing the highest strength class at 105 MPa. The most recent version of NS 3473 was published in 2003 and later withdrawn in 2010. [6] Since then, the applicable standard for the design of concrete structures has transitioned to NS-EN 1992, where the highest recommended characteristic compressive strength remains at 105 MPa. However, it is important to note that many offshore concrete structures were designed according to NS 3473, as this was the prevailing standard during the time of their design.

Table 4-1: Norwegian standards for design of concrete structures after 1962

Norwegian Standards	**NS 427A**	**NS 3473**	**NS 3473**	**NS-EN 1992**
Valid from	1962	1973	1989	2004
Highest compressive strength	450 kp/cm^2	65MPa	105MPa	105MPa

The rapid production of new standards provides an image on how fast the industry developed from the 1970s until the 2000s. New improved methods made it possible to design concrete structures with much higher strength, which is clearly shown in Figure 4-1 below. The development in compressive strength in offshore concrete structures are illustrated by a graph, where the x-axis provides different offshore structures by the year they were built, and the y-axis provides the compressive strength of the concrete. The dark blue columns represent the required characteristic strength, and the light blue columns represent the achieved characteristic strength in the structures. A clear increase in the compressive strength can be seen from the early 1970's until 2016.

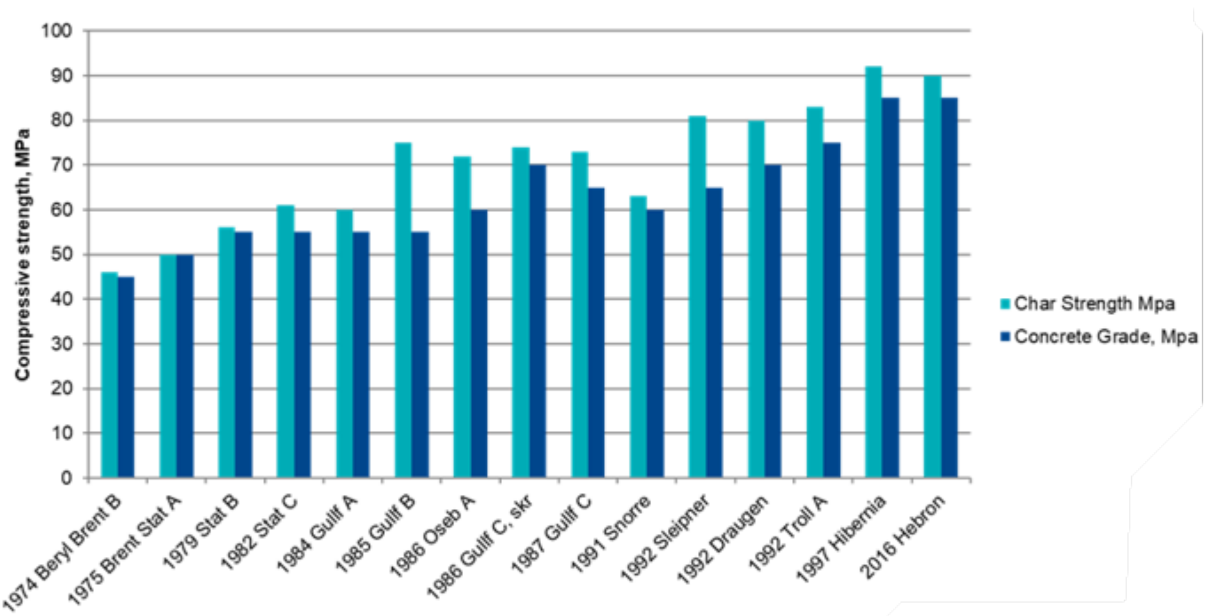

Figure 4-1: Compressive strength in offshore structures from 1974 to 2016 [7]

4.1.2 Properties of High Strength Concrete

Today, normal strength concrete is categorized as concrete with density between 2000 kg/m^3 to 2600 kg/m^3 and a compressive strength between 20 MPa to 55 MPa [8]. This type of concrete is widely used in concrete structures since it is easy to handle and place, and for most structures satisfy the strength requirements. Nevertheless, higher strength concrete is beneficial in specific types of constructions such as high-rise buildings, bridges, and as we have seen especially for offshore structures. The definition of high-strength concrete has changed progressively during the development of the concrete industry. Today, concrete with a compressive strength above 55 MPa is considered high-strength concrete, with a recommended upper limit of 105 MPa [8].

Normal Portland cement was used in concrete production until 1978 when a more advanced type of cement was developed. By optimizing the components of normal strength concrete, high strength concrete was created, which included the use of high-quality cement and optimized aggregates, as well as the composition of water, cement, aggregates, additives, and admixtures in the concrete mix. As the years went by, further enhancements were made to improve the properties of the concrete and to meet the curing temperature requirements for the higher strength concrete types.

Silica fume as an additive has had a major impact in the development of higher strength concrete but was not introduced into the Norwegian concrete industry until the late 1970s. Typically, the concrete mixes made for compressive strength of 55-65 MPa did not include silica fume, but as the required compressive strength and workability of the concrete where increased, silica fume of 2-5% of the cement weight were incorporated into the concrete mix. Silica fume will create additional bonds in the concrete resulting in an increased compressive strength and is therefore an important factor in producing high-strength concrete. The use of silica fume in development began around 1987, coinciding with the design of Gullfaks C. As the development progressed, the typical percentage of silica fume utilized increased to 5-8%. [6]

When producing high strength concrete, a low water-to-cement ratio is used to achieve high density and a less porous structure, resulting in high compressive strength. As the density of the concrete mix increases, the workability of the concrete is decreased. Chemical admixtures are therefore another important factor in high-strength concrete production. Plasticizers and superplasticizers allow for lower water/cement ratios while still maintaining adequate workability in the fresh concrete. In the 1970s, plasticizing admixtures in the form of lignosulfonates were used, until they in the 1980s were replaced by the superplasticizers naphthalene and melamine. Today another type of superplasticizers, polycarboxylates, is typically used. Without these water-reducing admixtures, high-strength concrete would be very difficult to produce. [6]

In Table 4-2 below, the development in typical concrete mixes in offshore structures from 1975 to 2017 is shown.

Table 4-2: Typical concrete mixes in offshore structures from 1975 to 2017 [7]

	Unit	**1975**	**1990**	**2017**
Cement	kg/m³	460	410	350
Silica fume	%		2	5-8
Fly ash	%			20
Sand	kg/m³	780	940	940
Coarse aggregate	kg/m³	1000	945	940
SP	l/m³	4	6	3
w/c		0.41	0.40	0.36
Slump	mm	120	240	240
1975: Lignosulfonate P		~ 8% Electrostatic fracturing		
1990: Naphthalene/Melamine SP		~ 15% Electrostatic failure		
2017: Polycarboxylate SP		~ 40% Steric hindrance		

4.2 Relation between Capillary Absorption and Concrete Rehabilitation

As advancements were made in enhancing the properties of concrete to achieve higher strength, corresponding changes in the hardened concrete and its mechanical properties occurred. The rehabilitation methods designed for conventional strength concrete may not necessarily be optimal for higher strength and more contemporary concrete. The effectiveness of concrete rehabilitation greatly relies on achieving good adhesion, which is closely connected to the capillary action between the concrete and the repair material employed. Before delving into the effects of high strength concrete and the utilization of silica fume on the capillary suction of concrete, it is essential to grasp the concept of capillary action and its relationship to concrete rehabilitation.

4.2.1 Capillary Action Theory

Capillary suction is one of the main mechanisms for moisture transport in concrete. Water is drawn into the pores due to adhesive forces between the applied water and the pore surface. The forces are determined by the diameter of the pores in the concrete, the surface tension in the water and the contact angle between the water and the pore surface. To understand this concept further, we will look at the theory behind capillary suction.

In the illustration given in Figure 4-2 we see two glass tubes placed in water. The tube with the larger diameter has drawn water to a level just above the surface, whereas the tube with the smaller diameter has drawn the water to a considerably greater height. This is due to capillary action. [9]

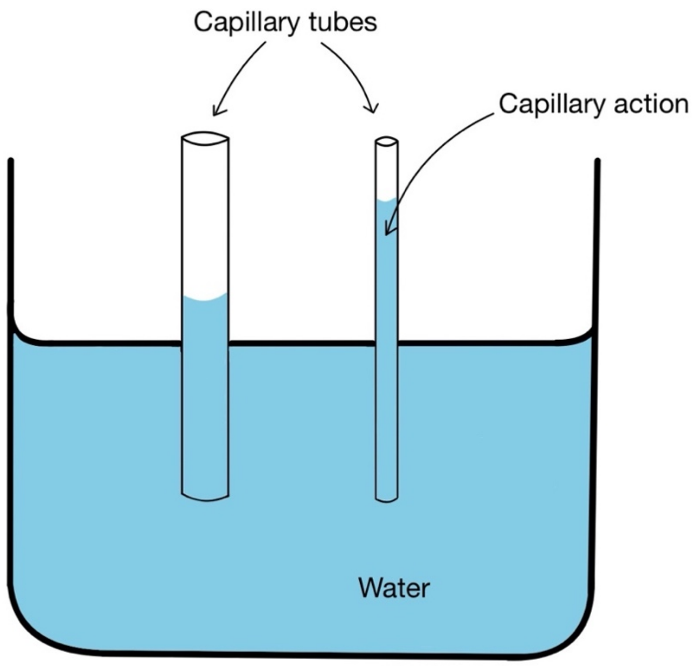

Figure 4-2: Illustration of capillary action

When the radius of the tube is smaller the pressure P_w [Pa] below the meniscus becomes larger, resulting in a greater height h [m]. This pressure phenomenon can be expressed by Laplace's law, where σ [N/m] is the surface tension, α is the contact angle between the water and the tube, and r [m] is the radius of the tube.

$$P_w = \frac{2 \cdot \sigma \cdot cos\alpha}{r} \quad (4.1)$$

When the pressure below the meniscus becomes equal to the pressure above, the water has reached equilibrium and is at its peak height. Assuming no friction, the water height in the tube can be expressed by the following equation.

$$h = \frac{P_w}{\rho \cdot g} = \frac{2 \cdot \sigma \cdot cos\alpha}{\rho \cdot g \cdot r} \quad (4.2)$$

The glass tube in the water is a simplified illustration of the capillary pores of the concrete when the concrete is in contact with water/liquid substances [9].

4.2.2 Determination of Capillary Absorption of Hardened Concrete

The capillary absorption of hardened concrete can be found by laboratory testing. Statens vegvesen's handbook R210 [10] describes method *426, Kapillær sugehastighet og porøsitet,* where the capillary absorption rate and the porosity of the hardened concrete is established by placing the test piece in a water reservoir and measuring the water absorption in the concrete's capillary pore system over time.

The calculated parameters from the test are the capillarity coefficient, k, and the resistance coefficient, m. The capillarity coefficient, k, describes the speed of the water absorption before the waterfront reaches the concrete surface. It is dependent on the total amount of water absorbed, and therefore on the total pore volume of the concrete. The resistance coefficient, m, describes the relative time it takes for the waterfront to reach a height h, and gives an expression of the fineness of the capillary pore system. Finer pores give an increased resistance coefficient resulting in a reduced rate of water absorption.

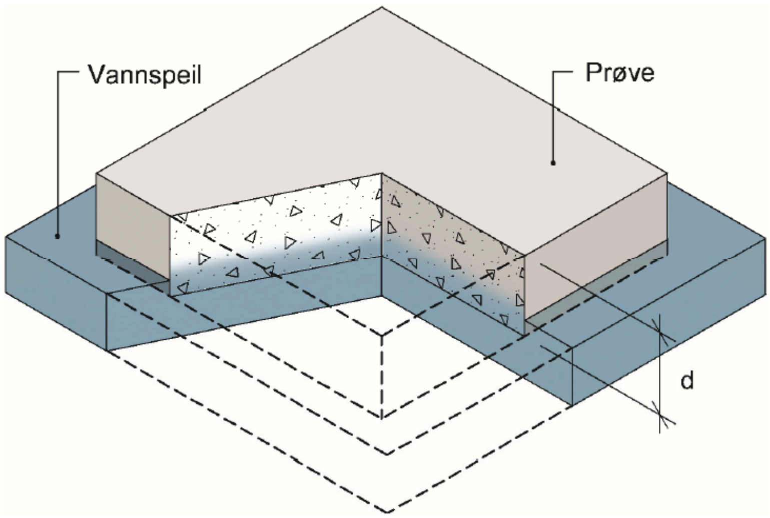

Figure 4-3: Illustration of the setup of the capillary absorption test method [11]

In the following description, the procedure of the method as given by Statens Vegvesen [10] is presented.

4.2.2.1 Equipment

To perform the testing, the following equipment is needed.

- Small stone saw
- Splitting machine
- Plastic containers with a grate in the bottom and a lid with a moisture-absorbing lining
- Scale with an accuracy of 0.01 g
- Stopwatch
- Clean, damp cloth
- Ventilated drying cabinet (105 °C)

4.2.2.2 Preparation of Test Specimens

Test specimens are prepared from cast cylinders or drilled cores. A diameter of 100 mm, minimum 90 mm, should be aimed for. The specimens are cut into discs with a thickness of 20 mm ± 1 mm. The discs should be flat and parallel.

A set of tests normally consists of 4 specimens of ø100 mm discs. When using discs with a diameter less than 100 mm, the number of discs should be adjusted such that the total area is at least:

- 20,000 mm^2 for concrete with $d_{maks} \leq 16$ mm
- 25,000 mm^2 for concrete with $d_{maks} > 16$ mm

The exposed surface should normally be a sawn surface.

4.2.2.3 Procedure

The test is performed by the following steps:

- Measurement of disc thickness using a caliper
- Potential painting of the side surfaces with epoxy or latex paint (only for diameter < 90 mm)
- Drying in a ventilated drying cabinet at 105°C until the weight loss is less than 0.01% per hour (alternatively for 7 days if constant drying time is more suitable), followed by a minimum of 2 hours of cooling in air at room temperature, covered with plastic wrap, weighing (weight g_1)

- Four days of suction from the water reservoir. The entire suction surface must be in contact with the water, without the water level rising more than 1-2 mm on the side surface. The box must be covered with a lined lid that prevents dripping of condensed water. Weighing after:
    - 10 and 30 minutes
    - 1, 2, 3, 4 and 6 hours
    - 1, 2, 3 and 4 days (weight after 4 days, g_5)

  When weighing, the following procedure must be followed for each disc:
    - The disc is taken up from the grid while making sure it doesn't drip on other discs
    - The disc is wiped off with a damp cloth and weighed
    - The disc is returned to the grid

The weights are registered in a form as given in Attachment 1.

4.2.2.4 Results

The method presents several parameters that should be calculated, but for our purpose it is only necessary to calculate the resistance coefficient, m, and the capillarity coefficient, k.

$$k = \frac{Q_{cap}}{\sqrt{t_{cap}}}\ , \qquad [\frac{kg}{m^2\sqrt{s}}] \tag{4.3}$$

$$m = \frac{t_{cap}}{h^2}\ , \qquad [\frac{s}{m^2}] \tag{4.4}$$

Where Q is the measured absorption values (expressed as the amount of absorbed water per unit area in kg/m^2), with Q_{cap} as the absorption value which corresponds to the waterfront just reaching the top surface of the sample, measured at given times t and h is the value describing the height the water rises, i.e., the thickness of the disc.

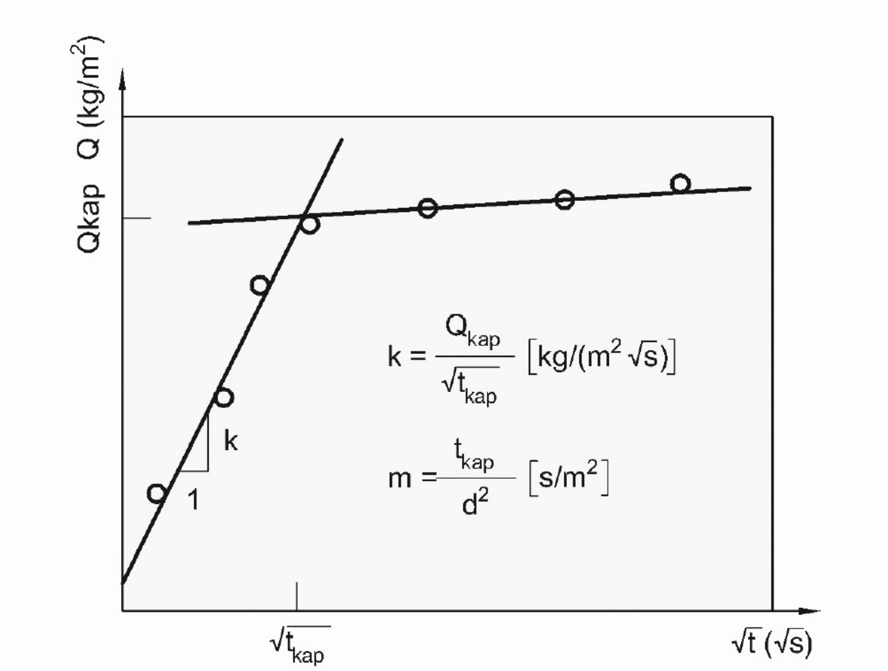

Figure 4-4: Example of results curve when measuring capillary absorption [11]

The intersection of the two curve parts (t_{cap}, Q_{cap}) can either be determined graphically or by linear regression analysis.

4.2.3 Pre-wetting in Concrete Rehabilitation

As described in chapter 3, pre-wetting of the concrete is an important step to ensure good adhesion when rehabilitating concrete. The techniques used for pre-wetting of the concrete affects the capillary suction in the concrete and therefore the bond created between the concrete and the repair material applied. As the properties of modern concrete has developed, it is interesting to look into the existing techniques for pre-wetting and investigate whether they are applicable to achieve optimal capillary action for good adhesion. In the following subchapters, the desired moisture condition of the concrete for optimal capillary action and the typical methods used to attain this condition is described.

4.2.3.1 Saturated Surface-dry Condition

When describing pre-treatment methods in concrete rehabilitation, it is common to state that the concrete should be saturated surface-dry (SSD) and slightly absorbent before applying the new coat [4]. The initial moisture level in the concrete before placing the repair material will have a great effect on the total absorbed water and the rate of absorption i.e., the capillary suction. High initial moisture level results in lower rate of absorption at the beginning, faster reduction in the rate of absorption and therefore lower total absorbed water compared to concrete with low initial moisture level. [12] How one controls that the concrete is indeed at SSD-condition is not clearly defined. The method normally practiced in the field for deciding the correct moisture level is simply just by visualization after what is assumed to be enough pre-wetting [13]. To acquire a better understanding of this concept, one needs to know the conditions that define a saturated surface-dry concrete.

Saturated surface-dry condition is defined as the condition where the concrete's capillary pores are saturated with water to a depth of several millimeters while the surface has no free water and is only slightly damp. The SSD-condition is important for the substrate to achieves its equilibrium. If the substrate is not sufficiently pre-wetted, we can get two types of disequilibrium. The first one is the case where the concrete substrate has too low moisture content. This state will result in capillary action pulling the water out of the new cementitious or epoxy cementitious repair material, resulting in issues such as incomplete hydration of the repair material and weak bonding between the old and new concrete. The second and opposite state is when the concrete substrate is too wet. Instead of achieving capillary action that pulls the repair material into the pores, helping increase the adhesion, we get surface pressure almost pushing the repair material away, resulting in a weak interface and low adhesion. The free water can also interfere with the repair material's water-to-cement ratio, making it weaker in strength. [13]

When the concrete has been saturated to the point where it is visually dark but has no free water on its surface, it is said to be saturated surface dry. At this state, the concrete should be slightly absorptive such that it attracts the repair material into the outer surface pores, creating good bonding without disturbing the properties of the repair material. Figure 4-5 shows the visual image of the saturated surface-dry condition.

Figure 4-5: Concrete at a dry state (left) and at a saturated surface dry state (right)

4.2.3.2 Pre-Wetting Methods

In scholarly literature it is typically stated that pre-wetting the concrete for at least a day prior to the application of the repair material is necessary for successful concrete rehabilitation. However, it is also stated that for concrete with low capillary suction, an assessment with regards to the necessity of pre-wetting must be made for each case. [4] The methods stated in many sources are developed with regards to normal concrete and may therefore not be as applicable to high strength concrete. Since there are no official methods defined on how to pre-wet the repair surface when rehabilitating modern high strength concrete, this report will discuss RaKon AS' procedures as given in Attachment 2 and Attachment 3. Although these procedures are not strictly adhered to in practical applications, they will serve as a foundation source for this thesis.

According to RaKon's procedure given in Attachment 2 mortar is placed by hand for smaller repairs where it is impractical or difficult to access with dry shotcrete mortar. Depending on the time passed after hydro blasting, or if just chiseling is performed, it is common to spray or brush water on the surface to achieve what is visually described as saturated surface-dry condition before applying the repair material. Any visible water on the concrete surface should be wiped away prior to the application of the mortar.

In the case of larger repairs, the mortar is sprayed on by dry shotcrete application as described in Attachment 3. When weather conditions are uncertain, the preferred approach is to wet the concrete for a minimum of 30 minutes before applying the mortar. However, in good weather conditions, the concrete should be pre-wetted for approximately 2 hours. It is also described that for the especially larger repair areas the concrete should be pre-wetted for at least a day before spraying of the mortar. Nonetheless, if the concrete is hydro blasted within 5 days, light pre-wetting is suggested as it is assumed that the concrete is already fully saturated with water.

As discussed in Chapter 3, the removal of damaged concrete is commonly achieved through two methods: chiseling or hydro blasting. Hydro blasting involves the application of pressurized fresh water into the pores and cracks of the concrete, generating internal pressure that breaks up the concrete and dissolves the aggregate. While hydro blasting is not typically classified as a pre-wetting method, it does introduce moisture into the concrete and can potentially impact the capillary suction of the concrete depending on its properties and the time elapsed between hydro blasting and the application of the repair material. If the pressure within the concrete pores from hydro blasting has not sufficiently dissipated, it is possible that the capillary action in the concrete may be insufficient for achieving proper adhesion or may not occur at all. In the worst-case scenario, excess pressure within the concrete may result in the outward displacement of the repair material.

The methods regarding pre-wetting are often described depending on the weather conditions, the chosen technique of chiseling and the type of repair material that is used, rather than the properties of the concrete which the repair material is applied to. It is therefore interesting to examine the effects of the composition of modern high strength concrete to assess whether there is need for a more thorough description for pre-wetting dependent on the concrete grade and the amount of silica fume in the concrete mix.

4.3 The Effect of Low Water-to-Cement Ratio and Silica Fume on Capillary Absorption in High Strength Concrete

As we delve into the topic of capillary absorption and its influence on adhesion in concrete rehabilitation, it is imperative to investigate the consequences of the composition of modern high strength concrete. In chapter 2.3.4, we previously explored silica fume as an additive in concrete mixes and its general impact on concrete properties. However, in this particular chapter, our attention will be directed towards silica fume's effect on the intricate capillary pore system within concrete. This is significant, as it can potentially affect the approach to achieving optimal adhesion in concrete rehabilitation. In addition to studying the influence of silica fume, we will also establish the impact of a low water-to-cement ratio on capillary absorption. By thoroughly examining how these variables affects the capillary pore system, we aim to uncover valuable insights that can inform effective strategies for improving adhesion in concrete rehabilitation.

Furthermore, within this chapter, a comprehensive overview will be provided, including a detailed account of a significant study conducted by SINTEF in 1988, titled "Capillary Absorption as a Quality Criterion" [5]. This seminal study holds considerable significance within the field and serves as a key reference for understanding the influence of silica fume and different water-to-cement ratio on capillary absorption. By leveraging the insights gained from prior research, we can enhance our understanding of the role of these variables in modulating capillary absorption and its implications for achieving optimal adhesion in concrete rehabilitation.

4.3.1 Theoretical Foundation

As previously elaborated in Chapter 2.2, the water-to-cement ratio plays a crucial role in determining the pore volume of concrete. A higher w/c ratio leads to an increased volume of pores, which in turn reduces the strength and density of the concrete. Conversely, when the w/c ratio is smaller and the amount of water is insufficient for complete cement hydration, the unreacted cement particles serve as a robust aggregate within the concrete and the pore volume decreases.

Another important factor which affects the pore structure of the concrete is the addition of silica fume in the cement. When silica fume is added to the concrete mix, it will act both as a reactive pozzolan and an effective filler. In chapter 2.3.4, it has been elucidated that the incorporation of silica fume into the concrete mix results in the formation of a reaction mass that effectively replaces coarse capillary pores that are evenly distributed throughout the concrete. This phenomenon is attributed to the pozzolanic reaction that takes place between the silicon dioxide present in the silica fume and the calcium hydroxide released by the cement. The reaction can be represented by the following equation:

$$Ca(OH)_2 + SIO_2 + H_2O \rightarrow CSH \qquad (4.5)$$

The outcome of this reaction is the formation of calcium silicate hydrate (CSH), which is the main binder in concrete. As a result, the incorporation of silica fume leads to the densification of the concrete, as the newly formed CSH fills the voids left by the capillary pores. This densification contributes to a reduction in porosity and an increase in the overall homogeneity of the concrete matrix. This pozzolanic reaction is a significant mechanism by which silica fume enhances the properties of high-strength concrete.

Silica fume is composed of tiny, smooth spherical particles of silicon oxide. These particles are incredibly small, ranging from 1 to 5/1000 mm in size, which is about 1/100 of the size of a cement grain. Additionally, silica fume boasts an exceptionally high surface area of around 20,000 m^2/kg, allowing it to absorb and bind significant amounts of water. This unique combination of properties results in a micro filler effect, where silica fume replaces coarse pores in the concrete that would typically be filled with pore water. Although this may slightly increase the total porosity of the concrete, it ultimately leads to a more homogeneous mixture and a reduction in permeability, which outweighs the porosity increase. [2] Notably, concrete incorporating silica fume exhibits an elevated number of gel pores and a decreased number of capillary pores in comparison to concrete without silica fume. [14]

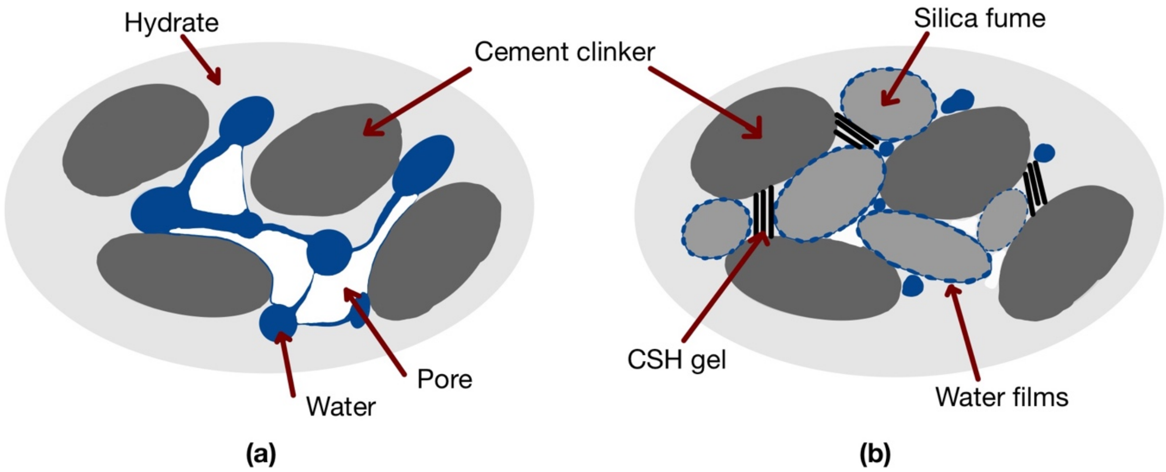

Figure 4-6: Illustration of cement paste microstructure: (a) without silica fume and (b) with silica fume

The addition of silica fume to the concrete mix requires an increased amount of water to achieve the desired consistency. To mitigate this, water reducing admixtures, as previously discussed in chapter 2.3.3, are essential to maintain workability without the need for excessive additional water. Water reducing admixtures are divided into two main types called plasticizers and superplasticizers. The most common plasticizers are lignosulfonates which are produced from natural products, while super plasticizers are synthetic substances. The water reducing admixtures affect the attractive and repulsive forces that always act between particles, altering the rheological properties of the cement paste. The cement particles in the mix will naturally be drawn to each other due to the attracting forces, but the plasticizer counteracts the attractive forces and therefore has a dispersing effect on the particles. The plasticizers also help reduce the diffusion rate of water into the cement grains. The use of plasticizing admixtures is believed to have some influence on the moisture-mechanical properties of concrete, because the additives affect the surface tension between pore water and pore walls, and thus the capillary absorption. [14] When discussing the effect of silica fume and low w/c-ratio on the capillary absorption, it is therefore important to also acknowledge the possible effect of these admixtures.

4.3.2 Previous Studies: *Capillary absorption as a quality criterion,* SINTEF 1988

In 1988, Sverre Smeplass performed a study with SINTEF named “Kapillærabsorpsjon som kvalitetskriterium” [5] which translates to “Capillary absorption as a quality criterion”. The objectives of the experimental program were to assess the correlation between water absorption and material composition, the reproducibility of the method, the sensitivity to variations in concrete composition, and the testing procedure itself, particularly regarding sample preparation. For the purpose of this thesis, it is especially the correlation between water absorption and the material composition, and the sensitivity to variations in concrete composition that is interesting to examine.

4.3.2.1 Method

The method used to determine the capillary absorption of the test specimens became the foundation for the method described in Statens Vegvesen’s handbook R210 [10] and is therefore the same as described in chapter 4.2.2. The study included two types of parameters which were material parameters and experimental parameters. The material parameters included concrete quality, i.e., w/c-ratio, use of silica fume and curing conditions. The study included 8 different concrete compositions, where the water-cement ratio varied in four levels from 0.40 to 0.70. In half of the concrete samples, 5% of the cement was replaced with silica dust. For the selected mixtures, a paste content of 31% (excluding any air) was chosen. The cement was a pure Portland cement without the addition of fly ash, with a Blaine value of approximately 4000 m^2/kg. A melamine-based, plasticizing admixture was used in the concrete with water/cement ratios lower than 0.70. The dosage of the admixture was done subjectively in order to achieve a slump of around 15 cm. No consideration was given to the admixture's effect on capillary absorption when the results were assessed.

In Table 4-3 and Table 4-4 below the respective concrete compositions of the concrete with and without silica fume is described.

Table 4-3: SINTEF study - Concrete compositions with silica fume [5]

Delmatr. (kg/m³)	E70S	E60S	E50S	E40S
Sement (P30)	290	322	360	409
Vann	214	203	190	173
Silika	16	17	19	22
Pukk	860	860	860	860
Sand	1052	1052	1052	1052
Rescon HP(S)		2	4	7
Luftdemper	0,1	0,1	0,1	0,1
Silikastøv	5 %	5 %	5 %	5 %
V/C+S	0,70	0,60	0,50	0,40

Table 4-4: SINTEF study - Concrete compositions without silica fume [5]

Delmatr. (kg/m³)	E70	E60	E50	E40
Sement (P30)	307	341	382	435
Vann	216	204	191	174
Silika	-	-	-	-
Pukk	860	860	860	860
Sand	1052	1052	1052	1052
Rescon HP(S)	-	2	4	7
Luftdemper	0,1	0,1	0,1	0,1
Silikastøv	0 %	0 %	0 %	0 %
V/C+S	0,70	0,60	0,50	0,40

Table 4-5 presents the measured compressive strength of the test specimens 28 and 265 days after casting.

Table 4-5: SINTEF study - Measured compressive strength at 28 and 265 days of age. [5]

Alder (døgn)	v/c+s	Trykkfasthet (MPa)	
		0 % SiO_2	5 % SiO_2
28 d	0,7	35,2	45,7
	0,6	44,3	52,9
	0,5	54,7	61,5
	0,4	63,9	76,9
265 d	0,7	40,7	52,0
	0,6	52,5	59,0
	0,5	63,4	71,2
	0,4	75,5	87,5

4.3.2.2 Results

The test was originally performed on specimens with different initial moisture levels. The differences in moisture levels were achieved by using different moisture conditioning and showed that the degree of saturation not only affects the amount of absorbed water, but also the speed and the course of the absorption. The absorption rate was lower in the initial phase and decreased more rapidly at high initial moisture levels than at low moisture levels. This result was unambiguous for all concrete qualities, but the tendency was most pronounced at low water/cement ratios and with the use of silica dust. The results showed that the silica concrete consistently had higher moisture levels after moisture conditioning than the concrete without silica. Results for the capillarity coefficient and resistance coefficient could not be obtained for specimens with higher initial moisture levels. Therefore, the following results are only based on specimens dried at 105°C.

As the graph in Figure 4-7 shows, the concrete with silica fume had significantly higher resistance coefficient than the corresponding concrete (same w/c) without silica fume. Additionally, it was observed that higher w/c-ratio exhibited lower resistance coefficients.

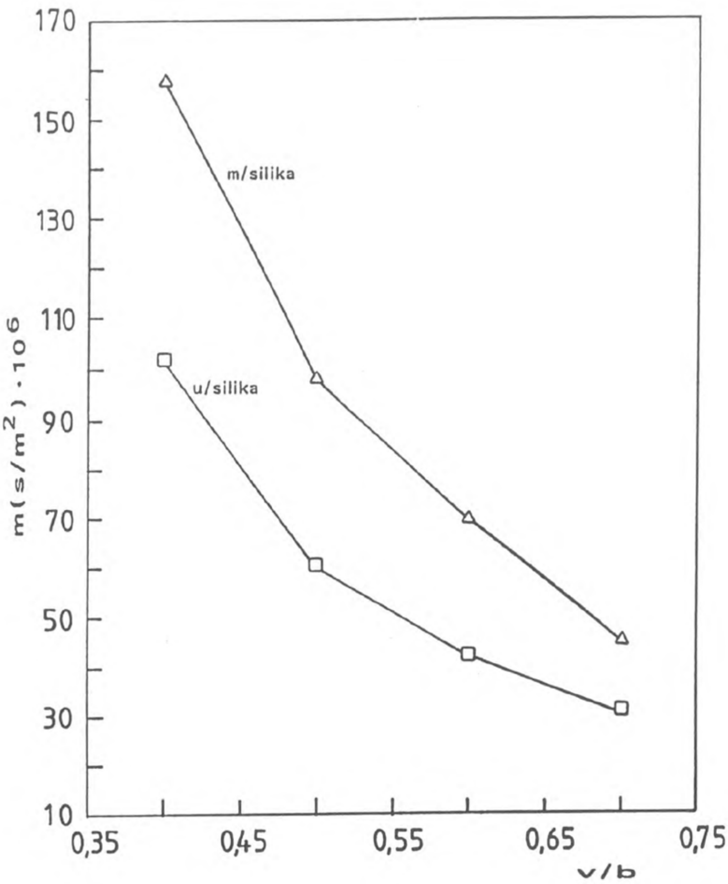

Figure 4-7: SINTEF study - Measured resistance coefficient, m, as a function of water/cement ratio and silica dosage. Water stored samples and moisture conditioning at 105°C for 3 days. Average values for 4 test pieces. [5]

Further, the graph in Figure 4-8 shows that the observed capillarity coefficients increased unambiguously with increasing water/cement ratio. The concrete with silica fume had significantly lower capillarity coefficients than the concrete without silica.

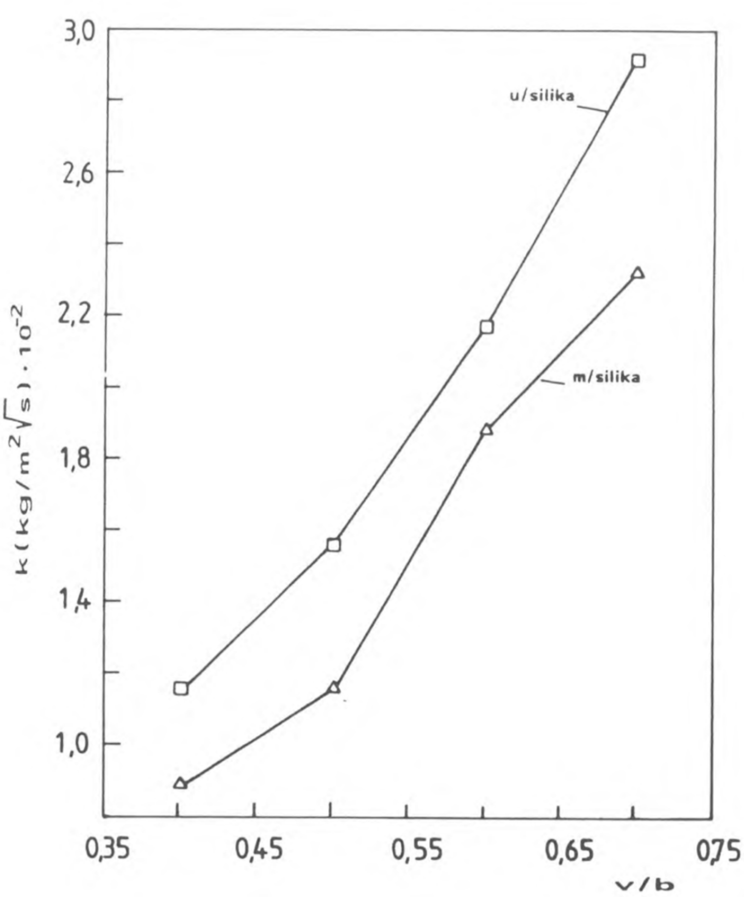

Figure 4-8: SINTEF study - Measured capillarity coefficient, k, as a function of water/cement ratio and silica dosage. Water stored samples and moisture conditioning at 105°C for 3 days. Average values for 4 test pieces. [5]

According to the results, the relationship between material composition and material properties was not as well defined for the capillarity coefficient as for the resistance coefficient. This was assumed to be because the resistance coefficient is mainly dependent on the pore size distribution in the capillary pore system, while the capillarity coefficient also depends on the concrete's total capillary pore volume, and thus becomes sensitive to local differences in aggregate distribution, etc.

4.3.2.3 Conclusion

The resistance coefficient, capillarity coefficient and capillary absorption were, according to the tests, unambiguously dependent on the water/cement ratio. As the w/c-ratio decreases, the capillary coefficient decreases, and the resistance increases.

The use of silica dust (5% cement replacement) gave changes in resistance coefficient and capillarity coefficient corresponding to the effect of a reduction in the water/cement ratio of 1/10. The determination of resistance coefficient and capillarity coefficient was also particularly sensitive to differences in moisture levels in the test pieces after moisture acclimatization.

4.4 Implications for Capillary Absorption in High Strength Concrete and Concrete Rehabilitation

The incorporation of silica fume in high strength concrete has a significant impact on capillary absorption by enhancing the material's density and reducing its porosity. Moreover, the lower water-to-cement (w/c) ratio, characteristic of high strength concrete compared to regular concrete, further influences capillary absorption properties. These factors result in a reduction in the volume of capillary pores and a decrease in the available pore volume for capillary suction. Consequently, the combination of silica fume and a lower w/c ratio in high strength concrete theoretically leads to a decrease in capillary absorption.

The impact of reduced capillary absorption in high strength concrete with silica fume can potentially affect the adhesion of repair materials to the existing concrete substrate during rehabilitation. Achieving good adhesion between the repaired concrete and the repair material can be challenging, especially when the substrate is not properly prepared or when the repair material is not applied correctly. The complex and multifaceted effects of silica fume and lower w/c ratio on capillary absorption in high strength concrete necessitate further research and laboratory testing to fully understand their implications on adhesion in concrete rehabilitation.

The findings from this literature review provide valuable insights that can inform the experimental investigations in the upcoming chapter of this thesis. In the next part, laboratory testing will be conducted to explore capillary absorption of modern high strength concrete, as well as the adhesion properties of high strength concrete with silica fume, specifically in the context of pre-wetting methods in concrete rehabilitation. This research aims to advance our understanding of the intricate relationship between capillary absorption and adhesion in high strength concrete.

5. Laboratory Tests

The laboratory testing phase of this research project focuses on investigating key aspects of concrete rehabilitation. Building upon the findings of the literature study, this chapter aims to provide a deeper understanding of the capillary suction properties of high strength concrete and the effectiveness of various pre-wetting techniques in enhancing adhesion. By conducting in-depth laboratory tests, we aim to gain valuable insights into the need for tailored repair techniques, mainly focusing on pre-wetting methods, based on the specific characteristics of the concrete being repaired.

Bond strength tests, specifically the pull-off method, will be employed to evaluate the strength of the bond between repaired concrete and the repair material. The tests will mainly focus on assessing the adhesion achieved through different pre-wetting techniques, while also looking into the materials, repair techniques and after treatments. By conducting pull-off tests, we can quantitatively measure the strength of the bond and make informed comparisons between different repair techniques.

Additionally, the laboratory testing aims to further explore the capillary suction of high strength concrete, which constitutes the second primary objective. Through the measurement of capillary absorption, valuable insights can be gained regarding the porous structure and moisture retention capabilities of high strength concrete. By assessing the influence of the composition of high strength concrete on capillary suction, we aim to determine its impact on moisture movement within the concrete and potentially identify the need for additional pre-wetting methods to optimize the adhesion of repaired concrete.

The results obtained from these laboratory tests will be thoroughly analyzed and discussed in the subsequent results and discussion chapter. Through this analysis, we will gain valuable insights into the capillary absorption properties of high strength concrete, the impact of silica fume on moisture movement, and the efficacy of various pre-wetting techniques in achieving optimal adhesion. These findings will not only advance our understanding of concrete rehabilitation but also aim to provide practical guidance for selecting and implementing appropriate pre-wetting methods based on the specific concrete type.

5.1 Tensile Bond Strength Tests

5.1.1 Methodology

For the purpose of this thesis, two different types of concrete will be subjected to testing. The first type is based on a recipe derived from a typical gravity-based offshore structure (GBS). This particular recipe represents a more traditional concrete composition commonly used in offshore structures dating back to around 1987. However, it is important to note that for the castings conducted in this study, more modern types of cement will be used compared to those employed in existing GBS structures, as explained in Chapter 4.1. The water-to-cement (w/c) ratio for the GBS-type concrete castings prepared for this thesis is 0.42. In Table 5-1 the recipe used for the concrete mix is given.

Table 5-1: GBS concrete recipe for bond strength testing

Recipe for GBS concrete	Batch 416 kg
Cement Anlegg FA	94 kg
Silica fume (dry, silica/C in %)	3 kg (3.19%)
Sand (0-5mm)	178 kg
Coarse aggregates (5-20mm)	140 kg
SP	1 %
w/c - ratio	0.42

The second type of concrete to be tested is specifically formulated to resemble the composition of an existing offshore foundation for wind turbines (FWT). This concrete mixture represents a more contemporary approach to offshore structures, reflecting a design from 2022. The water-to-cement (w/c) ratio for the FWT concrete castings prepared for this thesis is 0.37. In Table 5-2 the recipe used for the concrete mix is given.

Table 5-2: FWT concrete recipe for bond strength testing

Recipe for FWT concrete	Batch 440 kg
Cement Anlegg FA	103.4 kg
Silica fume (dry, silica/C in %)	3.3 kg (3.19%)
Sand (0-5mm)	195.8 kg
Coarse aggregates (5-20mm)	154 kg
SP	1.1 %
w/c - ratio	0.37

Due to limited availability of materials, the recipe is based on a material in which Weber Norway uses for coarse dry concrete. This material has a drop in the sand curve of the composition and is therefore not 100% comparable to other recipes.

The mortar material for the repair in the bond strength testing is delivered by Weber Norway. Weber Rep 05 is the material used as a bonding agent for hand applied repair, Rep 65 is used as the repair mortar for hand applied repair, and Sprøyterep T is used as the repair mortar for dry shotcrete application. Table 5-3 gives a description of the properties of the repair materials.

Table 5-3: Weber Norway repair material description [15]

Product	Repair class	Exposure class	28 days strength (MPa)	Grain size (mm)	Layer thickness (mm)
Weber Sprøyterep T	-	x	60	2	< 50
Weber Rep 65	R4	x	> 50	2	5-50
Weber Adhesion Rep 05	-	x	-	0.25	1-3

The rehabilitation procedures provided by RaKon AS, as outlined in Attachment 2 and Attachment 3, have served as the initial framework for the selected methods in the laboratory testing. Both types of high strength concrete, GBS and FWT, will undergo the same repair methods. For each concrete type, two main blocks measuring 40x40x40 cm3 will be cast, allowing for testing on five sides of the blocks. One of the blocks will be repaired using hand-applied repair techniques, while the second block will undergo the dry shotcrete application method. Following the repair process, the blocks will be stored in a controlled indoor environment and securely wrapped in plastic foil.

In order to assess the impact of post-treatment methods, four smaller additional blocks will be cast using the same concrete types. These blocks will have two sides designated for testing purposes. Following the selection of similar repairs, these blocks will be stored outside, exposed to normal weather conditions. Additionally, two smaller blocks will be cast and fully submerged in water for a duration of 6 days prior to the repair process. These variations in post-treatment methods aim to provide a comprehensive understanding of their effects on the repaired concrete structures.

Considering the limited time available, the concrete will have a curing period of only 7 days before the repair is carried out. This timeframe allows for the development of approximately 60-75% of the strength typically achieved at 28 days. The tensile bond strength test will be conducted 14 days after the repair, specifically 21 days after the initial casting of the specimens. In addition to the castings specifically prepared for this thesis, four core samples have been generously provided for comparison purposes. Two of these samples originate from an existing gravity-based offshore structure (GBS) dating back to 1987, while the other two are from an existing offshore foundation for wind turbines (FWT) constructed in 2022. These additional samples will be integrated into a larger substrate, allowing for the execution of repairs and bond strength tests on these specimens as well.

5.1.2 Hand Applied Repair

Table 5-4 shows the set up for the blocks that will be repaired by placing repair mortar by hand. Side A-E represent the sides on the main blocks, Extra A-B represent the additional blocks which are stored outside, and Extra G represent the additional blocks which are pretreated by being submerged in water.

Table 5-4: Laboratory testing method: Hand applied repair

	Pre-treatment	Method	Repair mortar	Post treatment
Side A	Stored at 20°C, covered in plastic. Pre moist 30 - 60 min before.	Rep 65 mortar is applied by throwing mortar onto substrate.	Rep 65	Stored at 20°C, covered in plastic.
Side B	Stored at 20°C, covered in plastic. Pre moist 30 - 60 min before.	Rep 65 mortar brushed into substrate before wet in wet application.	Rep 65	Stored at 20°C, covered in plastic.
Side C	Stored at 20°C, covered in plastic. Pre moist 30 - 60 min before.	Rep 05 adhesion mortar brushed into substrate before wet in wet application with Rep 65.	Rep 05 + Rep 65	Stored at 20°C, covered in plastic.
Side D	Stored at 20°C, covered in plastic. No Pre moist of substrate.	Rep 65 mortar brushed into substrate before wet in wet application.	Rep 65	Stored at 20°C, covered in plastic.
Side E	Stored at 20°C, covered in plastic. No Pre moist of substrate.	Rep 05 adhesion mortar brushed into substrate before wet in wet application with Rep 65.	Rep 05 + Rep 65	Stored at 20°C, covered in plastic.
Extra A	Stored at 20°C, covered in plastic. Pre moist 30 - 60 min before repair.	Rep 65 mortar brushed into substrate before wet in wet application.	Rep 65	Stored outside exposed to normal weather.
Extra B	Stored at 20°C, covered in plastic. Pre moist 1 day and 30 - 60 min before repair.	Rep 65 mortar brushed into substrate before wet in wet application.	Rep 65	Curing membrane, stored outside.

5.1.3 Dry Shotcrete Application

Table 5-5 shows the set up for the blocks that will be repaired by placing repair mortar by spraying. Side A-D represent the sides on the main blocks, Extra E-F represent the additional blocks which are stored outside, and Extra G represent the additional blocks which are pretreated by submerging in water. Finally, Extra Orig. A-B represent the core samples obtained from existing offshore structures, casted into larger substrates.

Table 5-5: Laboratory testing method: Dry shotcrete application

	Pre-treatment	**Method**	**Repair mortar**	**Post treatment**
Side A	Stored at 20°C, covered in plastic. Waterjet 5 days before and pre moist before repair.	Sprøyterep T applied by dry shotcrete.	Dry shotcrete Sprøyterep T	Stored at 20°C, covered in plastic.
Side B	Stored at 20°C, covered in plastic. Waterjet 1 day before and pre moist before repair.	Sprøyterep T applied by dry shotcrete.	Dry shotcrete Sprøyterep T	Stored at 20°C, covered in plastic.
Side C	Stored at 20°C, covered in plastic. Waterjet 1 day before.	Sprøyterep T applied by dry shotcrete.	Dry shotcrete Sprøyterep T	Stored at 20°C, covered in plastic.
Side D	Stored at 20°C, covered in plastic. No pre moist.	Sprøyterep T applied by dry shotcrete.	Dry shotcrete Sprøyterep T	Stored at 20°C, covered in plastic.
Extra E	Stored at 20°C, covered in plastic. Waterjet 1 day before and pre moist before repair.	Sprøyterep T applied by dry shotcrete.	Dry shotcrete Sprøyterep T	Stored outside exposed to normal weather.
Extra F	Stored at 20°C, covered in plastic. Waterjet 1 day before and pre moist before repair.	Sprøyterep T applied by dry shotcrete.	Dry shotcrete Sprøyterep T	Curing membrane, stored outside.

Extra G	Stored fully submerged in water for 6 days.	Sprøyterep T applied by dry shotcrete.	Dry shotcrete Sprøyterep T	Stored at 20°C, covered in plastic.
Extra orig. A	Waterjet 1 day before and pre moist before repair.	Sprøyterep T applied by dry shotcrete.	Dry shotcrete Sprøyterep T	Stored at 20°C, covered in plastic.
Extra orig. B	No pre moist of substrate.	Sprøyterep T applied by dry shotcrete.	Dry shotcrete Sprøyterep T	Stored at 20°C, covered in plastic.

5.1.4 Measurement of Bond Strength by Pull-off Method

The method used to determine the pull-off bond strength of repair products and systems applied to a reference concrete is described in the Norwegian standard NS-EN 1542. The method of test is by direct dolly pull-off using a dolly bonded to the surface of the repair product or system, with the test area having been defined by coring through the surface. In the following description, the procedure of the method as given in NS-EN 1542 is summarized. [16]

5.1.4.1 Equipment

To perform the testing, the following equipment is needed.

- Mortar/concrete mixer.
- Compaction tools and equipment for repair grouts, mortars, and concretes.
- Standard laboratory climate.
- Molds for producing a uniform thickness of repair product.
- Vernier calipers accurate to not less than 0.1 mm.
- Rapid hardening two component epoxy adhesive.
- Circular dollies with a diameter of (50 ± 0.5) mm and with a thickness of at least 20 mm if made of steel, or with a thickness of at least 30 mm if made of aluminum.
- Grinding equipment, for cleaning adhesive from the used dollies.
- Steel wire brush and soft-bristled brush.

- Diamond core drill and barrel that enable the drilling of a (50 ± 1.0) mm cylinder through the repair product and system.
- Pull off test equipment.
- Concrete test specimens.

5.1.4.2 Preparation of Test Specimens

Minimum one test specimen is required for each repair product or system, from which five bond tests shall be carried out. A normal type of failure must be given in minimum three of the tests for the test to be acceptable.

The following steps are to be conducted when preparing the test specimens.

- The products and tools shall be stored in the standard laboratory climate, (21 ± 2)°C and (60 ± 10) % relative humidity, for at least 24 hours before testing.
- The surface of the reference concrete must be free from contamination, and therefore cleaned sufficiently before applying the repair product. The cleaning method depends on which pre-treatment method that is used. Cleaning can be done either with water, a brush, vacuum etc.
- The mixing technique for preparing the specimens shall be carried out as instructed by the manufacturer.
- The test specimens prepared in the vertical position shall be stored in this position for three days, before the specimens may be laid horizontal and curing continued.
- Following the curing period, the test specimen shall be conditioned for seven days by storage in a standard laboratory climate.
- At the end of the seven days, the specimen should be set up with the dollies in place such that testing can be conducted.

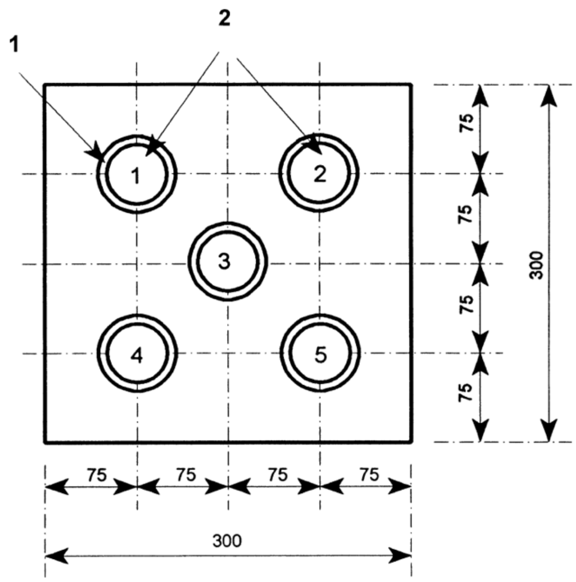

Figure 5-1: Plan of specimen showing dolly locations [16]

5.1.4.3 Procedure

The following steps describe the procedure which must be followed when carrying out the test.

- The test specimen must be fastened such that it cannot move. By using a diamond coring barrel, one should drill through the repair product or system to a depth of (15 ± 5) mm into the concrete substrate. The total drill-in depth, d_i, is given by the following formula:

$$d_i = d_d + (15 \pm 5)\ mm$$

  where d_d is the thickness of the mortar layer in mm.
- To fasten the dolly to the test specimen, a thin layer of adhesive must be applied to the specimen such that it forms a uniform layer between the dolly and the substrate. The dolly shall be placed in the center of the core while applying sufficient pressure. Any excess adhesive shall be removed immediately before leaving the adhesive to harden.
- The pull-off equipment shall be placed over the dolly and be secured such that it will not change position during the test.

- The load should be increased continuously and evenly at a rate of (0.05 ± 0.01) MPa/s until failure occurs. The failure load as well as the mean diameter of the specimen at the failure face (as the average result of measurements taken perpendicularly to each other, across the core, using the vernier calipers) shall be recorded.

5.1.4.4 Results

The results must be categorized into one of the following types of failure patterns by visual assessment.

- A: Cohesion failure in the concrete substrate.
- A/B: Adhesion failure between the substrate and the first layer (e.g. primer, bonding slurry or mortar).
- B: Cohesion failure in the first layer.
- B/C: Adhesion failure between the first and second layer.
- C: Cohesion failure in the second layer.

(Etc., as defined by the particular product or system under test)

- -/Y: Adhesion failure between the last layer and adhesive layer (e.g. C/Y in a two-layer repair system)
- Y: Cohesion failure in the adhesive layer.
- Y/Z: Adhesion failure between the adhesive layer and the dolly (which is Z).

In the case of a combined failure pattern, a visual inspection shall be carried out to determine the percentage of each failure pattern.

For each normal failure result, the tensile bond strength shall be calculated by the following formula,

$$f_h = \frac{4F_h}{\pi D^2}$$

where f_h is the bond of the test specimen in megapascals, F_h is the failure load in Newtons and D is the mean diameter of the test specimen in millimeter.

5.1.5 Execution of Preparatory Work for Bond Strength Tests

The concrete mix was thoroughly blended using a large pan mixer, enabling simultaneous mixing of the required quantity of concrete for each concrete type. Once the concrete mix reached a satisfactory consistency, it was poured into the formwork. During the pouring process, a vibrator was utilized to ensure even distribution of the mix and to eliminate any trapped air bubbles within the concrete. Following the pouring, the surface of the concrete was carefully smoothed out, and then the blocks were covered with plastic and stored in a controlled indoor environment at approximately 20°C. Figure 5-2 illustrates the appearance of the main concrete blocks immediately after casting.

Figure 5-2: Main concrete castings for bond strength tests, GBS (left) and FWT (right)

After one day of hardening, the concrete blocks were taken out of the formwork as shown in Figure 5-3.

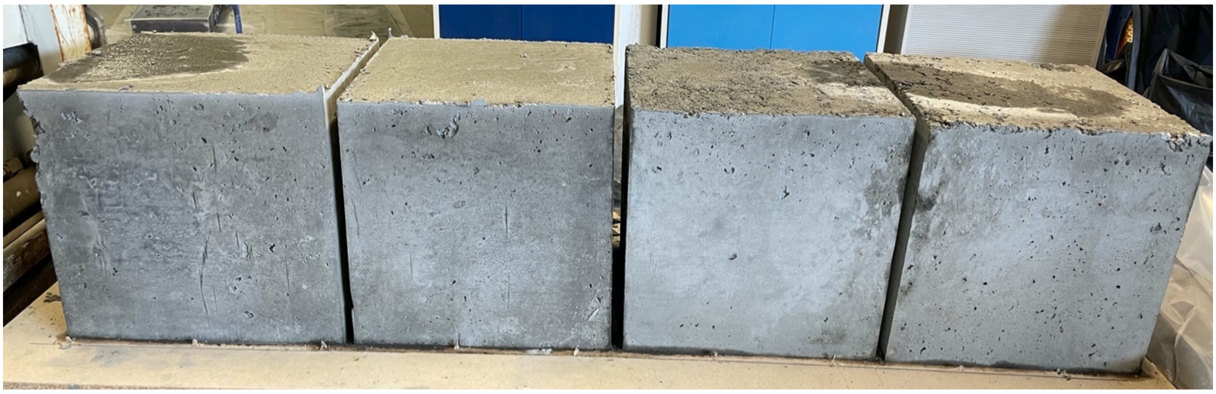

Figure 5-3: Main concrete castings (GBS left and FWT right) for bond strength tests: After one day of curing

The initial step involved polishing the concrete surface using a concrete polisher to eliminate the laitance present on the surface. Subsequently, a chisel machine was employed to create a rough and coarse texture on the surface, providing an ideal foundation for the repair material to adhere to. As the availability of equipment was limited, the surface preparation solely relied on the use of a chisel machine, omitting hydro blasting. Due to the regulations stipulated by the HMS which restrict the duration of chisel machine operation, and considering the time-consuming nature of the task, this process was spread over two days. Upon completion of the chiseling process, the concrete surface was subjected to air blasting, effectively removing any dust or residual substances.

Figure 5-4 below shows the execution of chiseling with a chisel machine, and the concrete surface after polishing and chiseling.

Figure 5-4: Concrete castings for bond strength tests: During and after chiseling with a chisel machine

Five days prior to the repairs, side A of the dry shotcrete application blocks underwent a high-pressure washing while in a vertical position. Subsequently, the sides were laid horizontally, and water was poured onto the surface. This method was chosen as an alternative to the conventional hydro blasting method typically employed on offshore structures. As discussed in Chapter 4.2.3.2, hydro blasting can create excessive pressure in the capillary pores of the concrete, caused by both the force applied and the amount of water in the pores. The method employed in this thesis aims to replicate this condition as closely as possible using the available resources.

Figure 5-5 depicts side A of each concrete casting type that will undergo repair using the dry shotcrete application method, immediately after the high-pressure washing process.

Figure 5-5: Main concrete castings for bond strength tests: Side A (GBS left, FWT right) after high pressure washing

On the day preceding the repair, sides B and C of the main blocks, as well as sides E and F of the extra blocks designated for the dry shotcrete application specimens, were subjected to the identical procedure. Seven days after casting, water was applied to the sides requiring pre-wetting using a pressure spray bottle, approximately 30-60 minutes prior to the repair process. To ensure the desired saturated surface dry condition was attained before the application of the repair material, multiple sprays were administered on certain sides due to variations in the timing of the repair execution. Figure 5-6 showcases two of the extra blocks following the completion of the pre-wetting process.

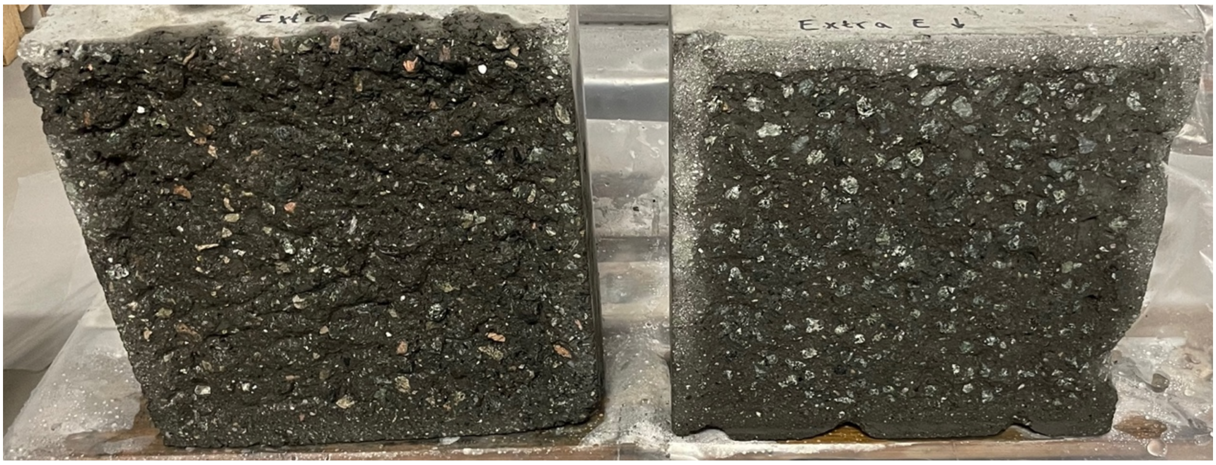

Figure 5-6: Extra concrete castings (FWT left, GBS right) for bond strength tests: After pre-wetting

Once the concrete castings had completed a seven-day curing period, the repair process was carried out. Figure 5-7 illustrates the execution of the hand applied repair. For the sides where adhesion mortar Rep 05 was selected, a brush was used to press the mortar into the surface, as depicted on the left side of the figure. On the right side, Rep 65 was applied according to the instructions provided in Table 5-4.

Figure 5-7: Concrete repair: Application of Rep 05 (left) and after hand application of Rep 65 (right)

Figure 5-8 shows one of the main concrete blocks which were repaired by dry shotcrete as described in Table 5-5. The repair was performed by a professional assuring sufficient placement of the mortar.

Figure 5-8: Concrete repair: Before (left) and after (right) dry shotcrete repair with Dry shotcrete Sprøyterep T

Subsequently, the main concrete blocks, fully saturated blocks, and core samples were stored indoors, protected by plastic coverings. The extra blocks, on the other hand, were placed outside. Two of the sides were treated with a curing membrane, as illustrated in Figure 5-9, while the remaining two sides were left exposed, following the instructions provided in Table 5-4 and Table 5-5.

Figure 5-9: Application of curing membrane on specimens Extra F

Following the completion of a seven-day curing period for the repair material, the repaired area underwent polishing to ensure its readiness for bond strength testing. Over the subsequent days, a total of 145 cores were drilled out for further analysis. In the final stages, the dollies were glued to the surface of the cores, rendering the specimens ready for testing after 21 days since casting and 14 days since the repair took place.

5.1.6 Execution of Bond Strength Tests

The bond strength testing was performed by the use of an automated pull-off tester called Proceq DY-206. In Figure 5-10 the typical plan of a specimen after the bond strength pull-off method has been executed is shown. Each core is placed at the top right corner of the core hole, showing the fracture surface.

Figure 5-10: Typical plan of specimen showing pulled out cores after bond strength testing

A visual assessment of each core was performed to categorize the failure patterns as described in chapter 5.1.4.4. The categorizes relevant for the executed tests are as follows:

- A: Cohesion failure in the concrete substrate.
- A/B: Adhesion failure between the substrate and the repair mortar. (Either Rep 05, Rep 65 or Sprøyterep T depending on method).
- B: Cohesion failure in the repair mortar. (Either Rep 65 or Sprøyterep T depending on method).
- Y: Cohesion failure in the adhesive layer.
- Y/Z: Adhesion failure between the adhesive layer and the dolly.

Picture documentation of all the specimens showing pulled out cores after bond strength testing including description of each failure pattern is given in Attachment 4 to Attachment 7.

The values obtained from the bond strength test on the specimens repaired by hand applied repair are given in Table 5-6 and Table 5-7. Below each value the failure categories including the percentage is given.

Table 5-6: Tensile bond strength for hand applied repair of GBS concrete

GBS - H:	**Tensile bond strength (MPa)**					**Mean Value**
	Core 1	**Core 2**	**Core 3**	**Core 4**	**Core 5**	
Side A	1.06	0.31	0.40	0.64	0.42	0.57
	100% A	87% A, 13% B	60% A, 40% A/B	40% A, 60% A/B	25% A, 75% A/B	
Side B	1.36	0.93	1.21	1.51	1.86	1.37
	90% A/B, 10% A	15% A, 85% A/B	15% A, 85% A/B	20% A, 80% B	20% A, 80% B	
Side C	1.11	1.28	1.60	1.04	1.14	1.23
	95% A/B, 5% B	95% A, 5% B	95% A, 5% B	95% A, 5% B	97% A/B, 25% B	
Side D	1.13	1.22	1.52	1.84	0.87	1.32
	95% A, 5% B	65% A, 35% B	65% A, 35% B	90% A, 10% B	90% A, 10% B	
Side E	1.10	1.43	1.82	1.8	1.18	1.47
	60% A, 40% B	50% A, 50% B	50% A, 50% B	50% A, 50% B	50% A, 50% B	
Extra A	0.82	1.76	1.46	1.10	0.84	1.20
	35% A/B, 65% B	25% A/B, 75% B	75% B, 25% Y/Z	40% A/B, 60% B	35% A/B, 65% B	
Extra B	1.17	1.31	0.84	1.32	1.09	1.15
	5% A, 95% A/B	10% A, 90% A/B	10% A, 90% A/B	10% A, 30% A/B, 60% B	15% A, 50% A/B, 40% B	

Table 5-7: Tensile bond strength for hand applied repair of FWT concrete

FWT-H:	**Tensile bond strength (MPa)**					**Mean Value**
	Core 1	**Core 2**	**Core 3**	**Core 4**	**Core 5**	
Side A	0.61	0.52	0.53	0.62	0.54	0.56
	90% A, 10% B	15% A, 85% B	5% A, 95% B	50% A, 50% B	95% A, 5% B	
Side B	1.51	1.58	1.51	0.85	1.2	1.33
	40% A, 40% A/B, 20% B	35% A, 5% A/B, 50% B	20% A, 15% A/B, 65% B	30% A, 15% A/B, 55% B	30% A, 15% A/B, 55% B	
Side C	0.80	1.00	0.67	0.86	1.07	0.88
	40% A, 60% B	20% A, 80% B	35% A, 65% B	45% A, 55% B	20% A, 80% B	
Side D	1.49	0.88	1.57	1.34	1.03	1.26
	65% A, 35% B	80% A, 20% B	10% A, 90% B	97% A, 3% B	85% A, 15% B	
Side E	1.01	1.24	1.65	1.18	1.3	1.28
	50% A, 50% B	30% A, 70% B	50% A, 50% B	40% A, 60% B	25% A, 75% B	
Extra A	1.87	1.46	0.68	1.19	1.24	1.29
	80% A, 20% B	80% A, 20% B	90% A, 10% A/B	65% A, 35% A/B	50% A, 50% A/B	
Extra B	1.68	1.14	0.65	0.86	0.78	1.02
	40% A, 60% B	40% A, 60% B	75% A, 25% B	65% A, 35% B	80% A, 20% B	

The values obtained from the bond strength test on the specimens repaired by dry shotcrete repair are given in Table 5-8 and Table 5-9. Below each value the failure categories including the percentage is given.

Table 5-8: Tensile bond strength for dry shotcrete repair of GBS concrete

GBS - S:	Tensile bond strength (MPa)					Mean Value
	Core 1	**Core 2**	**Core 3**	**Core 4**	**Core 5**	
Side A	1.99	2.67	1.67	2.11	1.88	2.06
	85% A, 15% B	85% A, 15% B	50% A/B, 50% B	40% A, 60% B	40% A, 60% B	
Side B	2.65	2.61	2.09	2.84	2.12	2.26
	100% A	100% A	80% A, 20% B	100% A	70% A, 30% B	
Side C	2.16	1.66	2.40	1.83	1.09	1.83
	100% A	50% A, 50% B	100% A	100% B	100% B	
Side D	1.28	0.73	1.27	1.41	1.60	1.26
	95% A, 5% B	100% A	100% A	95% A, 5% B	80% A, 20% B	
Extra E	1.54	1.58	2.39	1.1	1.09	1.54
	35% A, 65% B	100% B	100% B	97% A/B, 3% B	97% A/B, 3% B	
Extra F	1.58	1.13	1.86	1.37	1.35	1.46
	75% A/B, 25% B	60% A/B, 40% B	85% A/B, 15% B	85% A/B, 15% B	100% A/B	
Extra G	1.59	1.19	> 3.06	1.27	1.43	1.37
	95% A, 5% B	50% A/B, 50% B	100% A	95% A/B, 5% B	60% A/B, 40% B	
Extra orig. A	2.36	-	-	-	-	2.36
	65% A, 5% A/B, 30% B	-	-	-	-	
Extra orig. B	1.73	2.08	-	-	-	1.91
	100% A	10% A, 90% B	-	-	-	

Table 5-9: Tensile bond strength for dry shotcrete repair of FWT concrete

FWT - S:	**Tensile bond strength (MPa)**					**Mean Value**
	Core 1	**Core 2**	**Core 3**	**Core 4**	**Core 5**	
Side A	2.31	2.15	2.40	1.47	2.98	2.26
	5% A, 95% B	10% A, 90% B	70% A, 20% B	75% A, 25% B	60% A, 40% B	
Side B	1.55	1.74	2.12	2.07	2.77	2.05
	100% A	100% A	90% A, 10% B	50% A, 50% B	50% A, 50% B	
Side C	1.93	2.95	3.02	1.94	2.42	2.45
	100% B	100% A	65% A, 35% B	35% A, 65% B	85% A, 15% B	
Side D	1.26	1.85	1.09	0.66	1.70	1.31
	85% A, 15% B	90% A, 10% B	100% A	100% A	100% A	
Extra E	1.82	1.68	1.55	1.75	1.67	1.69
	100% B	100% B	100% B	100% B	100% B	
Extra F	1.21	1.95	2.35	1.42	1.45	1.68
	70% A, 30% B	100% B	95% B, 5% Y/Z	80% A, 20% B	95% A, 5% B	
Extra G	1.52	1.3	0.97	1.09	0.94	1.16
	90% A, 10% B	97% A, 3% B	93% A, 7% B	100% B	85% A, 15% B	
Extra orig. A	2.73	-	-	-	-	2.73
	90% A, 10% A/B	-	-	-	-	
Extra orig. B	0.27	-	-	-	-	0.27
	100% A/B	-	-	-	-	

5.2 Capillary Absorption Tests

5.2.1 Methodology

To facilitate a meaningful discussion on the relationship between bond strength and capillary absorption, the specimens for the capillary absorption test were sourced from the same existing offshore structures that served as the basis for the recipe used in the bond strength test specimens. This ensures a direct comparison and evaluation of the two sets of test results. One set of cores was obtained from an existing gravity based offshore structure (GBS) from 1987, while the other set was sourced from an offshore foundation specifically designed for wind turbines (FWT) from 2022. By including samples from these structures, we aim to provide a more comprehensive understanding of the bond strength and capillary absorption properties in the context of different concrete applications. The method used to determine the capillary absorption of the specimens is as described in Chapter 4.2.2.

The specific recipes used for the specimens are not publicly disclosed. However, Table 4-2 provides a representation of typical recipes for offshore structures, which were discussed in Chapter 4.1.2 during the investigation of high strength concrete. This table offers valuable insights into the characteristics of the recipes, offering a perspective on their composition and properties. The GBS concrete was composed with a water-to-cement (w/c) ratio of 0.43 and contained 2% silica fume, while the FWT concrete had a w/c ratio of 0.35 and included 5-8% silica fume.

5.2.2 Execution of Capillary Absorption Tests

The test specimens are prepared from drilled cores collected from the two offshore concrete structures. The specimens are cut into flat and parallel discs with a diameter of 95 mm ± 1 mm and thickness of 20 mm ± 1 mm. There is a total of 4 discs from GBS and 4 discs from FWT concrete. After the discs have been prepared, they are placed into a drying cabinet set to dry at 105 °C for 7 days i.e., until completely dried out. Figure 5-11 shows the test specimens after drying.

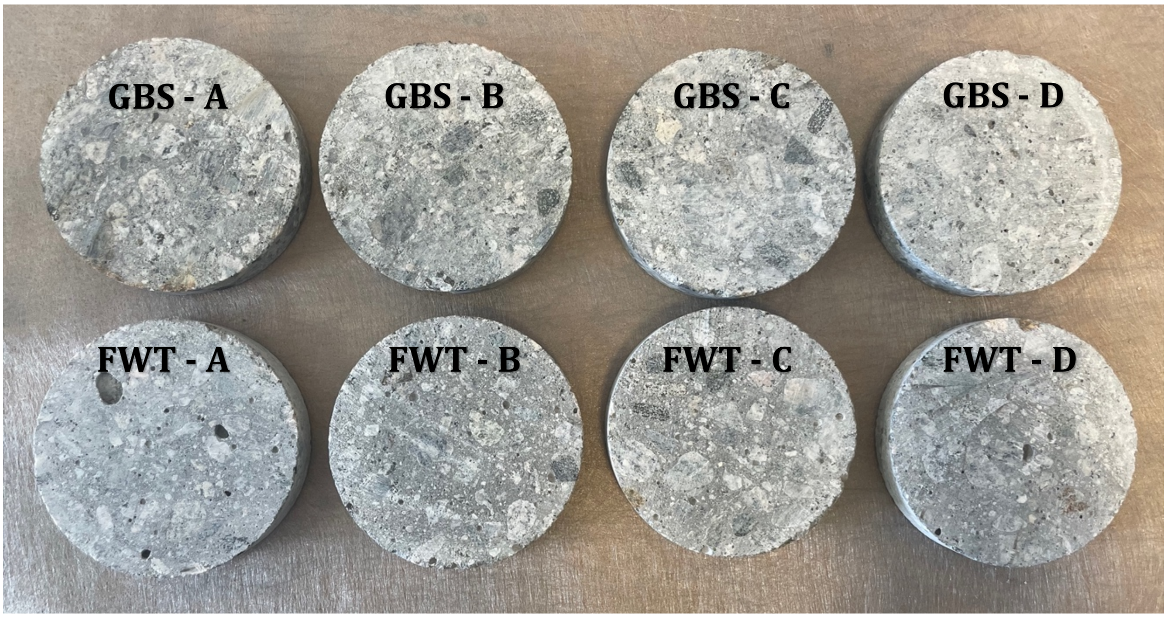

Figure 5-11: Capillary absorption test specimens after drying

Each specimen is placed in a plastic container with screws taped to the bottom, working as a grate as shown in Figure 5-12. The water level in the containers is adjusted to allow approximately a 1 mm rise on the side surface of the specimens. The specimens are positioned on the grid and covered with plastic lids, which are only removed during weighing. Throughout the testing process, the containers are diligently refilled to maintain the water level at 1 mm, ensuring consistent conditions for water absorption by the specimens.

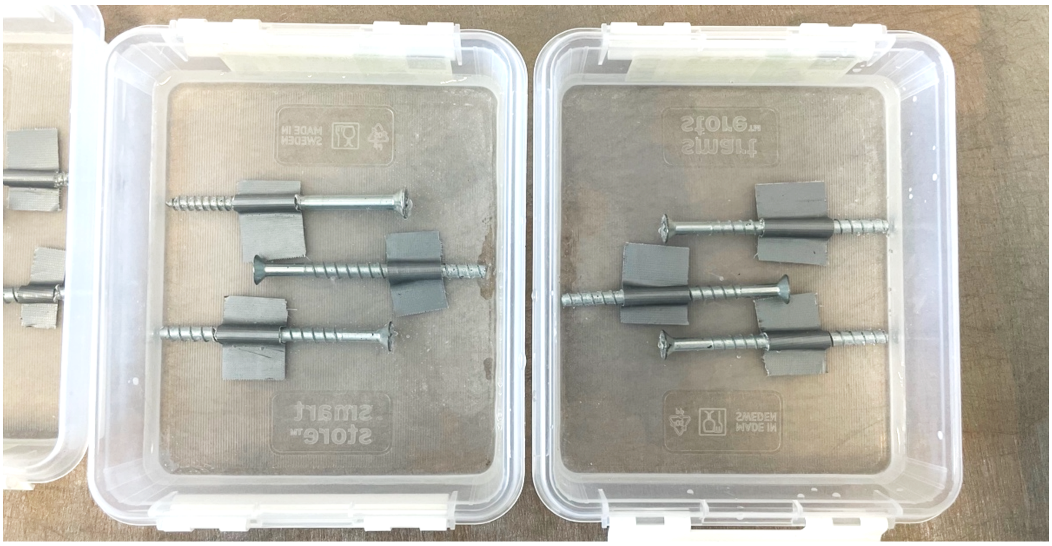

Figure 5-12: Plastic container for capillary absorption tests

The water fully covered the top surface of most specimens within 6 hours to 1 day after the start of the testing. However, for disc A and D of the GBS concrete, complete coverage was achieved between 1 and 2 days. In the regression analysis, the results obtained before and after the water reached the top surface will be treated separately and represented by two intersecting linear curves.

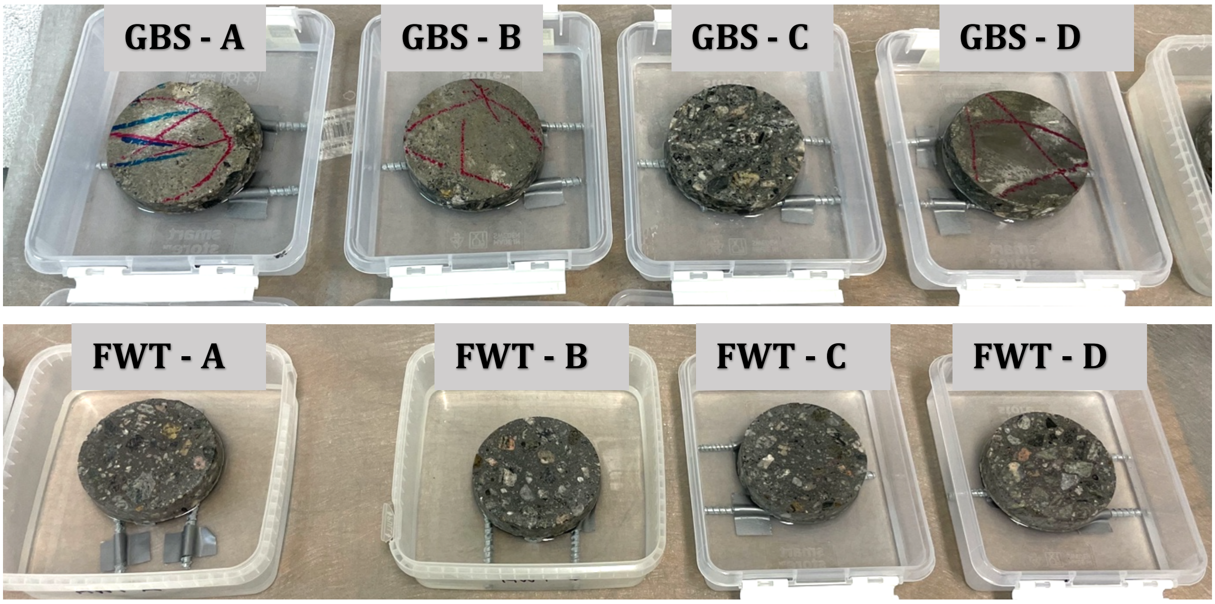

Figure 5-13: Capillary absorption test specimens after 1 day of suction

A stopwatch is used to measure the time at which the specimens should be weighed. The scale used for measuring the weight of the specimens have an accuracy of 0.1g.
Table 5-10 and Table 5-11 below shows the weight measurements registered from the capillary absorption test of the GBS and the FWT specimens.

Table 5-10: Capillary absorption tests: Numerical weight results, GBS

Date	**Time**	**Weight (g) after**	**GBS Test Specimen**			
			A	**B**	**C**	**D**
22.05.2023	13:30	Drying (g_1)	326.8	338.7	346.8	326.6
22.05.2023	13:40	10 min suction	328.1	340.3	348.5	328.7
22.05.2023	14:00	30 min suction	328.8	341.1	349.3	329.8
22.05.2023	14:30	1 hour suction	329.5	341.9	350.0	330.8
22.05.2023	15:30	2 hours suction	330.4	343.1	351.1	332.3
22.05.2023	16:30	3 hours suction	331.1	344.0	352.0	333.4
22.05.2023	17:30	4 hours suction	331.8	344.7	352.8	334.2
22.05.2023	19:30	6 hours suction	332.8	345.9	353.9	335.6
23.05.2023	13:30	1 day suction	337.0	349.6	356.6	339.1
24.05.2023	13:30	2 days suction	337.9	349.9	356.9	339.4
25.05.2023	13:30	3 days suction	337.9	349.9	356.9	339.5
26.05.2023	13:30	4 days suction	337.9	349.9	357.0	339.6
Measurement	**Diameter (mm)**		95.65	95.65	95.45	95.68
	Height (mm)		20.52	20.52	20.82	20.53

Table 5-11: Capillary absorption tests: Numerical weight results, FWT

Date	Time	Weight (g) after	FWT Test specimen			
			A	B	C	D
22.05.2023	13:31	Drying (g_1)	318.5	312.2	316.1	314.5
22.05.2023	13:41	10 min suction	321.2	314.7	318.4	317.0
22.05.2023	14:01	30 min suction	322.9	316.3	319.9	318.5
22.05.2023	14:31	1 hour suction	324.6	317.8	321.5	320.1
22.05.2023	15:31	2 hours suction	327.0	320.2	323.8	322.4
22.05.2023	16:31	3 hours suction	328.8	321.9	325.6	324.2
22.05.2023	17:31	4 hours suction	330.4	323.5	327.1	325.6
22.05.2023	19:31	6 hours suction	332.7	325.7	329.5	327.9
23.05.2023	13:31	1 day suction	334.5	327.4	331.3	329.4
24.05.2023	13:31	2 days suction	334.8	327.7	331.6	329.6
25.05.2023	13:31	3 days suction	334.9	327.8	331.7	329.7
26.05.2023	13:31	4 days suction	334.9	327.8	331.8	329.8
Measurement	**Diameter (mm)**		95.63	95.65	95.64	95.66
	Height (mm)		19.82	19.6	20.03	19.76

6. Results and Discussion

6.1 Tensile Bond Strength Tests

The analysis of the bond strength test results will encompass an evaluation of various factors. Primarily, the focus will be on assessing the effectiveness of different pre-wetting methods. Additionally, the discussion will encompass an examination of the concrete types, repair materials and methods employed, as well as the post treatment procedures.

6.1.1 Compressive and Flexural Strength

Table 6-1 indicates the compressive and flexural strength of the concrete test specimens, 28 days after casting. Compressive strength is measured by NS-EN 12390-3:2019 [17] and flexural strength is measured by NS-EN 12390-5:2019 [18].

It is worth mentioning that the tensile bond strength tests were carried out prior to the full development of the 28-day strength. In particular, the bond strength tests were conducted at the 21-day mark after casting. Furthermore, the casting process of all the specimens in this study was time-consuming, leading to a delay in casting the test specimens for compressive and flexural strength tests. This delay could potentially have resulted in weaker specimens compared to those used for the bond strength tests.

Table 6-1: Compressive and flexural strength of concrete castings after 28 days curing

After 28 days curing	**Compressive strength (MPa)**	**Flexural strength (MPa)**
GBS (w/c = 0.42)	71.5	9.7
FWT (w/c = 0.37)	74.7	10.2

6.1.2 Pre-wetting Method

The evaluation of different pre-wetting methods will primarily focus on the main concrete blocks specifically casted for this thesis, aiming to limit the influence of other factors on the results. These main concrete blocks were stored in a controlled indoor environment at approximately 20°C and covered with plastic. Further, a comparison with the two original concretes casted from cores of existing offshore structures will be executed to evaluate whether the main concrete blocks and the original concrete exhibit the same conclusion.

In the case of the castings repaired using hand application of repair materials, as depicted in Figure 6-1, the effect of pre-wetting appears to be correlated with the type of repair materials employed. When the substrates were pre-wetted 30-60 minutes before repair, achieving the condition of saturated surface-dry concrete as for side B, the highest bond strength was observed for substrates repaired solely with Rep 65 mortar. If we compare side B to side D which were repaired with similar repair mortar but had no pre-wetting, the pre-wetting method demonstrated a 4.89% higher bond strength. However, for substrates that were not pre-wetted, the use of adhesion mortar Rep 05 seemed to yield higher bond strength compared to using Rep 65 mortar alone. When Rep 05 were used in the repair, the pre-wetting method demonstrated a 22.90% lower bond strength compared to no pre-wetting.

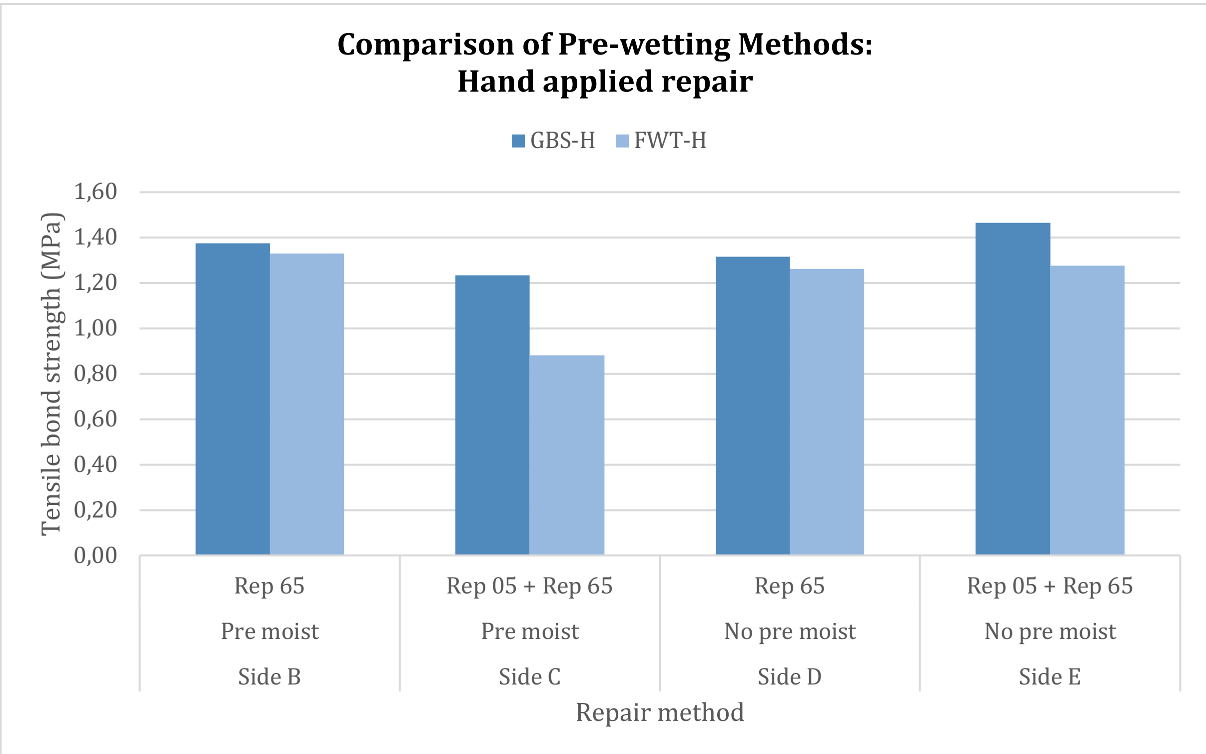

Figure 6-1: Graph presenting bond strength test results from hand applied repair for comparison of pre-wetting methods

While the overall differences in obtained values were not large, on average, the substrates that underwent no pre-wetting and were repaired with both Rep 05 and Rep 65 exhibited the best results during the testing.

When examining the overall impact of pre-wetting methods on the two concrete types repaired by hand application, as shown in Figure 6-2, it is found that pre-wetting the concrete led to an average decrease of 6.25% in bond strength for the GBS type concrete and 12.92% for the FWT type concrete, compared to no pre-wetting. These findings align with the discussions presented in the literature review, suggesting that higher strength concrete absorb less water and are therefore more sensitive to pre-wetting.

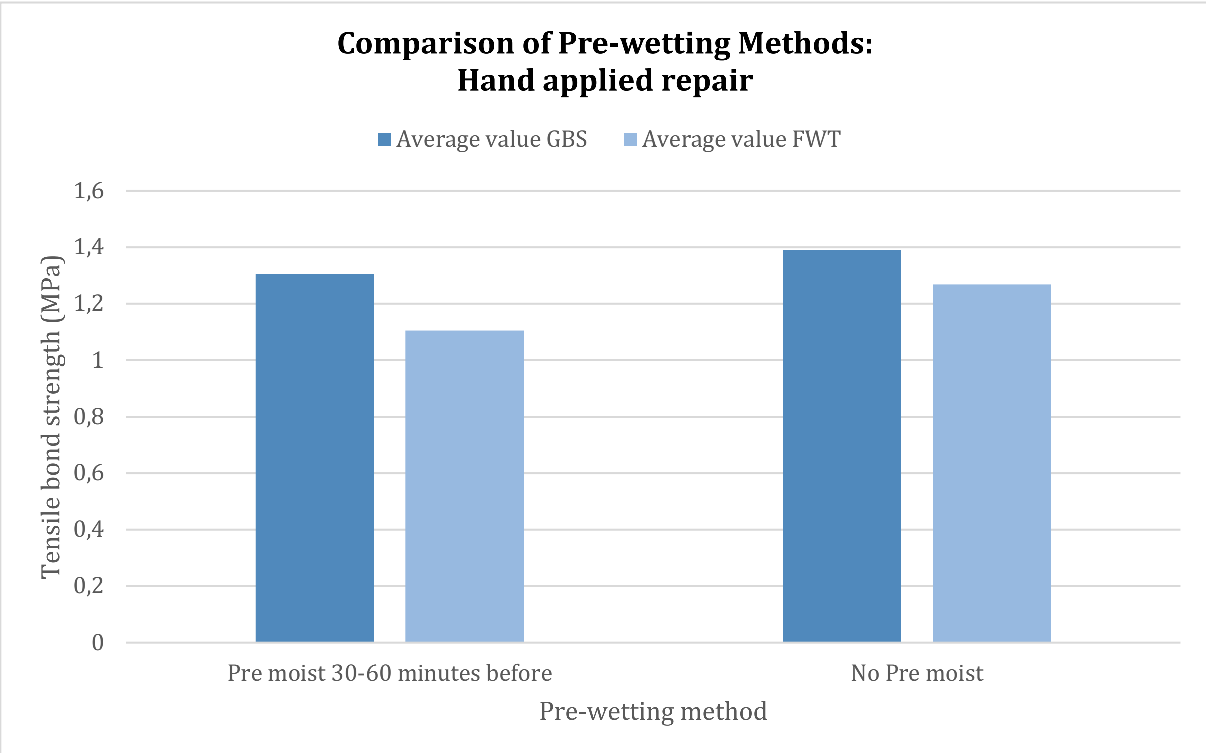

Figure 6-2: Graph presenting average bond strength test results from hand applied repair for comparison of pre-wetting methods

In the case of substrates repaired using the dry shotcrete repair method, different pre-wetting approaches yielded distinct results for the GBS and FWT concrete types, as can be seen in Figure 6-3. For the GBS concrete, the most favorable outcomes were achieved by water jetting the surface one day prior to the repair and pre-wetting the surface 30-

60 minutes before the repair. On the other hand, the FWT concrete exhibited the best results when only water jetting the surface one day before the repair and no pre-wetting on the day of the repair. These findings further align with the theory that higher strength concrete absorb less water and therefore requires less pre-wetting. However, it is evident that the method of no pre-wetting of the substrate resulted in the lowest bond strength for both concrete types. On average the bond strength decreased 38.67% for the GBS concrete and 41.81% for the FWT concrete when subjected to no pre-wetting, which indicates that some form of pre-wetting is necessary before dry shotcrete repair.

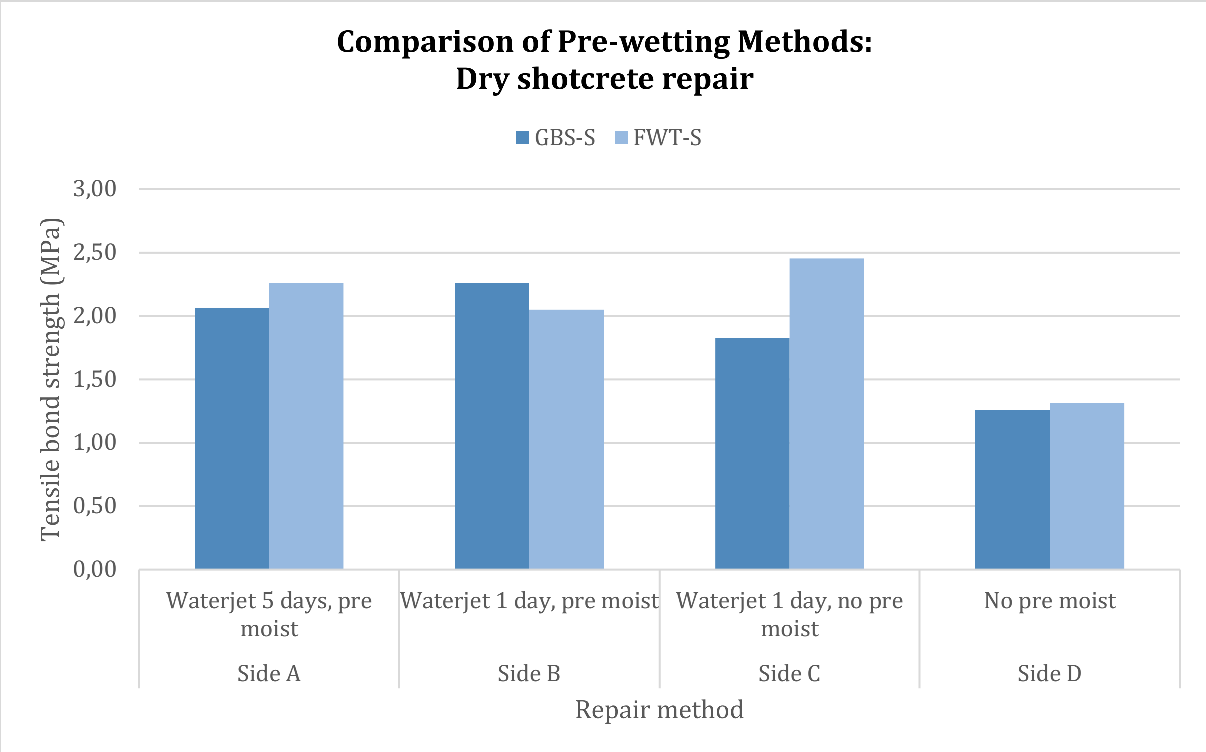

Figure 6-3: Graph presenting average bond strength test results from dry shotcrete repair for comparison of pre-wetting methods

In addition to investigating the main concrete blocks casted for the purpose of this thesis, it is very interesting to see how the cores sampled from real offshore structures react to pre-wetting in comparison to no pre-wetting. It is important to note that the results for the Extra Original B specimen of the FWT concrete were particularly unreliable due to the presence of a dust layer that formed during the application of the repair material. Therefore, it is recommended to exclude this specific value from the overall evaluation of the results. However, a comparison of the GBS concrete with and without pre-wetting is possible. As shown in Figure 6-4, it is clear that water jetting the surface 1 day prior and pre moist of the surface 30-60 minutes before the repair, resulted in the best bond strength. When the specimen was not pre-wetted, the average bond strength decreased 19.28%. The specimens collected from existing offshore structures therefore exhibit the same conclusion as for the main concrete blocks, i.e., that some form of pre-wetting is necessary for the dry shotcrete repair method.

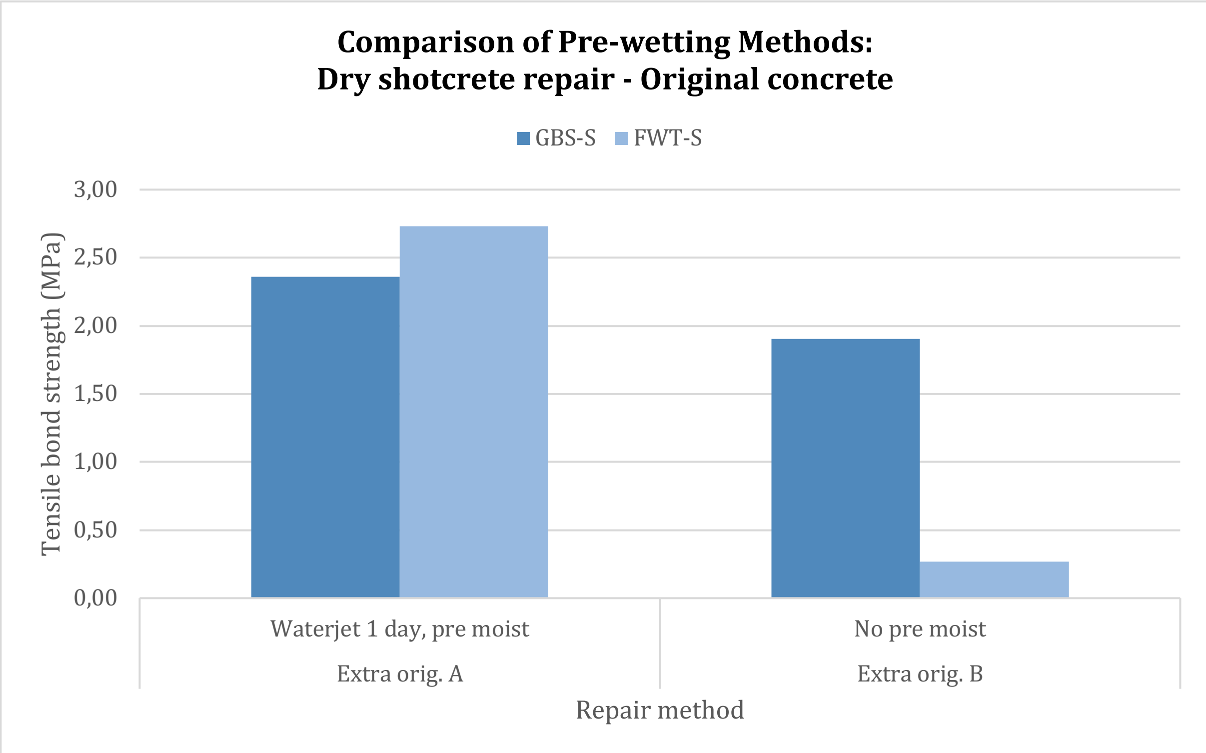

Figure 6-4: Graph presenting average bond strength test results from dry shotcrete repair for comparison of pre-wetting methods on original concrete

6.1.3 Concrete Type: GBS vs. FWT

Based on the analysis of the bond strength results obtained from the hand-applied repair as shown in Figure 6-5, a notable observation can be made. Generally, the GBS type concrete exhibited higher bond strength in comparison to the FWT type concrete. However, there was an exception observed for the repair method conducted on Extra A, which represents the sample stored outside without any subsequent treatment. It is possible that the orientation of the specimens exposed to outdoor conditions influenced their exposure to factors such as wind, rain, and other weather elements, potentially contributing to this anomaly.

On average, the GBS concrete demonstrated a 9.72% higher bond strength compared to the FWT concrete when being repaired by hand applied method. The variation in bond strength ranged from -7% to 40%. These findings suggest that the GBS concrete generally outperformed the FWT concrete in terms of bond strength, although there were certain instances where the FWT concrete exhibited comparable or even higher bond strength values.

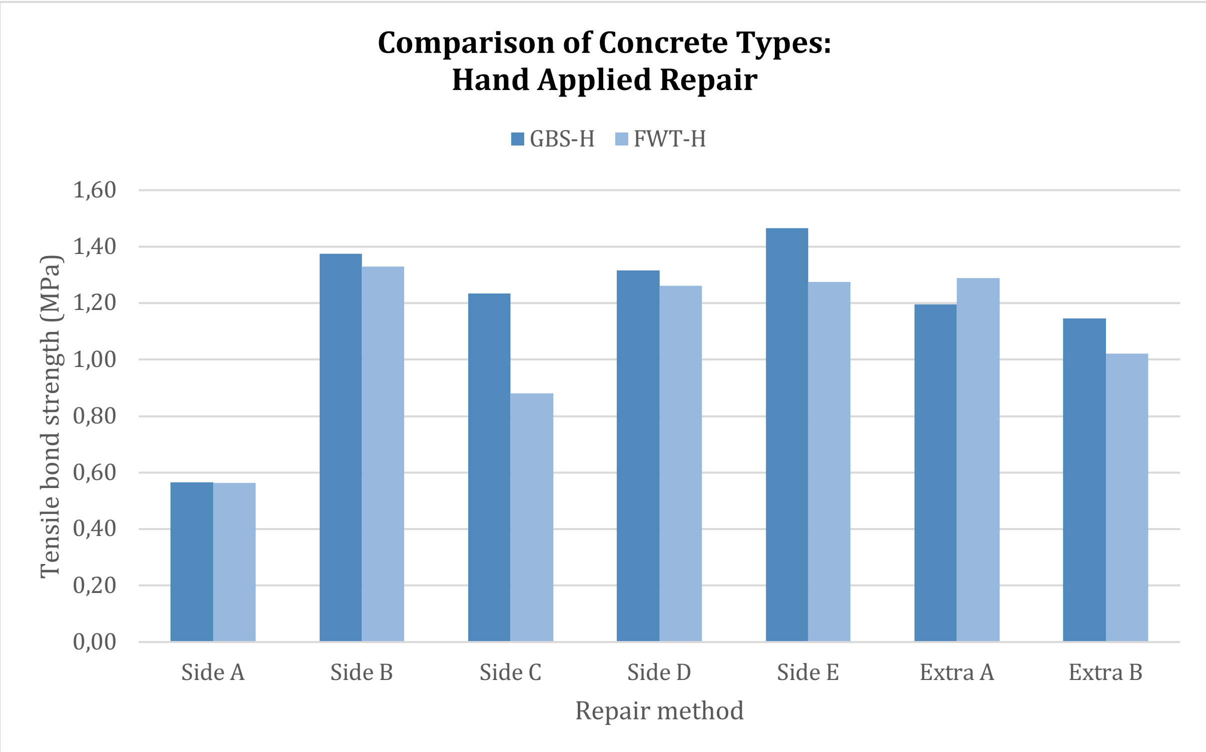

Figure 6-5: Graph presenting average bond strength test result from hand applied repair for comparison of concrete types

The results obtained from the dry shotcrete repair method, shown in Figure 6-6, were not as conclusive. However, out of the nine repair methods evaluated, six of them yielded higher bond strength values for the FWT concrete compared to the GBS concrete. It is also here important to note that the results for the Extra Original B specimen of the FWT concrete were particularly unreliable due to the presence of a dust layer that formed during the application of the repair material. Therefore, it is recommended to exclude this specific value from the overall evaluation of the results. Then it can be found that the GBS concrete demonstrated a 2.11% lower bond strength compared to the FWT concrete when being repaired by dry shotcrete repair.

Upon analyzing the Extra original A specimens sourced from existing offshore concrete structures, a significant enhancement in bond strength values becomes apparent, particularly for the FTW concrete. These specimens underwent the same repair and treatment procedure as side B of the main concrete blocks, involving water jetting one day prior and pre-wetting 30-60 minutes before repair. The observed increase in bond strength is in line with expectations, considering factors such as the substantial difference in the concrete's curing time, post-treatment techniques, and the surface chiseling method employed prior to repair.

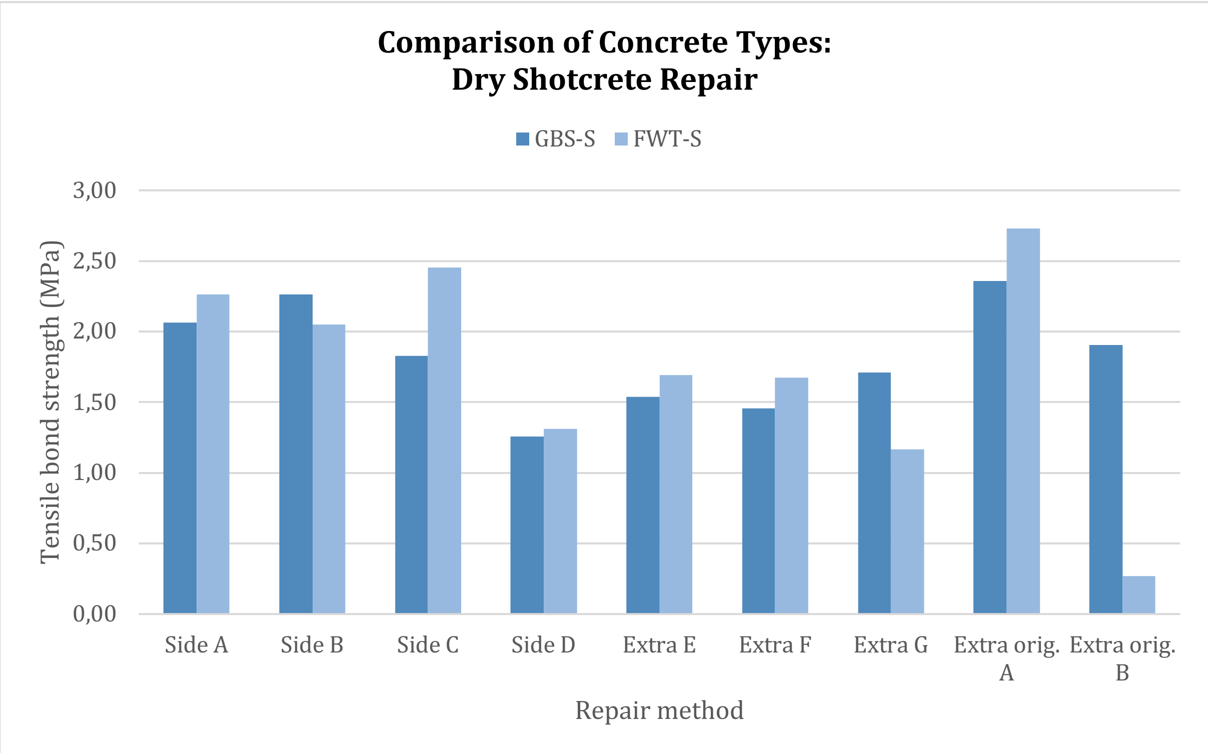

Figure 6-6: Graph presenting average bond strength test results from dry shotcrete repair for comparison of concrete types

6.1.4 Repair Material and Method

Upon calculating the average values for the results obtained from each repair method, a clear trend emerges, as depicted in Figure 6-7. The analysis reveals that the hand applying method in combination with the use of Rep 05 and/or Rep 65 mortar gave bond strength results 39.15% lower compared to the dry shotcrete method in combination with the Sprøyterep T mortar. It is commonly known that the execution of repair by hand application can present challenges with regards to working the mortar sufficiently into the concrete surface. This is assumed to affect the adhesion, and the findings of this study further substantiate this assumption.

As commented in Chapter 6.1.3 the results for the Extra Original B specimen for the dry shotcrete repair of the FWT type were particularly unreliable due to the presence of a dust layer that formed during the application of the repair material, and is therefore also excluded in the evaluation of these results.

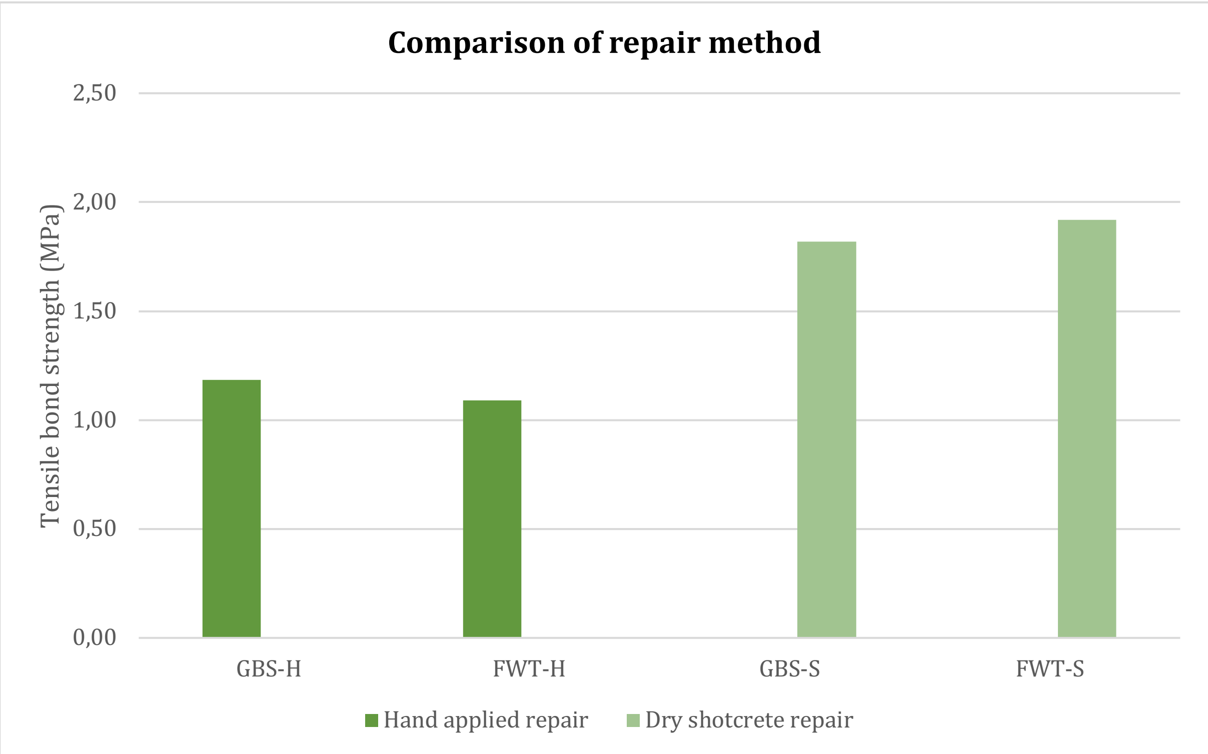

Figure 6-7: Graph presenting average bond strength test results from each repair method

Upon analyzing the various repair methods employed in the hand applying process, a notable observation arises regarding side A. This particular side, which underwent repair by throwing the repair mortar onto a horizontal surface, displayed significantly lower bond strength in comparison to the subsequent methods utilized on the other sides. It is important to note that the decision to employ this approach of throwing the repair mortar onto a horizontal surface was primarily driven by the simultaneous repair of the vertical sides, even though it is not regarded as an optimal method.

As elaborated in Chapter 6.1.2, the influence of the various repair mortars utilized in the hand applying method is contingent upon the pre-wetting method implemented prior to the repair. Consequently, this correlation is thoroughly addressed and examined in that specific chapter.

6.1.5 Post Treatment

As discussed in Chapter 6.1.4, it is evident that side A of the hand applied repair has been significantly impacted by the application method, resulting in noticeably lower values compared to the other results. Consequently, in the context of this analysis, it is appropriate to disregard these values.

Upon evaluation of the specimens repaired through hand application, it was found that the specimens stored indoors at about 20°C covered in plastic exhibited an average bond strength value that is 8.96% higher in comparison to the specimens stored outdoors. Among the two outdoor treatment methods, the application of a curing membrane resulted in the lowest bond strength value, as can be seen in Figure 6-8.

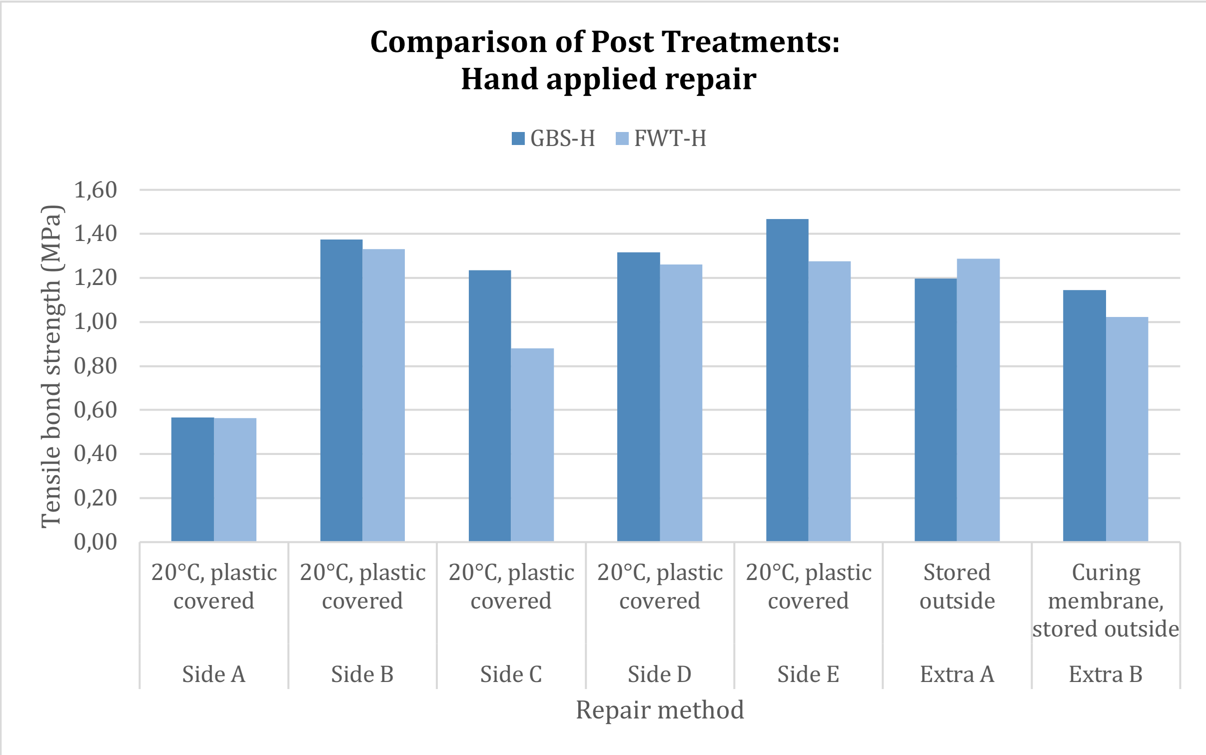

Figure 6-8: Graph presenting average bond strength test results from hand applied repair for comparison of post treatment

Evaluating the specimens repaired through dry shotcrete repair, as presented in Figure 6-9, it is found that the specimens stored indoors at about 20°C covered in plastic exhibited an average bond strength value that is 21.61% higher in comparison to the specimens stored outdoors. Among the two outdoor treatment methods, the application of a curing membrane resulted in the lowest bond strength value for the dry shotcrete application as well.

Side D of the dry shotcrete repair exhibits a significantly lower value compared to the other sides of the main concrete blocks. As discussed in the pre-wetting methods chapter 6.1.2, it was evident that some form of pre-wetting was necessary for the success of the dry shotcrete repair method. Hence, the lower values obtained on Side D could potentially be explained by the absence of pre-wetting on that particular side and may therefore not be a good representation of the specific post treatment. If we choose to neglect the results from side D, the indoors post treatment method resulted in an average bond strength value 35.24% higher compared to the outdoors treatments.

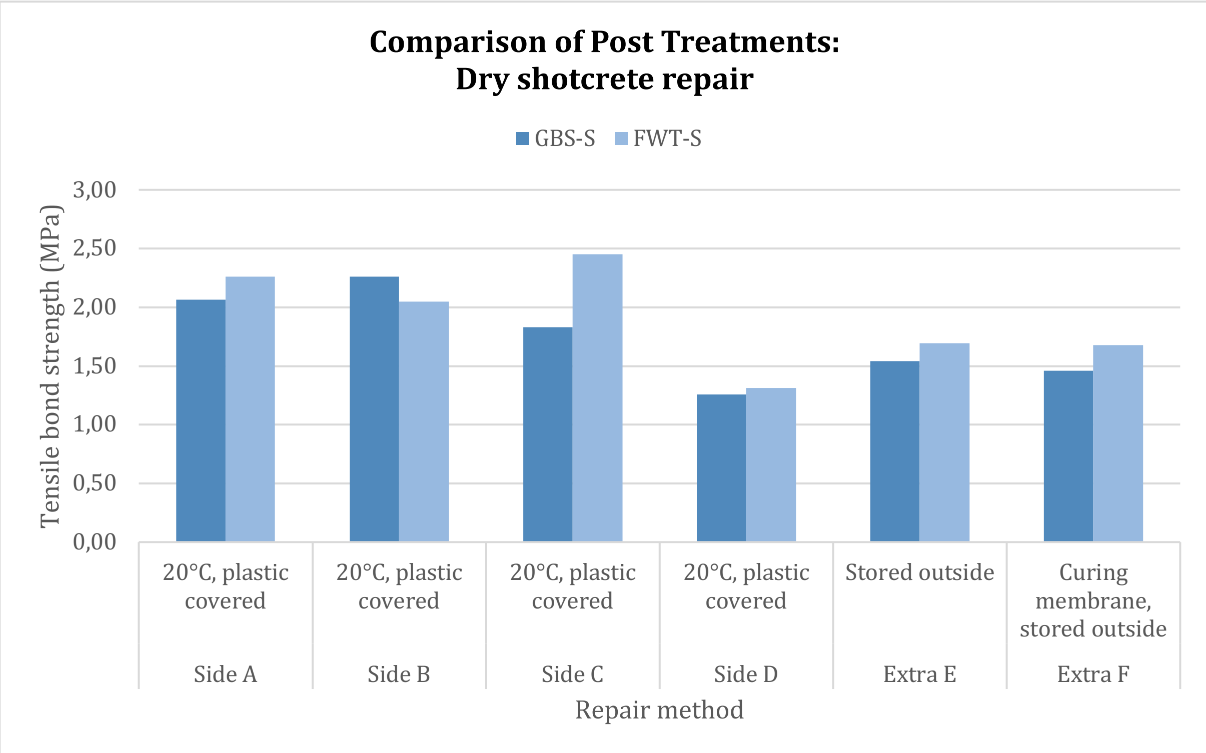

Figure 6-9: Graph presenting average bond strength test results from dry shotcrete repair for comparison of post treatment

The duration of specimen preparation before testing may have influenced the post-treatment of the repairs. It should be noted that during the preparatory work for the bond strength tests, the specimens stored indoors were left uncovered.

6.1.6 Influencing Factors

After analyzing the results from the bond strength tests, several factors need to be considered in validating the analysis.

In general, the obtained tensile bond strength values are lower than anticipated, which can be attributed to multiple factors. Firstly, the specimens used for the tests were specifically cast for the purpose of the thesis and had limited curing time. The concrete and had therefore not developed its full capacity when the tests were executed. Just one day after casting, the surface preparation process had to commence to ensure the feasibility of chiseling using the available equipment. The process of using a chisel machine is quite aggressive, causing the aggregates on the concrete surface to be crushed. This harsh treatment, compared to the gentler hydro blasting process, could potentially lead to a weaker surface for the repair mortar to adhere to. The observation that multiple failure patterns in the bond strength tests occurred at the concrete's top surface provides further support for this theory. Furthermore, the concrete underwent repairs only 7 days after being cast. Following the execution of the repairs, the polishing and drilling process had to commence with only a 7-day curing period for the mortar. The repair material was allowed to cure for a total of 14 days before the bond strength tests were conducted.

Apart from impacting the strength of the concrete, the abbreviated curing time may have also influenced the absorption properties of the concrete in the context of pre-wetting and appliance of the repair mortar. The presence of moisture in the concrete became evident during the chiseling and drilling processes.

As previously mentioned, due to the extensive time spent preparing the concrete for testing, a consequence was that the concrete remained uncovered for several hours throughout the curing period. It is also important to acknowledge that a lot of the work done on the specimens were performed by semi/non-professionals.

6.2 Capillary Absorption Tests

The analysis of the capillary absorption test results will encompass an evaluation of the difference in absorption of the two concrete types GBS and FWT with different water-to-cement ratios and amount of silica fume. The capillarity coefficient, k, and resistance coefficient, m, will be calculated for each of the four discs from the two concrete types. The findings will be analyzed and interpreted in light of the previous literature review conducted in the thesis. Further, the analysis will include a comparison of the test results with the results obtained from the study performed by Sverre Smeplass in 1988 [5], as presented in Chapter 4.3.2.

6.2.1 Comparison between Concrete Types

6.2.1.1 Capillary Absorption Results

Figure 6-10 presents the capillary absorption curves for each disc of the GBS type concrete. As can be seen, both the rate of absorption and total water absorbed varies between the four discs, which is to be expected to some degree due to differences in the composition of aggregates and the natural variation of pores in the specimens.

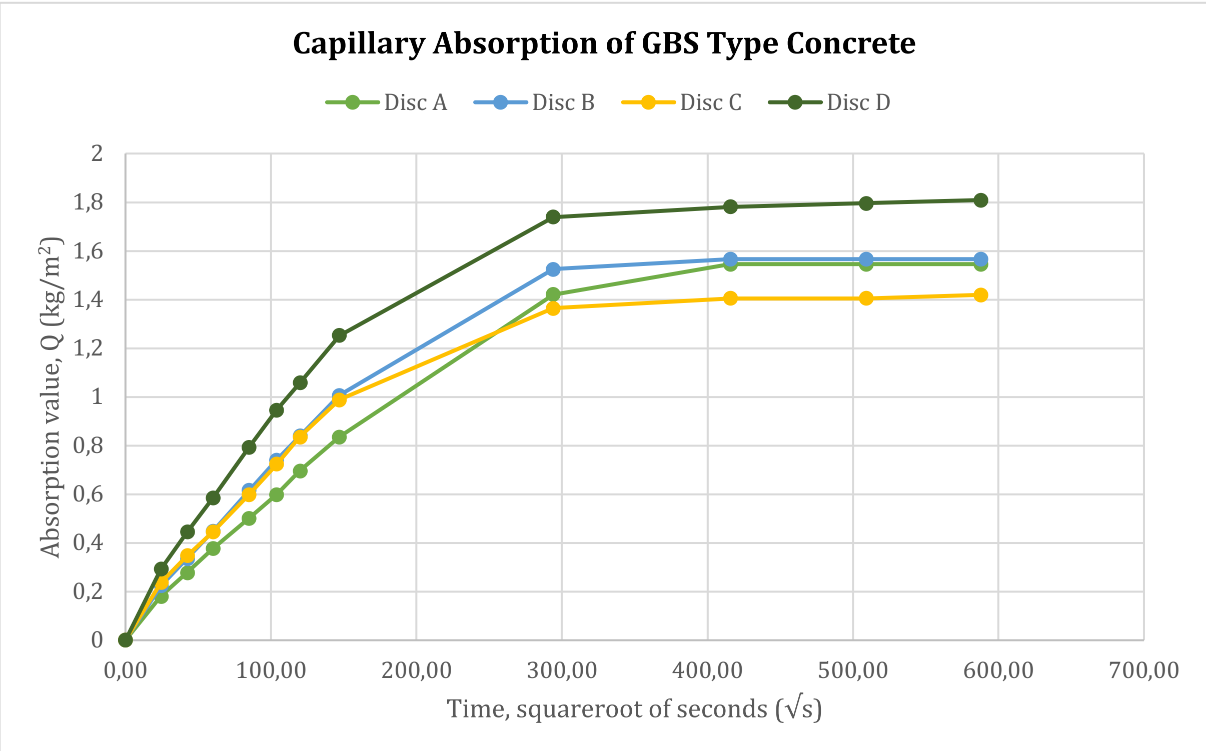

Figure 6-10: Graph presenting the capillary absorption from 4 discs of the GBS type concrete

Figure 6-11 presents the capillary absorption curves for each disc of the FWT type concrete. A variation in the absorption can be observed, however these specimens exhibit less variation compared to the GBS specimens.

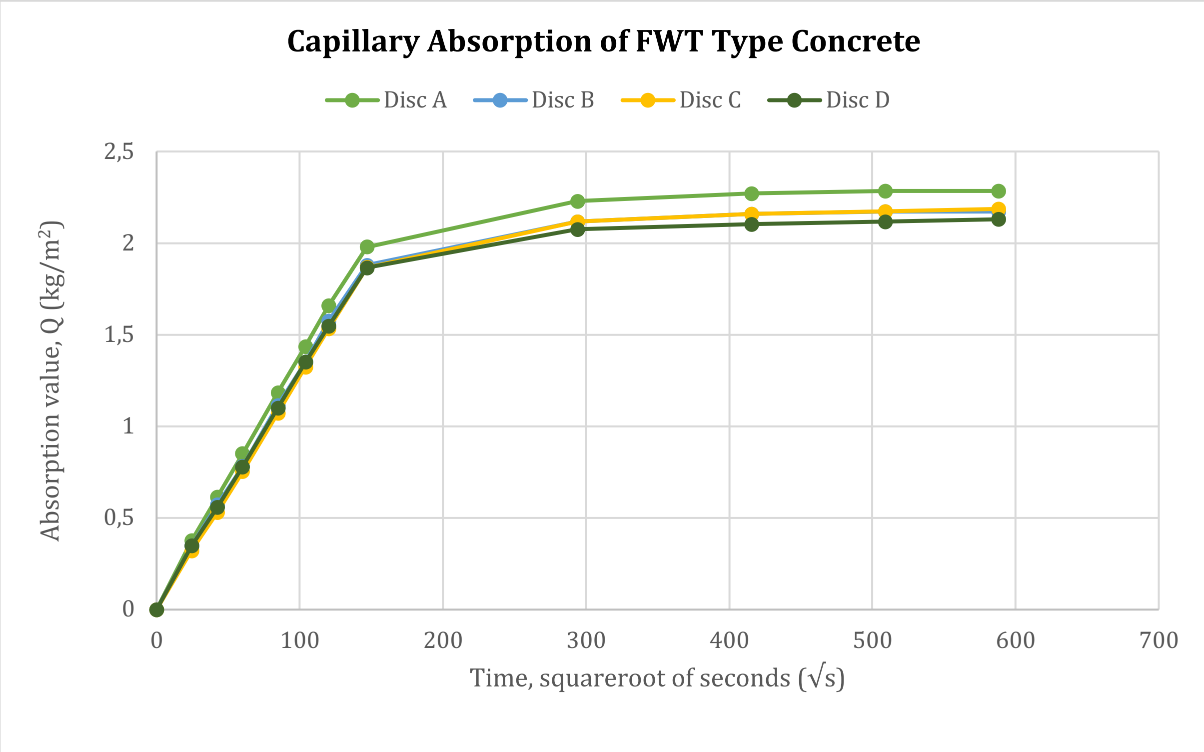

Figure 6-11: Graph presenting the capillary absorption from 4 discs of the FWT type concrete

To ensure a reliable representation of capillary absorption, the average values of each concrete type have been calculated and are presented in Figure 6-12. The middle values will be used for further analysis. On average the GBS specimens, with w/c-ratio equal to 0.43 and 2% silica fume, absorbed a total of 11.38 g water each throughout the absorption time, resulting in an average absorption value, Q, equal to 1.585 kg/m². The FWT specimens, with w/c-ratio equal to 0.35 and 5-8% silica fume, absorbed 15.75 g water on average, resulting in a final absorption value equal to 2.193 kg/m².

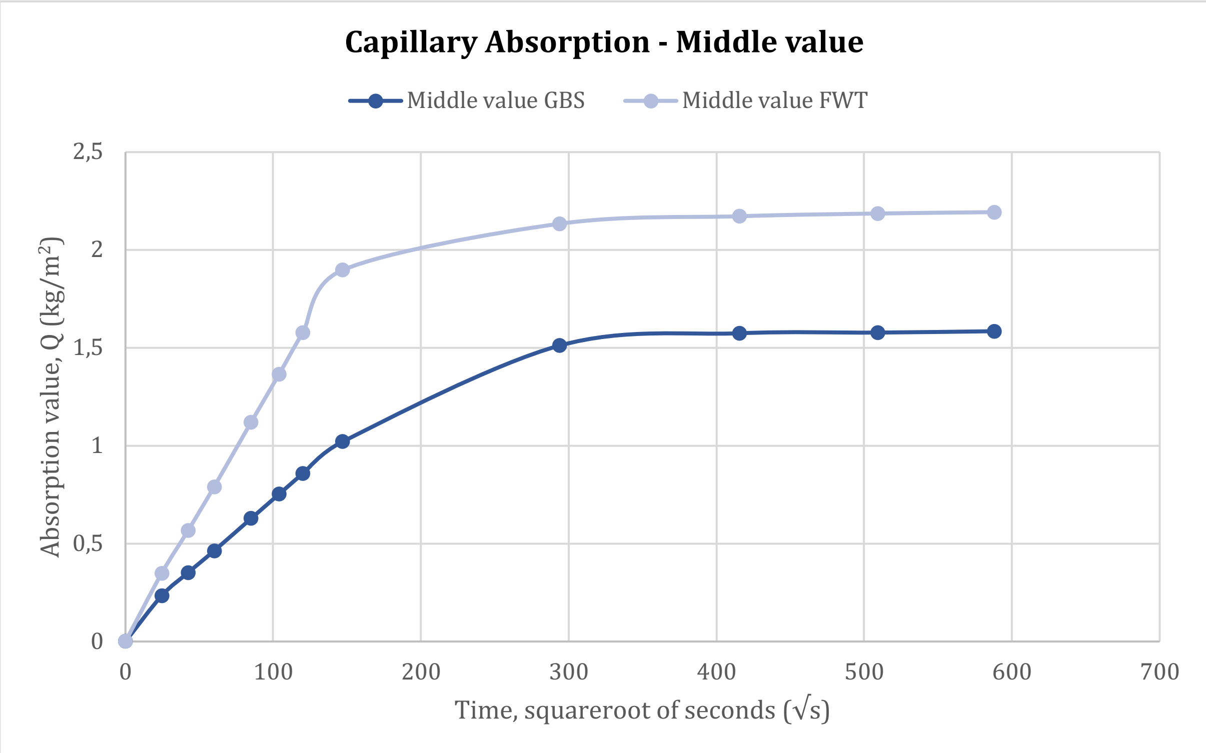

Figure 6-12: Graph presenting the capillary absorption middle value of 4 specimens each from GBS and FWT concrete

The values related to the graphs above can be found in Attachment 8 and Attachment 9. A linear regression analysis of each disc has been executed to obtain the necessary values for the calculations of the capillarity and resistance coefficient. The regression analysis presented both graphical and in tables are given in Attachment 10 to Attachment 25.

Table 6-2 below presents the capillarity coefficient, k, calculated from the obtained results of the capillary absorption test on the concrete type typical for gravity-based structures, GBS, and the concrete type typical for foundations for wind turbines, FWT. The capillarity coefficient from each disc is given in addition to the mean value. From the analysis it can be found that the mean capillarity coefficient for the GBS type concrete equals $0.66 \cdot 10^{-2}\ \mathrm{kg/m^2} \cdot \sqrt{\mathrm{s}}$, while the capillarity coefficient for the FWT type concrete equals $1.31 \cdot 10^{-2}\ \mathrm{kg/m^2} \cdot \sqrt{\mathrm{s}}$. The results indicate that the absorption rate for the GBS type concrete is about 50% lower compared to the FWT type concrete.

Table 6-2: Capillarity coefficient calculated through capillary absorption test of GBS and FWT type concrete

Specimen:	**Capillarity coefficient, k $(\mathrm{kg/m^2} \cdot \sqrt{\mathrm{s}}) \cdot 10^{-2}$**	
	GBS concrete w/c = 0.43 2% Silica fume	**FWT concrete** w/c = 0.35 5-8% Silica fume
Disc A	0.52	1.38
Disc B	0.71	1.30
Disc C	0.70	1.27
Disc D	0.70	1.29
Mean value	0.66	1.31

Table 6-3 below presents the resistance coefficient, m, calculated from the obtained results of the capillary absorption test on the GBS concrete type and the FWT concrete type. The resistance coefficient from each disc is given in addition to the mean value. From the analysis it can be found that the mean resistance coefficient for the GBS type concrete equals $13.15 \cdot 10^{7} (\mathrm{s/m^2})$, while the resistance coefficient for the FWT type concrete equals $6.51 \cdot 10^{7} (\mathrm{s/m^2})$. The results indicate that the resistance for the GBS type concrete is twice as high compared to the FWT type concrete.

Table 6-3: Resistance coefficient calculated through capillary absorption test of GBS and FWT type concrete

Specimen:	**Resistance coefficient, m $(s/m^2) \cdot 10^7$**	
	GBS concrete w/c = 0.43 2% Silica fume	**FWT concrete** w/c = 0.35 5-8% Silica fume
Disc A	22.09	6.42
Disc B	12.16	6.52
Disc C	9.29	6.75
Disc D	9.07	6.33
Mean value	13.15	6.51

Based on the theoretical framework presented in the literature review, these values indicate a contrary interpretation to what was anticipated. The concrete type with higher water-to-cement (w/c) ratio and less silica fume has actually absorbed water at approximately half the rate compared to the concrete with lower w/c-ratio and more silica fume. Moreover, the concrete with the lower w/c-ratio was expected to be denser, less porous, and therefore exhibit greater resistance, but the results suggest the opposite interpretation.

6.2.1.2 Accuracy of The Test Method

The testing procedures are based on an initial drying at 105°C, which according to SINTEF [5] causes some cracking of the concrete. This cracking primarily affects the suction behavior, i.e., the coefficient of resistance and the capillarity coefficient. The advantages of such rapid drying are that a well-defined initial state is achieved in a short time and that the obtained values for suction and microporosity have proven to be valuable for estimating the mass ratio and actual air content in the hardened concrete. The cracking during drying primarily influences the suction behavior (i.e., k and m). More gentle drying (e.g., at 40°C) results in greater density and better represents the performance properties of the concrete. However, a typical problem that arises when attempting to investigate in-situ capillary suction is that when drying at 40 degrees instead of 105 degrees, the water content remains high during testing, often leading to indistinct results. [5]

6.2.1.3 Accuracy of The Computational Model

According Statens Vegvesen's handbook R210 [10], the method as described in Chapter 4.2.2 should be analyzed by a regression analysis. The regression analysis can be used as a criterion for the placement of measurement points. The best configuration typically yields the highest correlation coefficients, and the highest emphasis should be placed on achieving high values of R-squared (R^2) for the steep part of the curve. Measurement points near the intersection point can potentially be excluded. According to Statens Vegvesen, the correlation coefficient from the regression analysis should in general not fall below 0.95 for the steep part of the curve and 0.90 for the horizontal part of the curve. If there are deviations, the calculation of m and k is discarded, and the results are only presented graphically. When determining the intersection point graphically, the quality of the determination of m and k should be evaluated subjectively. [10]

The regression analysis for each phase of each disc of the GBS and FWT concrete types are given in the Attachment 10 to Attachment 25. For all the measurements, the correlation coefficient R^2 of the steep part of the curve (phase 1) were above 0.95. However, for the horizontal part of the curve (phase 2), several specimens gave a correlation coefficient below 0.90. For disc B of the GBS specimens, the R-squared value of the horizontal part of the curve increased from 0.69 to 1.0 when the measurement at 1 day suction was excluded in the regression analysis. This was therefore applied when calculating the capillary and resistance coefficient. However, the regression analysis gave R^2 equal to 0.859 for GBS disc C, 0.861 for FWT disc A and 0.861 for FWT disc B, i.e., the correlation coefficient was below the recommended lower limit, 0.90, which is not ideal. Excluding values close to the intersection point did not improve the analysis.

6.2.2 Comparison with SINTEF Study (1988)

In addition to comparing the two different types of concrete tested for the purpose of this thesis, it is interesting to evaluate the result obtained in comparison to the capillary absorption study conducted by SINTEF in 1988 [5]. The methodology and results from this study has been elaborated in Chapter 4.3.2. The study included several concrete types, varying both with w/c-ratio and amount of silica fume in the concrete composition. The results obtained by SINTEF for the capillarity and resistance coefficients are given in the tables below.

v/c+s	Kapillaritetstall $(kg/m^2 \cdot \sqrt{s}) \cdot 10^{-2}$	
	0 % SiO_2	5 % SiO_2
0,7	2,92	2,33
0,6	2,17	1,89
0,5	1,56	1,16
0,4	1,15	0,89

Figure 6-13: SINTEF study - Measured capillarity coefficient, k, as a function of water/cement ratio and silica dosage. Water stored samples and moisture conditioning at 105°C for 3 days. Average values for 4 test pieces. [5]

v/c+s	Motstandstall $(s/m^2) \cdot 10^7$	
	0 % SiO_2	5 % SiO_2
0,4	10,20	15,80
0,5	6,03	9,84
0,6	4,26	7,03
0,7	3,11	4,56

Figure 6-14: SINTEF study - Measured resistance coefficient, k, as a function of water/cement ratio and silica dosage. Water stored samples and moisture conditioning at 105°C for 3 days. Average values for 4 test pieces. [5]

As previously presented, it was concluded that the resistance coefficient, capillarity coefficient and capillary absorption were unambiguously dependent on the water/cement ratio. As the w/c-ratio decreases, the capillary coefficient decreases, and the resistance increases. The use of silica fume (5% cement replacement) gave changes in resistance coefficient and capillarity coefficient corresponding to the effect of a reduction in the water/cement ratio of 1/10. The determination of resistance coefficient and capillarity coefficient was also particularly sensitive to differences in moisture levels in the test pieces after moisture acclimatization.

When comparing the test results from SINTEF with the findings of this study, clear contradictions arise. These disparities challenge the established beliefs and add an intriguing aspect to the research. Within the scope of this study, a lower capillarity coefficient was observed for the GBS concrete (w/c = 0.43, 2% silica) when compared to the FWT concrete (w/c = 0.35, 5-8% silica), suggesting that concrete with a lower w/c-ratio exhibited a heightened absorption rate. Additionally, the results indicated that the resistance of the lower w/c-ratio concrete was inferior to that of the higher w/c-ratio concrete. These contrasting findings deviate from the outcomes obtained by SINTEF in 1988.

Assuming a linear correlation between the various w/c ratios and the amount of silica fume included in SINTEF's study, we can estimate the expected values for both the GBS and FWT concrete as shown graphically in Figure 6-15 and Figure 6-16. According to SINTEF's results, concrete with 2% silica fume and a w/c ratio of 0.43 should have a capillarity coefficient of approximately $1.15 \cdot 10^{-2}$ kg/m$^2 \cdot \sqrt{s}$. However, the GBS concrete in this study exhibited a capillarity coefficient of $0.66 \cdot 10^{-2}$ kg/m$^2 \cdot \sqrt{s}$, indicating a deviation of 42.3% from the estimation based on SINTEF's results. As SINTEF's investigation only considered w/c ratios down to 0.4, it is less clear how the FWT specimens in this study, with a w/c ratio of 0.35, should be compared. Nevertheless, the study suggests that for w/c ratios below 0.4 and silica fume amounts equal to or above 5%, the capillarity coefficient should be below $0.89 \cdot 10^{-2}$ kg/m$^2 \cdot \sqrt{s}$.

However, the FWT concrete yielded a capillarity coefficient of $1.31 \cdot 10^{-2}\ \mathrm{kg/m^2} \cdot \sqrt{\mathrm{s}}$, indicating a deviation above 47.2% from SINTEF's estimation.

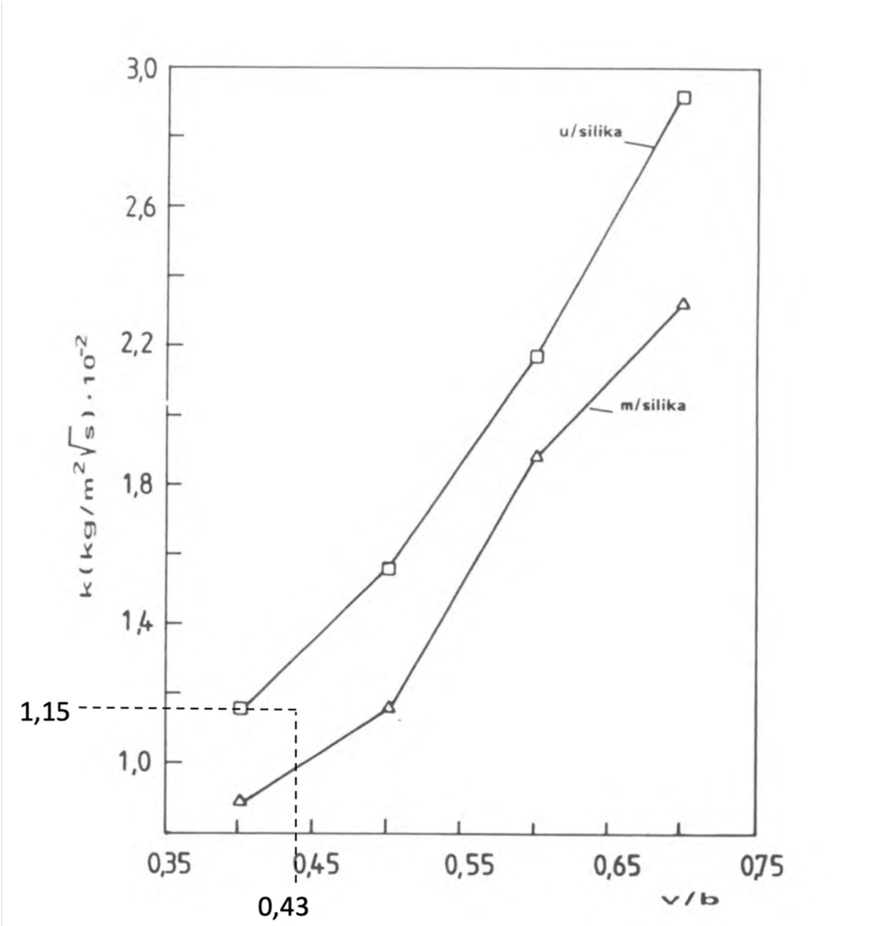

Figure 6-15: Estimation of the capillary coefficient of the GBS concrete based on results from SINTEF study

Further analysis concludes that according to SINTEF's results, the resistance coefficient for concrete containing 2% silica fume and with a water-to-cement (w/c) ratio of 0.43 should be approximately $10.97 \cdot 10^7\ \mathrm{s/m^2}$. The GBS concrete exhibited a resistance coefficient equal to $13.15 \cdot 10^7\ \mathrm{s/m^2}$, which is a deviation of 19,9% from SINTEF's estimation. As for concrete with water-to-cement (w/c) ratio below 0.4 and including 5-8% silica fume, the resistance number is expected to be above $15.8 \cdot 10^7\ \mathrm{s/m^2}$. The test results did however give a resistance coefficient equal to $6.51 \cdot 10^7\ \mathrm{s/m^2}$ for the FWT concrete, exhibiting a deviation above 58.9% from SINTEF's estimation.

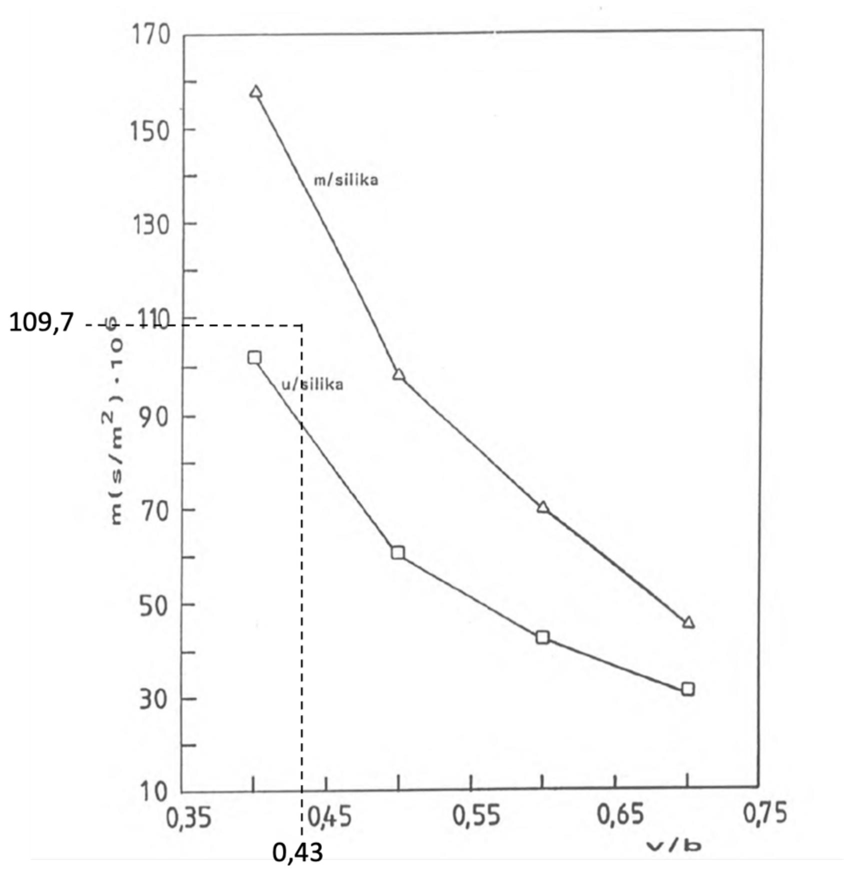

Figure 6-16: Estimation of the resistance coefficient of the GBS concrete based on results from SINTEF study

It should be noted that these results are influenced by numerous factors, and the values obtained by SINTEF are specifically associated with the precise composition of the concrete mix used in the specimens. The values can therefore only give an indication to some extent of what the values should be for the different w/c-ratios and amounts of silica fume. Although we observe deviations, the values obtained for the GBS and FWT concrete align best with the results from the lower w/c-ratios of SINTEF's study, implying that the capillary absorption is lower for high strength concrete on average.

6.2.3 Influencing Factors

As the results obtained by SINTEF indicated the opposite as the results from the tests obtained for the purpose of this thesis, it is important to evaluate the variables.

The test specimens used in the study performed by SINTEF was casted for the purpose of the study, and did therefore have equal curing conditions, treatments and curing time for each of the different water-to-cement ratios. Additionally, the concrete composition was based on the same materials such as cement, sand, aggregates etc. The test specimens used in this study was however collected from existing offshore concrete structures, and did therefore have different curing conditions, treatments and curing time for each of the different water-to-cement ratios. The concrete composition was also not based on the same materials, as the structures were built in different time periods of the concrete industry. When evaluating the results, it is crucial to consider both the differences between the concrete compositions in the two studies and the differences between the two types of concrete tested in this thesis. These factors can significantly impact the outcomes and should be considered for a comprehensive analysis.

7. Conclusion

Prior to presenting the conclusive findings of this study, it is crucial to revisit the primary objective of this thesis. The aim was to examine the impact of the properties of high strength concrete, including the use of silica fume, on the capillary suction and adhesion in concrete rehabilitation. Specifically, the goal was to ascertain whether and how the capillary absorption properties of the concrete should factor into the decision-making process for repairing and rehabilitating the structure, particularly related to pre-wetting, and whether customized criteria should be established accordingly.

7.1 Influencing Factors

It is crucial to emphasize that the conclusions drawn in this thesis are specific to the concrete and methods employed in this study. Further research is needed to arrive at more definitive conclusions on the subject. Below, we summarize the most significant influencing factors in this research study.

First and foremost, it is important to acknowledge the factors that may have influenced the results of the bond strength tests. The obtained tensile bond strength values were found to be lower than anticipated, which can be attributed to several reasons. Firstly, the specimens had limited curing time, which impacted their overall development and strength. The repairs were carried out only 7 days after the casting of the specimens, and the curing period for the mortar was also restricted. The execution of the aggressive chisel method may have weakened the concrete surface, affecting the adhesion of the repair mortar. Furthermore, the concrete specimens were left uncovered for several hours during the curing period, which could have affected the moisture content during curing. It is also important to note that the work performed on the specimens was conducted by semi/non-professionals, and some results were influenced by the presence of dust layers that had formed during the repair process.

Further, the factors which may have affected the capillary absorption results needs to be established. The study encompassed two distinct concrete types with a range of variables, including composition, curing conditions, time, post-treatments, and climate.

It is worth noting that the variables extended beyond just the water-to-cement (w/c) ratio and silica percentage. Regarding the test method, it is important to consider the factors that can influence the results. The concrete specimens were dried at 105 degrees Celsius for 7 days, which may have led to the development of cracks in the concrete. Additionally, it is important to acknowledge that the capillary absorption test method does not provide an in-situ representation of the concrete behavior.

Lastly, it is crucial to identify the factors that influence the assessment of the relationship between the various tests conducted and discussed in this thesis. It is important to acknowledge that the bond strength tests, and capillary tests performed in this study are not conducted on the same concrete specimens. Although the casted concrete in this study is based on the recipe used for the specimens in the capillary absorption tests, there are differences in composition, curing, treatment, and other factors. Further, the evaluation of the relationship between the findings of this study and those of the SINTEF study is affected by the fact that SINTEF's study includes the same variables for all the specimens, with only variations in w/c ratio and silica fume percentage in the presented results.

It is also important to acknowledge that several of the conclusions drawn are based on average values. In certain instances, results have been excluded after careful evaluation of their relevance and accuracy concerning the subject under discussion.

7.2 Summary of Findings

Based on the literature study conducted in the first part of this thesis, it was suggested that high-strength concrete, including silica fume, with a lower water-to-cement (w/c) ratio should theoretically exhibit lower capillary absorption compared to concrete with a higher w/c ratio. This led to the expectation that modern high-strength concrete structures would require less pre-wetting before repair in the context of concrete rehabilitation.

The findings from the bond strength tests revealed that pre-wetting the concrete prior to repair by hand application led to a decrease in average bond strength for both the concrete type based on a Gravity Based Structure (GBS) recipe and the concrete type based on a recipe for Foundations for Wind Turbines (FWT). Notably, the FWT concrete experienced a greater decrease compared to the GBS concrete when comparing with the results from no pre-wetting, indicating that concrete with lower w/c-ratio and higher silica fume percentage absorbs less moisture and at a slower rate, making it more sensitive to pre-wetting.

Similarly, in the dry shotcrete application, it was observed that GBS concrete performed better with more pre-wetting, while FWT concrete performed better with less pre-wetting. However, it was clear that some form of pre-wetting still is necessary for the dry shotcrete method. These results further support the theoretical prediction that concrete with lower w/c-ratio and higher silica fume percentage are more sensitive to pre-wetting. It should be emphasized that the necessity for pre-wetting was influenced not only by the properties of the concrete, but also by various other factors such as the specific repair material and application method utilized.

Furthermore, the capillary absorption tests revealed significant differences between the GBS and FWT concrete types. The GBS concrete exhibited approximately 50% lower absorption rate and twice the resistance compared to the FWT concrete with a lower w/c-ratio and higher silica fume percentage. The findings from this study challenge the established correlation between water-to-cement ratio and capillary absorption in SINTEF's 1988 study, as well as the conclusions drawn from the bond strength tests conducted in this research. It becomes evident that the variables present in existing offshore structures have a significant impact on capillary absorption.

Theoretical demonstrations of the influence of water-to-cement ratio and silica fume on capillary absorption can be observed in experiments conducted under controlled conditions. However, these experiments may not establish a robust foundation for comprehending how structures in real-world environments, with varying w/c ratios and silica fume percentage, will exhibit capillary suction unless the composition, casting and treatment procedures are accurately replicated. The observed differences in this study offer a practical representation of how factors may seem logical in theory and systematic in the laboratory but become more intricate and challenging to evaluate in the field. Numerous influencing factors come into play in real-world scenarios, making it more complex to establish how the capillary absorption properties of the concrete should factor into determining the appropriate approach for repairing and rehabilitating high strength concrete.

7.3 Suggestions for Further Work

While the result from this study provides informative insights on the effect of different repair methods, the contrary results from the capillary absorption tests indicate the need for further research and investigation. It becomes clear that laboratory tests on purpose-made concrete with limited variables, provide a theoretically accurate representation of the material, but does not reflect the conditions and behavior of concrete in real-world field applications. Further research is therefore necessary to determine whether and how the capillary absorption properties of the concrete should factor into the decision-making process for repairing and rehabilitating high strength concrete.

Firstly, performing repairs and conducting bond strength tests on actual offshore concrete structures in the field would provide a more accurate representation of the in-situ effects of pre-wetting methods and other factors during the repair process. Secondly, executing capillary absorption tests on the same exact concrete as used for the bond strength tests would facilitate a more reliable comparison and minimize variables between the tests. Finally, the development of capillary absorption tests for specimens with initial in field moisture levels could help evaluate the relation between capillary absorption and the necessary amount of pre-wetting in existing offshore concrete structures.

Bibliography

[1] SINTEF, "Excon - Grønn forvaltning av konstruksjoner for infrastruktur," March 2023. [Online]. Available: https://www.sintef.no/prosjekter/2023/excon-gronn-forvaltning-av-konstruksjoner-for-infrastruktur/. [Accessed June 2023].

[2] G. Pål , O. Morten and S. Sverre, Grunnleggende betongteknologi, Lillestrøm: Byggenæringens forlag, 2004.

[3] J. Rutle, Cementer: Fremstilling og egenskaper, Betokem AS, 1981.

[4] B. Kristiansen, J. Lindland and T. Østmoen, Betongrehabilitering: metoder og utførelse, Byggenæringens forlag, 1998.

[5] S. Smeplass, "Kapillærabsorpsjon som kvalitetskriterium," SINTEF, Forskningsinstituttet for cement og betong.

[6] I. Holand, Betongplattformer offshore, SINTEF, 1995.

[7] S. Hetland, "Offshore concrete platforms for the Sakhalin II development," in *Structural concrete*, 2009.

[8] SINTEF - Byggforskserien, 572.205 Betong: Typer, egenskaper og bruksområder, 2016.

[9] S. Jacobsen, Betongens permeabilitet: Vurdering av måleprinsipper og metoder, Norges byggforskningsinstitutt, 1996.

[10] Vegdirektoriatet, Håndbok R210: Laboratorieundersøkelser, Statens vegvesen, 2016.

[11] SINTEF - Byggforskserien, 520.031 Kvalitetskontroll og dokumentasjon av herdnet betong: Laboratoriemetoder, 2015.

[12] M. Maage, Betong: Regelverk, teknologi og utførelse, Byggenæringens forlag, 2015.

[13] Carboline AS, "CTSP Episode 195 - Saturated Surface Dry (SSD)," 2021. [Online]. Available: https://www.carboline.com/solution-spot/posts/saturated-surface-dry-ssd/. [Accessed february 2023].

[14] SINTEF, "Materialutvikling høyfast betong," 1992.

[15] Weber Norge, "Weber Saint-Gobain," 2019. [Online]. Available: https://www.weber-norge.no/losninger/betongrehabilitering#dokumentasjon. [Accessed Mai 2023].

[16] NS-EN 1542: Measurement of bond strength by pull-off, Standard Norge.

[17] NS-EN 12390-3:2019: Testing hardened concrete - Part 3: Compressive strength of test specimens, Standard Norge.

[18] NS-EN 12390-5:2019: Testing hardened concrete — Part 5: Flexural strength of test specimens, Standard Norge.

[19] NS-EN 1992-1-1: Eurocode 2 - Design of concrete structures, Standard Norge.

[20] J.-E. Clausen, Bygningsfysikk i praksis, Oslo: Universitetsforlaget, 1983.

[21] Portland Cement Association, "High-Strength Concrete," [Online]. Available: https://www.cement.org/cement-concrete/products/high-strength-concrete. [Accessed February 2023].

Attachments

Literature Study

Kapillærsug

Bestemmelse av kapillær sugehastighet og porøsitet

Prøvenr.:
Prosjekt:

Dato	Kl.	Vekt (g) etter	Prøvestykke merket						
		Tørking (g_1)							
		Start suging							
		10 min suging							
		30 min suging							
		1 time suging							
		2 time suging							
		3 time suging							
		4 time suging							
		6 time suging							
		1 døgn suging							
		2 døgn suging							
		3 døgn suging							
		4 døgn suging g_5							
		Vannmetting (luft) g_2							
		Vannmetting (vann) g_3							
		Trykkmetning (luft) g_4							
Mål	Diameter (mm)								
	Høyde (mm)								

Attachment 1: Form for determination of capillary suction and porosity [10]

4. Prosedyre for håndmørtling

Håndmørtling brukes på små reparasjoner, hvor det er uhensiktsmessig eller tilkomstsmessig vanskelig å ta i bruk sprøytemørtling.

Weber Rep 65 og Rep 05 heftbro blandes ihht blandingsforhold på pakke.

Sårgropa og et område på ca 10cm rundt sårgrop rengjøres for smuss og støv. Gjerne ved uht-utstyr om dette er tilgjengelig. Ved eksponert stål; rubbing med uht eller sandblåsing for å fjerne korrosjon. *Ved sandblåsing skal det rengjøres med vann eller trykkluft.*

- Påfør Rep 05 heftbro på armering, dersom man ikke går videre med reparasjon umiddelbart.
- Sårgropen forfuktes, og skal være svakt sugende før påføring av Rep 05. Det skal ikke være fritt vann på overflaten før påføring. påføres i tykkelse ca. 1-2 mm.
- Rep 05 heftbro påføres hele sårgropa, inkludert ca 10cm rundtom, og skal dekke godt, også på baksiden av armeringen dersom frilagt.
- Rep 65 reparasjonsmørtel påføres når weber rep 05 heftbro har stivnet noe, men ikke tørket.
- 50mm tykkelse er maks når man skal bygge i et sår. Det er bedre om vi bygger mindre på vertikale flater for å unngå at reparasjonen begynner å slippe. Fortsett å bygge opp sårgropen når det første laget er stivt nok.
- Som sluttfinish, når mørtelen har begynt å stivne, bør reparasjonen pusses over med et filsebrett, slik vi etterlater en estetisk fin ru og jevn overflate.
- Påfør Mapecure umiddelbart på reparasjon med egnet sprøyte eller kost, og kombiner med ettervanning der hvor det lar seg gjøre etter at reparasjonen har tørket nok til å hindre utvasking.

Hvis overdekningen til armering er mindre enn 60 mm kommer følgende i tillegg:

Området 5-10 cm rundt reparasjon sandblåses.

Sandblåst område samt reparert overflate primes med Mapepoxy LR og forsegles med 1 tykt lag Mapecoat CFS ihht generell prosedyre for overflatebehandling.

Ved forberedelse av KB installasjon gjelder følgende:

Hvis overdekningen til armering er mindre enn 20 mm må det sikres at det ikke forekommer kortslutning. Enten ved å kappe armering, eller blinde av. Det er også mulig å bygge overdekning i noen tilfeller.

Attachment 2: Procedure for hand mortar by RaKon

5. Prosedyre for sprøytemørtling

Ved sprøytmørtling kreves det erfaring og kompetanse for riktig utførelse. Dette er et håndverk, som skal utføres av faste ansatte i RaKon AS. Dette med grunnlag i kvalitetssikring og erfaringsbygging internt.

- Sprøytemørtling skal ikke foretas i vind på grunn av faren for separering av tørrstoff og vann. Vindforholdet må evalueres på sted ved sprøyting.
- Før sprøytemørtling, skal underlaget rengjøres og være fritt for støv, sementslam, olje, fritt vann etc. Det skal alltid rubbes med UHT om mulig 10-15cm utenfor skadeområde for å sikre optimal heft. Om det ikke er mulig å bruke UHT kan man sandblåse, dette gir ikke like god heft, og er ikke foretrukket metode. Sandblåst overflate skal rengjøres grundig med trykkluft eller vann.
- Ved usikre værforhold kan underlaget forvannes godt i min. 30 min før sprøytemørtling igangsettes. Dersom man har gode værforhold utover dagen skal sårgropen forvannes i ca 2 timer. Større områder som skal mørtles skal forvannes minst 1 døgn før sprøytemørtling. Dersom skaden er vannmeislet innenfor 5 dager – trenger overflaten kun lett forvanning – da betongen allerede er mettet med vann.
- Ved oppstart av sprøyting, skal det alltid sprøytes på plate eller ved siden av sårgrop inntil det visuelt kan kontrolleres at vanndoseringen er riktig. Når ønsket mengde er oppnådd, skru av mørteltilførsel og vask området rundt godt.
- Ved oppstart skal hele såret sprøytes med noe bløtere masse for at ikke støv og prell skal legge seg på flaten og redusere heften.
- Sprøytemørtelen skal være velkomprimert og uten lagdeling, sandlommer eller porøse partier. Om man får varierende mix ut av munnstykket, skal man stoppe opp og sjekke om vannringen i munnstykket er tett/gå over Reed.
- Ujevnheter skal skrapes ned etter hvert for å hindre at de forplanter seg til overflaten. Sårene skal sprøytes ca 1 cm tykkere enn tilsiktet avtrekkingsnivå.
- Ferdig sprøytet overflate skjæres av forsiktig med murersverd. Det får ikke tilføres rørelser i sprøytemørtelen, da er det stor risiko for at en lager bom. Overflatestrukturen skal være tilnærmet lik omkringliggende betongoverflater. I overganger mellom reparasjoner og reparasjoner og eksisterende betong, skal det ikke være sprang eller lepper inn på eksisterende betong utenfor utmeislet sår.
- Prelltap og løse partikler fra sprøytemørtelen ut på tilgrensende flater skal vaskes/fjernes mens mørtelen ennå er fersk. Her må man passe på å ikke vende munnstykke mot reparasjoner slik at man vasker ut mørtelen.

Hvis overdekningen til armering er mindre enn 60 mm kommer følgende i tillegg:

Området 5-10 cm rundt reparasjon sandblåses.

Sandblåst område samt reparert overflate primes med Mapepoxy LR og forsegles med 1 tykt lag Mapecoat CFS ihht generell prosedyre for overflatebehandling.

Ved forberedelse av KB installasjon gjelder følgende:

Hvis overdekningen til armering er mindre enn 20 mm må det sikres at det ikke forekommer kortslutning. Enten ved å kappe armering, eller blinde av. Det er også mulig å bygge overdekning i noen tilfeller

Attachment 3: Procedure for spray mortar by RaKon

Bond strength tests

GBS - H:	Picture documentation of bond strength test	Failure pattern
Side A	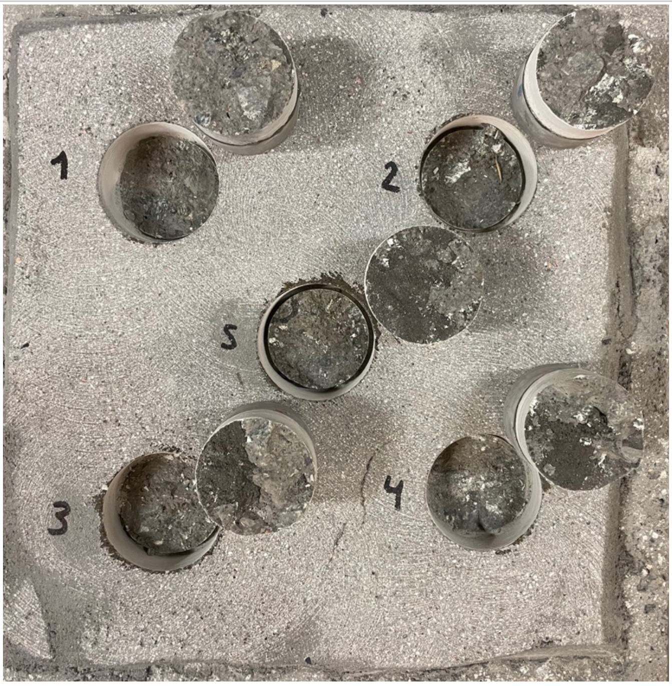	**1:** 100% cohesion failure in the concrete substrate (A).
		2: 80% cohesion failure in the concrete substrate. (A), 7% crushed aggregate: possible crushing of aggregate during chiseling (A), 13% cohesion failure in the mortar (B).
		3: 60% cohesion failure in the concrete substrate (A), 40% adhesion failure between the substrate and the mortar (A/B).
		4: 40% cohesion failure in the concrete substrate (A), 60% adhesion failure between the substrate and the mortar (A/B).
		5: 25% cohesion failure in the concrete substrate (A), 75% adhesion failure between the substrate and the mortar (A/B).
Side B	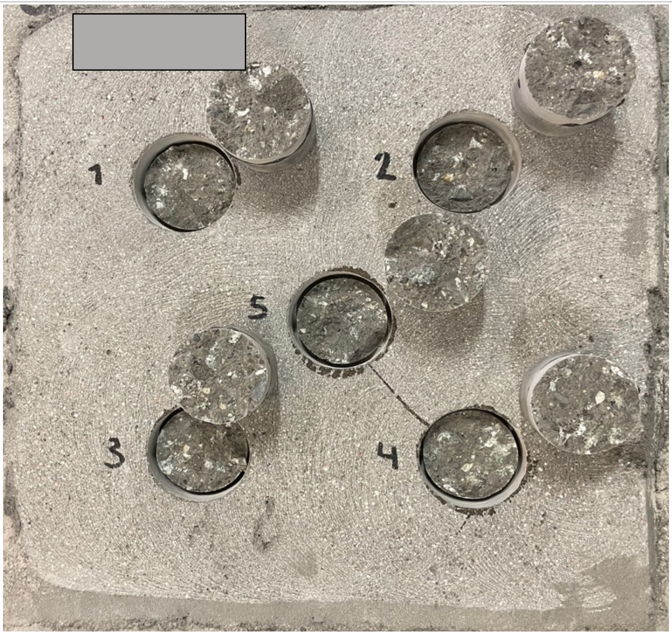	**1:** 90% adhesion failure between the substrate and the mortar (A/B), 10% cohesion failure in the concrete substrate (A).
		2: 15% cohesion failure in the top of concrete substrate (A), 85% adhesion failure between the substrate and the mortar (A/B).
		3: 15% cohesion failure in the top of concrete substrate (A), 85% adhesion failure between the substrate and the mortar (A/B).

		4: 20% cohesion failure in the concrete substrate (A), 80% cohesion failure in the mortar (B).
		5: 20% cohesion failure in the concrete substrate (A), 80% cohesion failure in the mortar (B).
Side C	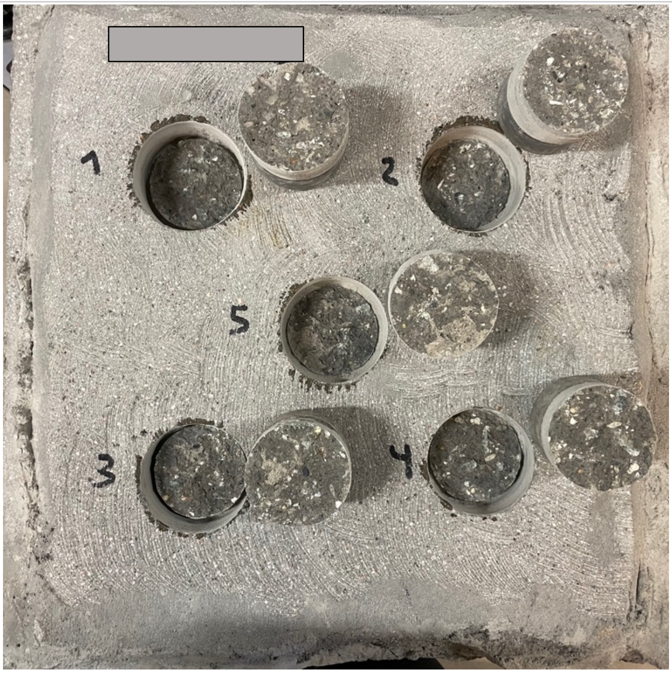	**1:** 95% adhesion failure between the substrate and the mortar (A/B), 5% cohesion failure in the mortar (B).
		2: 95% cohesion failure in the concrete substrate (A), 5% cohesion failure in the mortar (B).
		3: 95% cohesion failure in the concrete substrate (A), 5% cohesion failure in the mortar (B).
		4: 95% cohesion failure in the concrete substrate (A), 5% cohesion failure in the mortar (B).
		5: 97% adhesion failure between the substrate and the mortar (A/B), 25% cohesion failure in the mortar (B).

Side D		**1:** 95% cohesion failure in the concrete substrate (A), 5% cohesion failure in the mortar (B).
		2: 65% cohesion failure in the concrete substrate (A), 35% cohesion failure in the mortar (B).
		3: 65% cohesion failure in the concrete substrate (A), 35% cohesion failure in the mortar (B).
		4: 90% cohesion failure in the concrete substrate (A), 10% cohesion failure in the mortar (B).
		5: 90% cohesion failure in the concrete substrate (A), 10% cohesion failure in the mortar (B).
Side E	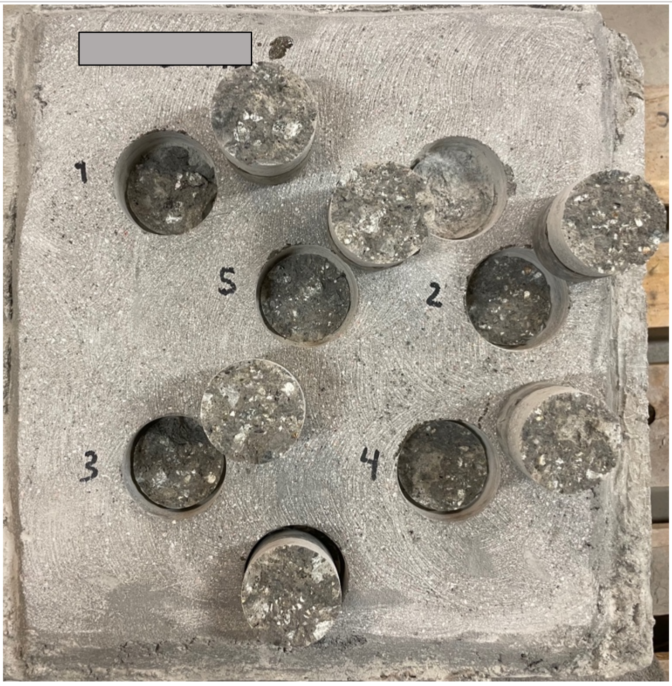	**1:** 60% cohesion failure in the concrete substrate (A), 40% cohesion failure in the mortar (B).
		2: 50% cohesion failure in the concrete substrate (A), 50% cohesion failure in the mortar (B).
		3: 50% cohesion failure in the concrete substrate (A), 50% cohesion failure in the mortar (B).
		4: 50% cohesion failure in the concrete substrate (A), 50% cohesion failure in the mortar (B).
		5: 50% cohesion failure in the concrete substrate (A), 50% cohesion failure in the mortar (B).

Extra A	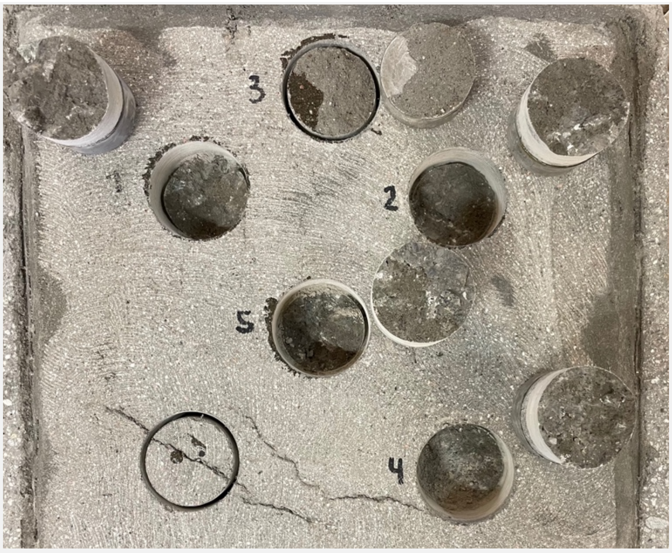	**1:** 35% adhesion failure between the substrate and the mortar (A/B), 65% cohesion failure in the mortar (B). **2:** 25% adhesion failure between the substrate and the mortar (A/B), 75% cohesion failure in the mortar (B). **3:** 75% cohesion failure in the mortar (B), 25% adhesion failure between the adhesive layer and the dolly (Y/Z). **4:** 40% adhesion failure between the substrate and the mortar (A/B), 60% cohesion failure in the mortar (B). **5:** 35% adhesion failure between the substrate and the mortar (A/B), 65% cohesion failure in the mortar (B).
Extra B		**1:** 5% cohesion failure in the concrete substrate (A), 95% adhesion failure between the substrate and the mortar (A/B). **2:** 10% cohesion failure in the concrete substrate (A), 90% adhesion failure between the substrate and the mortar (A/B). **3:** 10% cohesion failure in the concrete substrate (A), 90% adhesion failure between the substrate and the mortar (A/B). **4:** 10% cohesion failure in the concrete substrate (A), 30% adhesion failure between the substrate and the mortar (A/B), 60% cohesion failure in the mortar (B).

		5: 15% cohesion failure in the concrete substrate (A), 50% adhesion failure between the substrate and the mortar (A/B), 40% cohesion failure in the mortar (B).

Attachment 4: Picture documentation and description of failure pattern from bond strength tests on hand applied repair of GBS concrete

FWT - H:	Picture documentation of bond strength test	Failure pattern
Side A	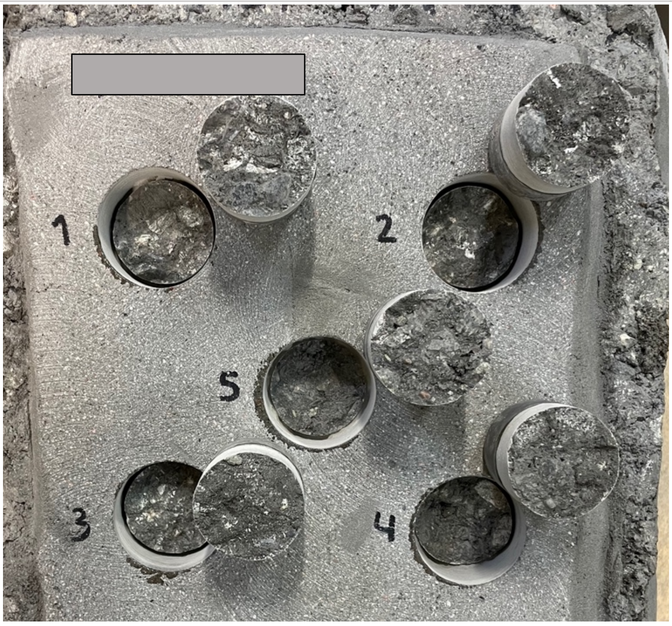	**1:** 90% cohesion failure in the concrete substrate (A), 10% cohesion failure in the mortar (B).
		2: 15% cohesion failure in the concrete substrate (A), 85% cohesion failure in the mortar (B).
		3: 5% cohesion failure in the concrete substrate (A), 95% cohesion failure in the mortar (B).
		4: 50% cohesion failure in the concrete substrate (A), 50% cohesion failure in the mortar (B).
		5: 95% cohesion failure in the concrete substrate (A), 5% cohesion failure in the mortar (B).
Side B	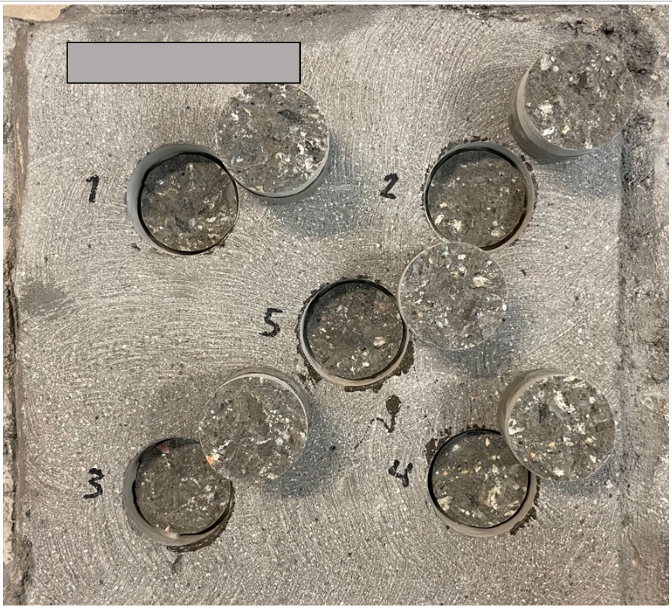	**1:** 40% cohesion failure in the concrete substrate (A), 40% adhesion failure between the substrate and the mortar (A/B), 20% cohesion failure in the mortar (B).
		2: 35% cohesion failure in the concrete substrate (A), 5% adhesion failure between the substrate and the mortar (A/B), 60% cohesion failure in the mortar (B).
		3: 20% cohesion failure in the concrete substrate (A), 15% adhesion failure between the substrate and the mortar (A/B), 65% cohesion failure in the mortar (B).
		4: 30% cohesion failure in the concrete substrate (A), 15% adhesion failure between the substrate and the mortar (A/B), 55%

		cohesion failure in the mortar (B).
		5: 30% cohesion failure in the concrete substrate (A), 15% adhesion failure between the substrate and the mortar (A/B), 55% cohesion failure in the mortar (B).
Side C	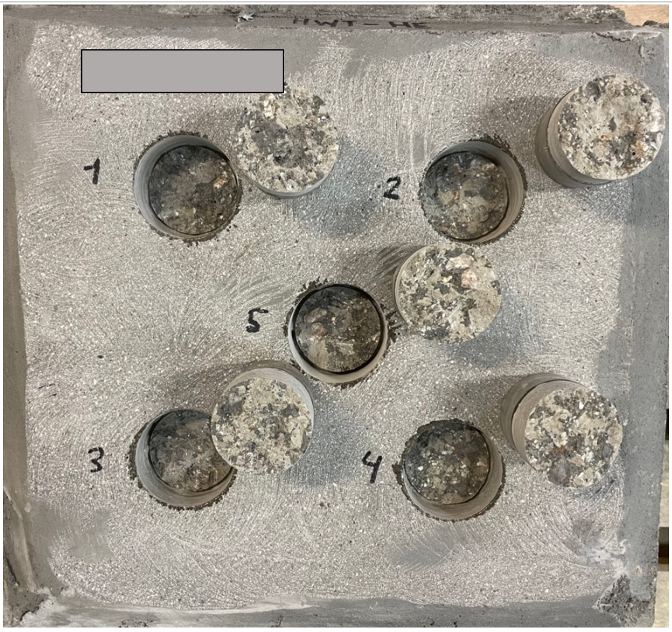	**1:** 40% cohesion failure in the concrete substrate (A), 60% cohesion failure in the mortar (B).
		2: 20% cohesion failure in the concrete substrate (A), 80% cohesion failure in the mortar (B).
		3: 35% cohesion failure in the concrete substrate (A), 65% cohesion failure in the mortar (B).
		4: 45% cohesion failure in the concrete substrate (A), 55% cohesion failure in the mortar (B).
		5: 20% cohesion failure in the concrete substrate (A), 80% cohesion failure in the mortar (B).
Side D	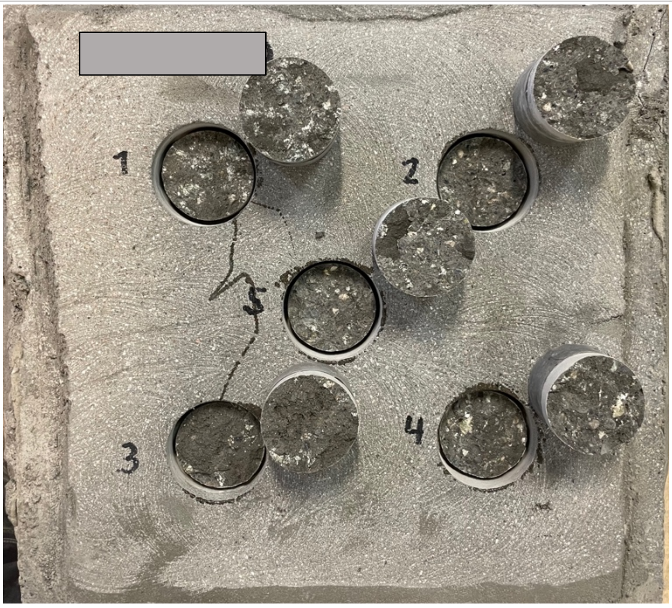	**1:** 65% cohesion failure in the concrete substrate (A), 35% cohesion failure in the mortar (B).
		2: 80% cohesion failure in the concrete substrate (A), 20% cohesion failure in the mortar (B).
		3: 10% cohesion failure in the concrete substrate (A), 90% cohesion failure in the mortar (B). Brushed in repair mortar has dried too quick.
		4: 97% cohesion failure in the concrete substrate (A), 3% cohesion failure in the mortar (B).

		5: 85% cohesion failure in the concrete substrate (A), 15% cohesion failure in the mortar (B).
Side E	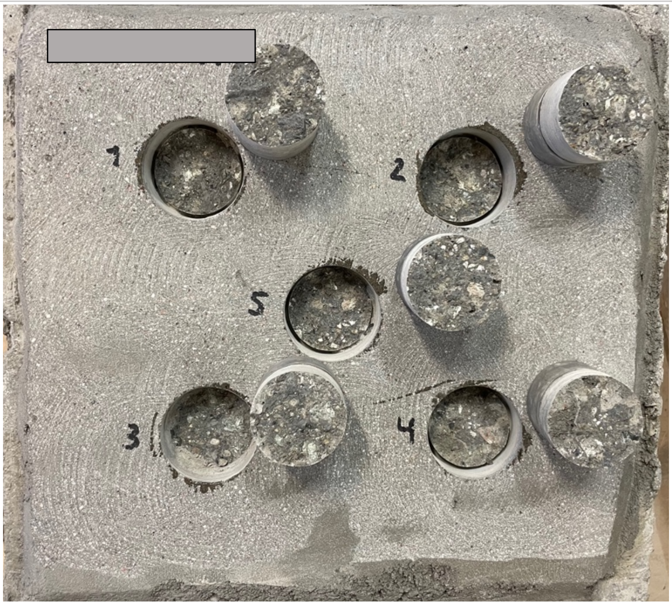	**1:** 50% cohesion failure in the concrete substrate (A), 50% cohesion failure in the mortar (B).
		2: 30% cohesion failure in the concrete substrate (A), 70% cohesion failure in the mortar (B).
		3: 50% cohesion failure in the concrete substrate (A), 50% cohesion failure in the mortar (B).
		4: 40% cohesion failure in the concrete substrate (A), 60% cohesion failure in the mortar (B).
		5: 25% cohesion failure in the concrete substrate (A), 75% cohesion failure in the mortar (B).
Extra A	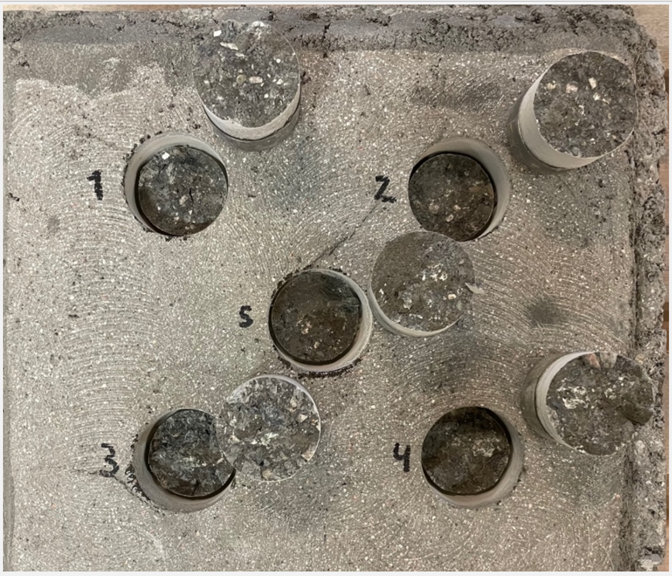	**1:** 80% cohesion failure in the concrete substrate (A), 20% cohesion failure in the mortar (B).
		2: 80% cohesion failure in the concrete substrate (A), 20% adhesion failure between the substrate and the mortar (A/B).
		3: 90% cohesion failure in the concrete substrate (A), 10% adhesion failure between the substrate and the mortar (A/B).
		4: 65% cohesion failure in the concrete substrate (A), 35% adhesion failure between the substrate and the mortar (A/B).
		5: 50% cohesion failure in the concrete substrate (A), 50% adhesion failure between the substrate and the mortar (A/B).

Extra B		**1:** 40% cohesion failure in the concrete substrate (A), 60% cohesion failure in the mortar (B). **2:** 40% cohesion failure in the concrete substrate (A), 60% cohesion failure in the mortar (B). **3:** 75% cohesion failure in the concrete substrate (A), 25% cohesion failure in the mortar (B). **4:** 65% cohesion failure in the concrete substrate (A), 35% cohesion failure in the mortar (B). **5:** 80% cohesion failure in the concrete substrate (A), 20% cohesion failure in the mortar (B).

Attachment 5: Picture documentation and description of failure pattern from bond strength tests on hand applied repair of FWT concrete

GBS-S	Picture documentation of bond strength test	Failure pattern
Side A		**1:** 85% cohesion failure in the concrete substrate (A), 15% cohesion failure in the mortar (B).
		2: 85% cohesion failure in the concrete substrate (A), 15% cohesion failure in the mortar (B).
		3: 50% adhesion failure between the substrate and the mortar (A/B), 50% cohesion failure in the mortar (B).
		4: 40% cohesion failure in the concrete substrate (A), 60% cohesion failure in the mortar (B).
		5: 40% cohesion failure in the concrete substrate (A), 60% cohesion failure in the mortar (B).
Side B	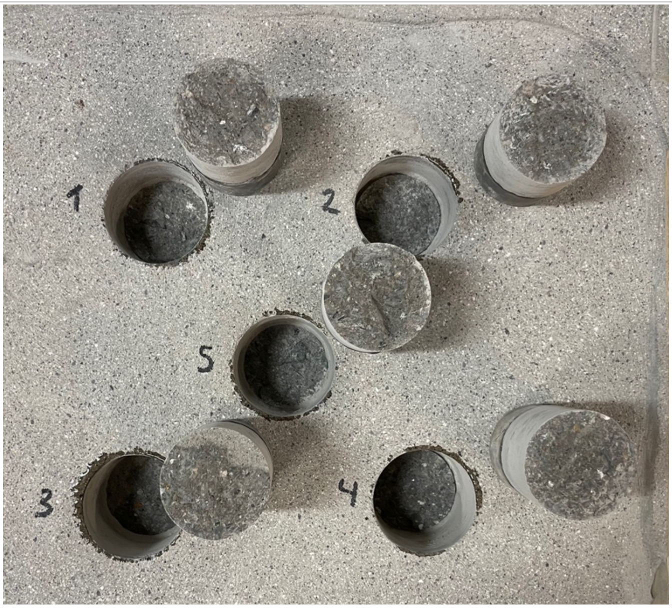	**1:** 100% cohesion failure in the concrete substrate (A).
		2: 100% cohesion failure in the concrete substrate (A).
		3: 80% cohesion failure in the concrete substrate (A), 20% cohesion failure in the mortar (B).
		4: 100% cohesion failure in the concrete substrate (A).
		5: 70% cohesion failure in the concrete substrate (A), 30% cohesion failure in the mortar (B).

Side C	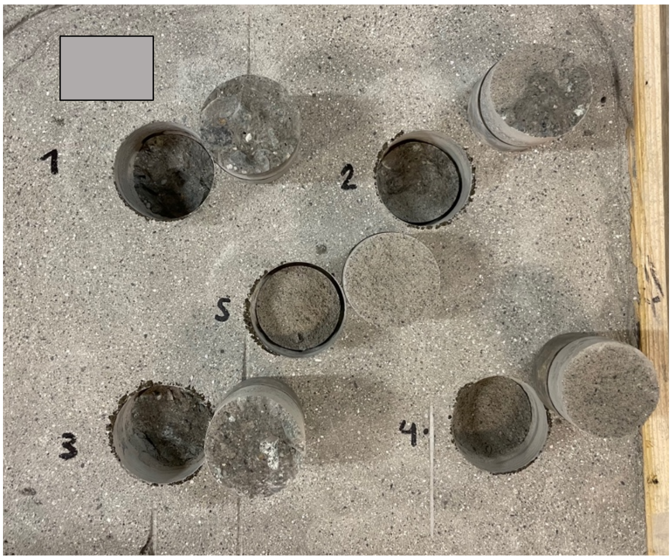	**1:** 100% cohesion failure in the concrete substrate (A). **2:** 50% cohesion failure in the concrete substrate (A), 50% cohesion failure in the mortar (B). **3:** 100% cohesion failure in the concrete substrate (A). **4:** 100% cohesion failure in the mortar (B). Possible dust layer. **5:** 100% cohesion failure in the mortar (B). Possible dust layer.
Side D	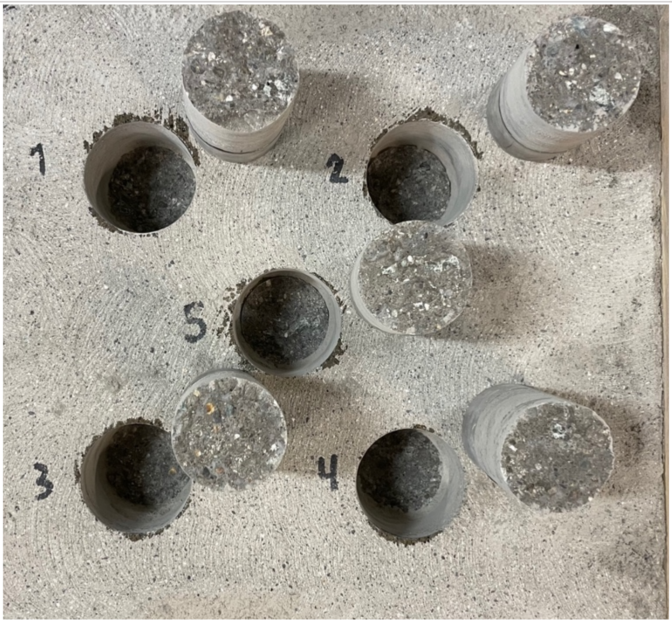	**1:** 95% cohesion failure in the concrete substrate (A), 5% cohesion failure in the mortar (B). **2:** 100% cohesion failure in the concrete substrate (A). **3:** 100% cohesion failure in the concrete substrate (A). **4:** 95% cohesion failure in the concrete substrate (A), 5% cohesion failure in the mortar (B). **5:** 80% cohesion failure in the concrete substrate (A), 20% cohesion failure in the mortar (B).

Extra E	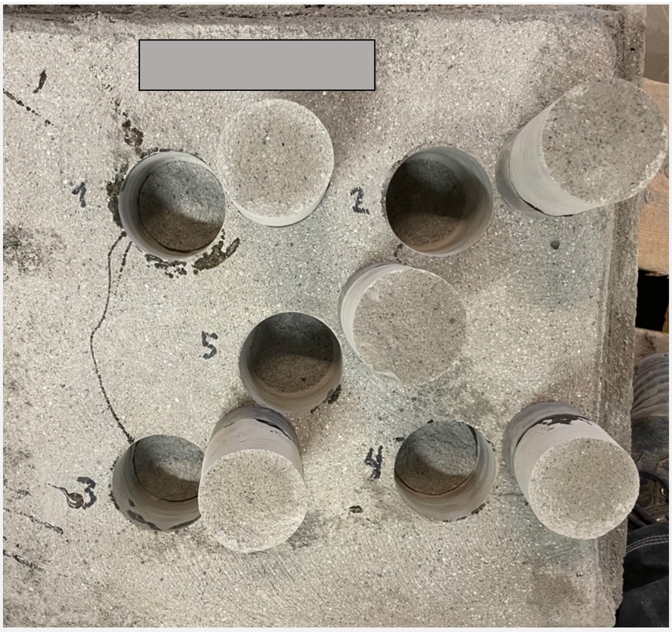	**1:** 35% cohesion failure in the concrete substrate (A), 65% cohesion failure in the mortar (B). **2:** Incomplete gluing of dolly, ca. 70%, 100% cohesion failure in the mortar (B). **3:** 100% Cohesion failure in the mortar (B). **4:** 97% adhesion failure between the substrate and the mortar (A/B), 3% cohesion failure in the mortar (B). **5:** 97% adhesion failure between the substrate and the mortar (A/B), 3% cohesion failure in the mortar (B).
Extra F		**1:** 75% adhesion failure between the substrate and the mortar (A/B), 25% cohesion failure in the mortar (B). **2:** 60% adhesion failure between the substrate and the mortar (A/B), 40% cohesion failure in the mortar (B). **3:** 85% adhesion failure between the substrate and the mortar (A/B), 15% cohesion failure in the mortar (B). **4:** 85% adhesion failure between the substrate and the mortar (A/B), 15% cohesion failure in the mortar (B). **5:** 100% adhesion failure between the substrate and the mortar (A/B)

Extra G	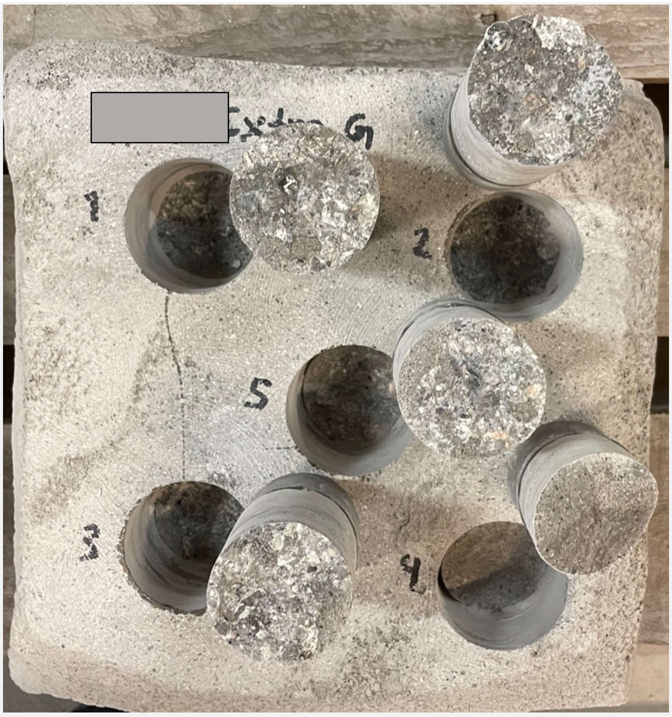	**1:** 95% adhesion failure between the substrate and the mortar (A/B), 5% cohesion failure in the mortar (B). **2:** 50% adhesion failure between the substrate and the mortar (A/B), 50% cohesion failure in the mortar (B). **3:** 100% cohesion failure in the concrete substrate (A). Air pocket, insufficient casting. **4:** 95% adhesion failure between the substrate and the mortar (A/B), 5% cohesion failure in the mortar (B). **5:** 60% adhesion failure between the substrate and the mortar (A/B), 40% cohesion failure in the mortar (B). Dust issue.
Extra orig. A		**1:** 65% cohesion failure in the concrete substrate (A), 5% adhesion failure between the substrate and the mortar (A/B), 30% cohesion failure in the mortar (B).

Extra orig. B		**1:** 100% cohesion failure in the concrete substrate (A).
		**2:** 10% cohesion failure in the concrete substrate (A), 90% cohesion failure in the mortar (B).

Attachment 6: Picture documentation and description of failure pattern from bond strength tests on dry shotcrete repair of GBS concrete

FWT-S	Picture documentation of bond strength test	Failure pattern
Side A	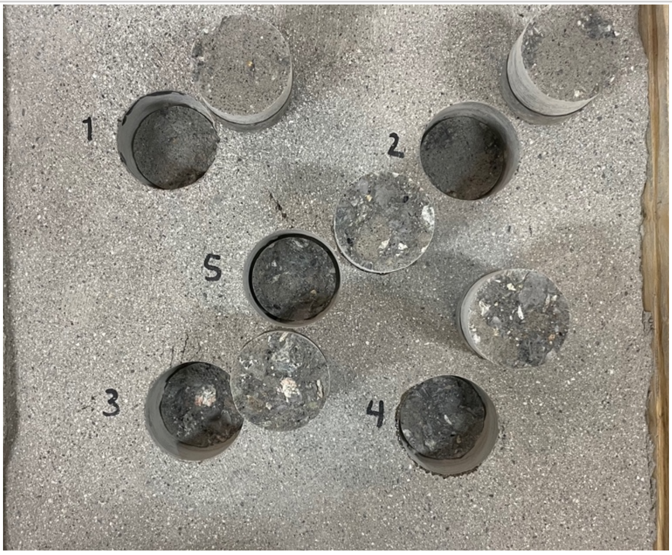	**1:** 5% cohesion failure in the concrete substrate (A), 95% cohesion failure in the mortar (B).
		2: 10% cohesion failure in the concrete substrate (A), 90% cohesion failure in the mortar (B).
		3: 70% cohesion failure in the concrete substrate (A), 20% cohesion failure in the mortar (B).
		4: 75% cohesion failure in the concrete substrate (A), 25% cohesion failure in the mortar (B).
		5: 60% cohesion failure in the concrete substrate (A), 40% cohesion failure in the mortar (B).
Side B	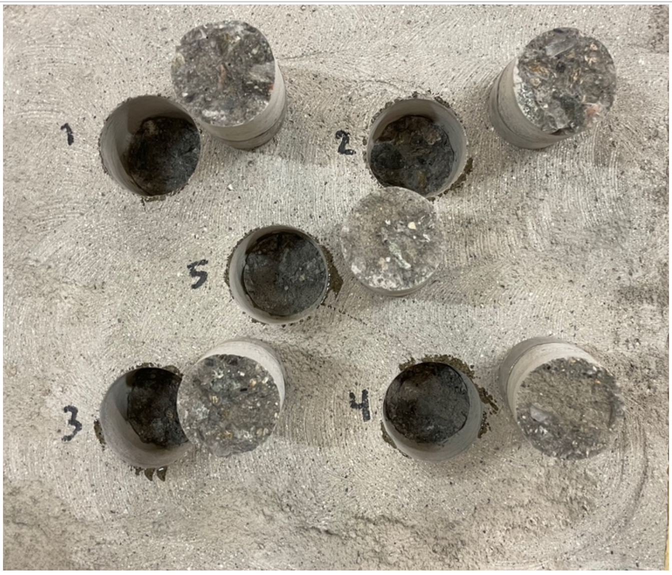	**1:** 100% cohesion failure in the concrete substrate (A).
		2: 100% cohesion failure in the concrete substrate (A).
		3: 90% cohesion failure in the concrete substrate (A), 10% cohesion failure in the mortar (B).
		4: 50% cohesion failure in the concrete substrate (A), 50% cohesion failure in the mortar (B).
		5: 50% cohesion failure in the concrete substrate (A), 50% cohesion failure in the mortar (B).

Side C	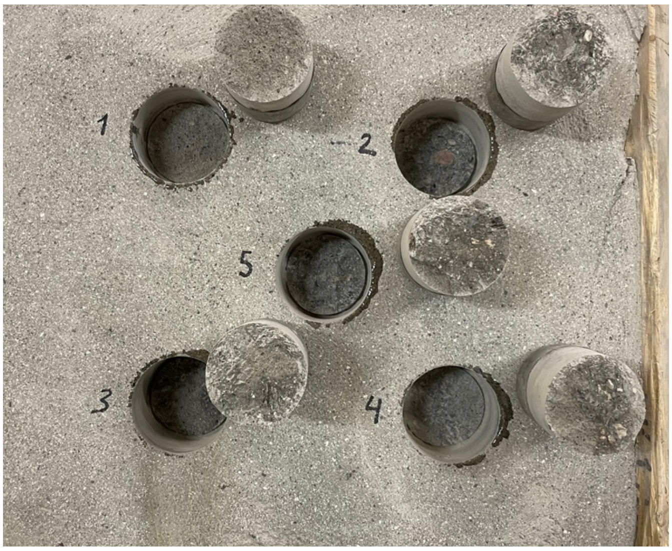	**1:** 100% Cohesion failure in the mortar (B). **2:** 100% cohesion failure in the concrete substrate (A). **3:** 65% cohesion failure in the concrete substrate (A), 35% cohesion failure in the mortar (B). **4:** 35% cohesion failure in the concrete substrate (A), 65% cohesion failure in the mortar (B). **5:** 85% cohesion failure in the concrete substrate (A), 15% cohesion failure in the mortar (B).
Side D	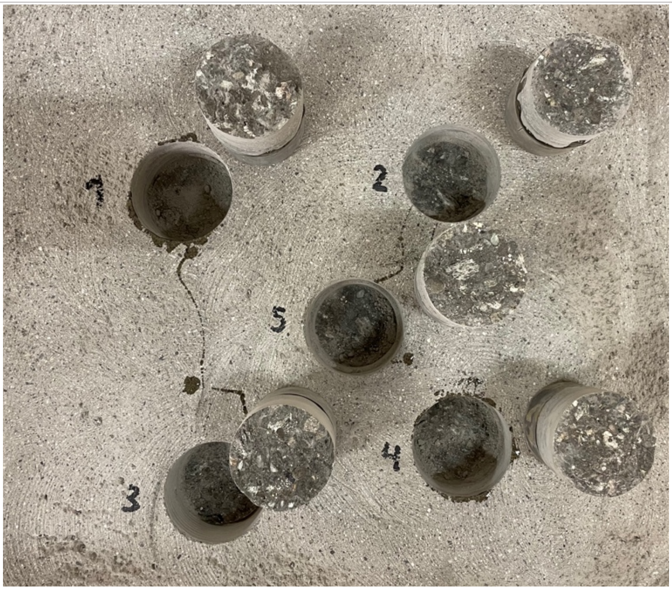	**1:** 85% cohesion failure in the concrete substrate (A), 15% cohesion failure in the mortar (B). **2:** 90% cohesion failure in the concrete substrate (A), 10% cohesion failure in the mortar (B). **3:** 100% cohesion failure in the concrete substrate (A). Possible crushing of aggregate during chiseling. **4:** 100% cohesion failure in the concrete substrate (A). **5:** 100% cohesion failure in the concrete substrate (A).

Extra E	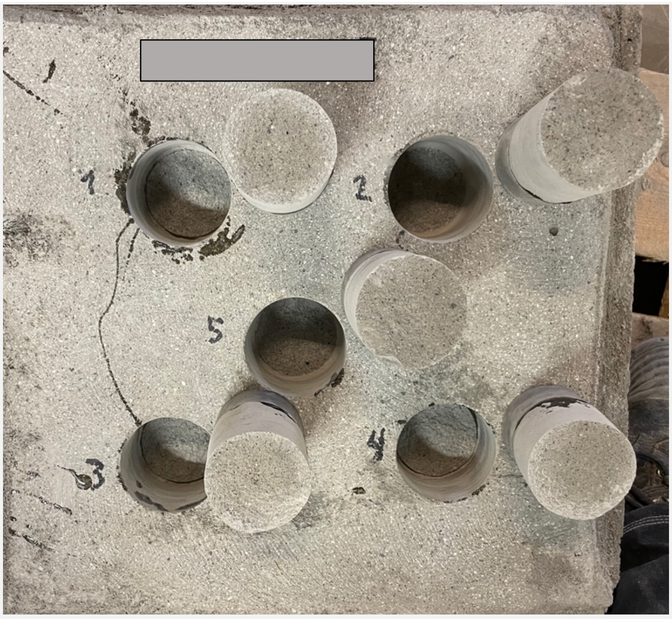	**1:** 100% cohesion failure in the mortar (B). Possible issue with depth of core drilling due to thick mortar layer.
		2: 100% cohesion failure in the mortar (B). Possible issue with depth of core drilling due to thick mortar layer.
		3: 100% cohesion failure in the mortar (B). Possible issue with depth of core drilling due to thick mortar layer.
		4: 100% cohesion failure in the mortar (B). Possible issue with depth of core drilling due to thick mortar layer.
		5: 100% cohesion failure in the mortar (B). Possible issue with depth of core drilling due to thick mortar layer.
Extra F		**1:** 70% cohesion failure in the concrete substrate (A), 30% cohesion failure in the mortar (B).
		2: 100% Cohesion failure in the mortar (B).
		3: 95% cohesion failure in the mortar (B), 5% adhesion failure between the adhesive layer and the dolly (Y/Z).
		4: 80% cohesion failure in the concrete substrate (A), 20% cohesion failure in the mortar (B).
		5: 95% cohesion failure in the concrete substrate (A), 5% cohesion failure in the mortar (B).

Extra G	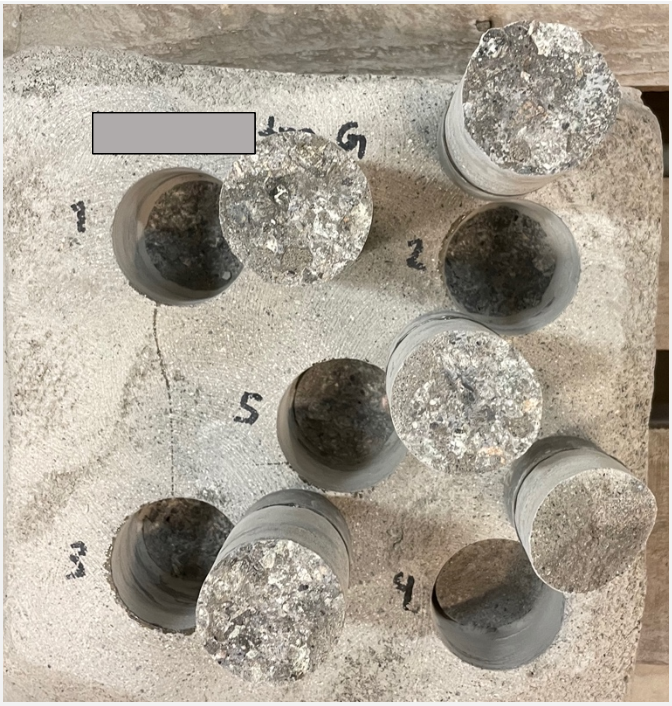	**1:** 90% cohesion failure in the concrete substrate (A), 10% cohesion failure in the mortar (B). **2:** 97% cohesion failure in the concrete substrate (A), 3% cohesion failure in the mortar (B). **3:** 93% cohesion failure in the concrete substrate (A), 7% cohesion failure in the mortar (B). **4:** 100% Cohesion failure in the mortar (B). Dust issue. **3:** 85% cohesion failure in the concrete substrate (A), 15% cohesion failure in the mortar (B).
Extra orig. A		**1:** 90% cohesion failure in the concrete substrate (A), 10% adhesion failure between the substrate and the mortar (A/B).
Extra orig. B		**1:** 100% adhesion failure between the substrate and the mortar (A/B). Dust issue.

Attachment 7: Picture documentation and description of failure pattern from bond strength tests on dry shotcrete repair of FWT concrete

Capillary absorption tests

GBS concrete																	
Date	Time	Weight (g) after	Minutes	Square sec sqrt(t)	Test specimen weight (g)				Total water absorbed (g)				Absorption value, Q (kg/m2)				Middle value GBS
					A	B	C	D	A	B	C	D	Disc A	Disc B	Disc C	Disc D	
22.05.2023	13:30	Drying (g_1)	0	0,00	326,8	338,7	346,8	326,6	0	0	0	0	0	0	0	0	0
22.05.2023	13:40	10 min suction	10	24,49	328,1	340,3	348,5	328,7	1,3	1,6	1,7	2,1	0,181	0,224	0,237	0,292	0,233
22.05.2023	14:00	30 min suction	30	42,43	328,8	341,1	349,3	329,8	2	2,4	2,5	3,2	0,278	0,336	0,348	0,445	0,352
22.05.2023	14:30	1 hour suction	60	60,00	329,5	341,9	350,0	330,8	2,7	3,2	3,2	4,2	0,376	0,447	0,445	0,584	0,463
22.05.2023	15:30	2 hours suction	120	84,85	330,4	343,1	351,1	332,3	3,6	4,4	4,3	5,7	0,501	0,615	0,598	0,793	0,627
22.05.2023	16:30	3 hours suction	180	103,92	331,1	344,0	352,0	333,4	4,3	5,3	5,2	6,8	0,599	0,741	0,724	0,946	0,752
22.05.2023	17:30	4 hours suction	240	120,00	331,8	344,7	352,8	334,2	5	6	6,0	7,6	0,696	0,839	0,835	1,058	0,857
22.05.2023	19:30	6 hours suction	360	146,97	332,8	345,9	353,9	335,6	6	7,2	7,1	9	0,835	1,007	0,988	1,252	1,021
23.05.2023	13:30	1 day suction	1440	293,94	337,0	349,6	356,6	339,1	10,2	10,9	9,8	12,5	1,420	1,524	1,364	1,739	1,512
24.05.2023	13:30	2 days suction	2880	415,69	337,9	349,9	356,9	339,4	11,1	11,2	10,1	12,8	1,546	1,566	1,405	1,781	1,575
25.05.2023	13:30	3 days suction	4320	509,12	337,9	349,9	356,9	339,5	11,1	11,2	10,1	12,9	1,546	1,566	1,405	1,795	1,578
26.05.2023	13:30	4 days suction	5760	587,88	337,9	349,9	357,0	339,6	11,1	11,2	10,2	13	1,546	1,566	1,419	1,809	1,585
	Measurement	Diameter (mm)			95,65	95,45	95,68	95,68									
		Height (mm)			20,52	20,82	20,53	19,96									
		Surface area (mm2)			7181,90	7151,90	7186,41	7186,41									

Attachment 8: Capillary absorption values – GBS concrete specimens

FWT concrete																	
Date	**Time**	**Weight (g) after**	**min**	**Square sec sqrt(t)**	**Test specimen weight (g)**				**Total water absorbed (g)**				**Absorption value (kg/m2)**				**Middle value FWT**
					A	**B**	**C**	**D**	**A**	**B**	**C**	**D**	**Disc A**	**Disc B**	**Disc C**	**Disc D**	
22.05.2023	13:31	Drying (g_1)	0	0,00	318,5	312,2	316,1	314,5	0	0	0	0	0	0	0	0	0
22.05.2023	13:41	10 min suction	10	24,49	321,2	314,7	318,4	317,0	2,7	2,5	2,3	2,5	0,376	0,348	0,320	0,348	0,348
22.05.2023	14:01	30 min suction	30	42,43	322,9	316,3	319,9	318,5	4,4	4,1	3,8	4	0,613	0,571	0,529	0,557	0,567
22.05.2023	14:31	1 hour suction	60	60,00	324,6	317,8	321,5	320,1	6,1	5,6	5,4	5,6	0,850	0,780	0,752	0,780	0,790
22.05.2023	15:31	2 hours suction	120	84,85	327,0	320,2	323,8	322,4	8,5	8	7,7	7,9	1,184	1,114	1,072	1,100	1,118
22.05.2023	16:31	3 hours suction	180	103,92	328,8	321,9	325,6	324,2	10,3	9,7	9,5	9,7	1,435	1,351	1,323	1,350	1,365
22.05.2023	17:31	4 hours suction	240	120,00	330,4	323,5	327,1	325,6	11,9	11,3	11,0	11,1	1,658	1,573	1,532	1,545	1,577
22.05.2023	19:31	6 hours suction	360	146,97	332,7	325,7	329,5	327,9	14,2	13,5	13,4	13,4	1,978	1,880	1,866	1,865	1,897
23.05.2023	13:31	1 day suction	1440	293,94	334,5	327,4	331,3	329,4	16	15,2	15,2	14,9	2,229	2,116	2,117	2,074	2,134
24.05.2023	13:31	2 days suction	2880	415,69	334,8	327,7	331,6	329,6	16,3	15,5	15,5	15,1	2,271	2,158	2,159	2,102	2,172
25.05.2023	13:31	3 days suction	4320	509,12	334,9	327,8	331,7	329,7	16,4	15,6	15,6	15,2	2,284	2,172	2,173	2,116	2,186
26.05.2023	13:31	4 days suction	5760	587,88	334,9	327,8	331,8	329,8	16,4	15,6	15,7	15,3	2,284	2,172	2,187	2,130	2,193
	Measurement	Diameter (mm)			95,63	95,65	95,64	95,66									
		Height (mm)			19,82	19,6	20,03	19,76									
		Surface area (mm2)			7178,90	7181,90	7180,40	7183,41									

Attachment 9: Capillary absorption values – FWT concrete specimens

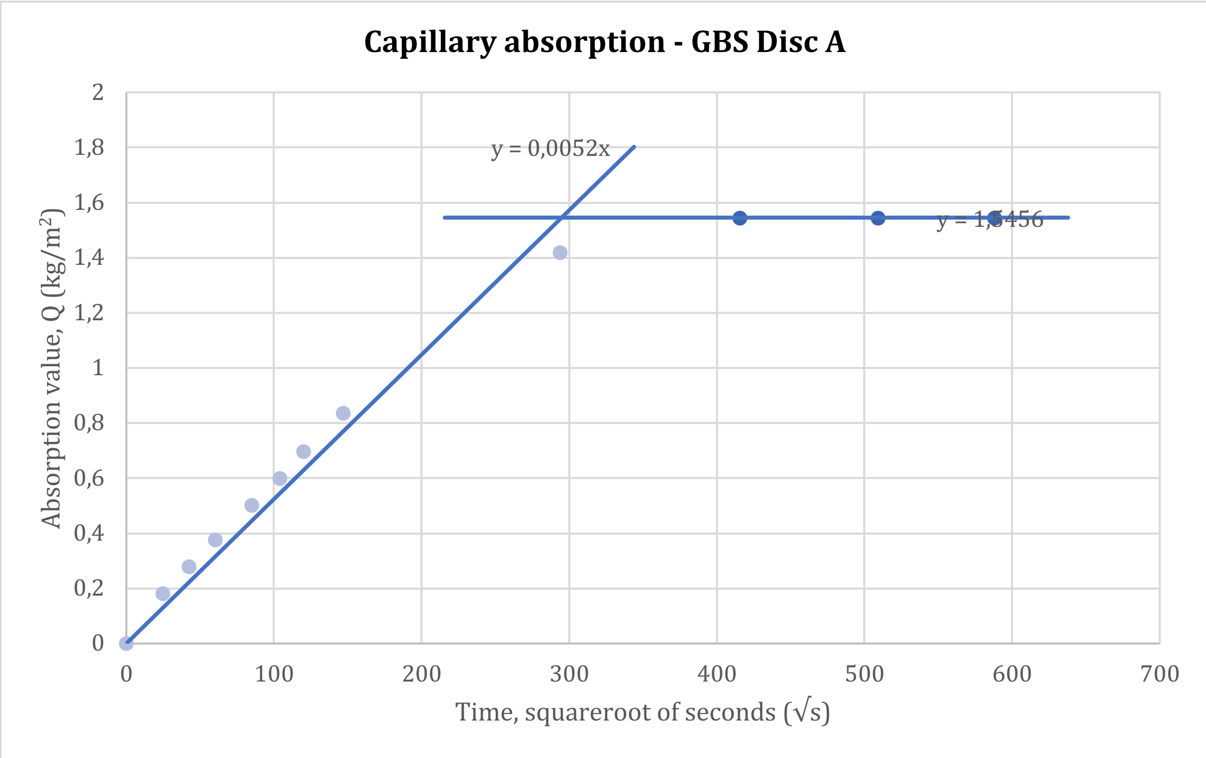

Attachment 10: Capillary absorption trend lines for GBS Disc A

Regression output Phase 1	
Multiple R	0,9942122
R-squared	0,9884579
Adjusted R-squared	0,986809
Standard Err.	0,0481685
Observations	9

Regression output Phase 2	
Multiple R	1
R-squared	1
Adjusted R-squared	1
Standard Err.	0
Observations	3

Calculations		
	h	0,02
x	√t	297,23
y	Q_cap	1.55
	k	0,0052
	m	220865325

Attachment 11: Regression analysis GBS Disc A

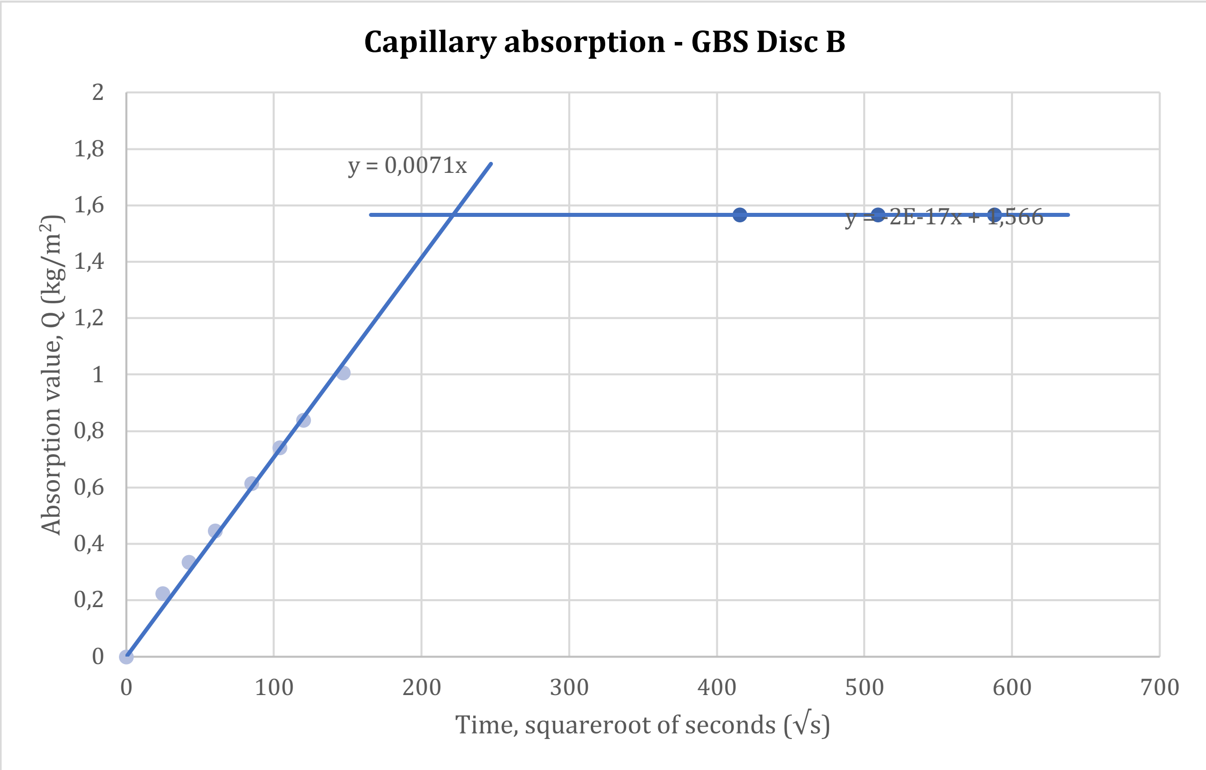

Attachment 12: Capillary absorption trend lines for GBS Disc B

Regression output Phase 1	
Multiple R	0,998407
R-squared	0,9968165
Adjusted R-squared	0,996286
Standard Err.	0,0205215
Observations	8

Regression output Phase 2	
Multiple R	1
R-squared	1
Adjusted R-squared	1
Standard Err.	0
Observations	3

Calculations		
	h	0,02
x	√t	220,56
y	Q_cap	1.57
	k	0,0071
	m	1.22E+08

Attachment 13: Regression analysis GBS Disc B

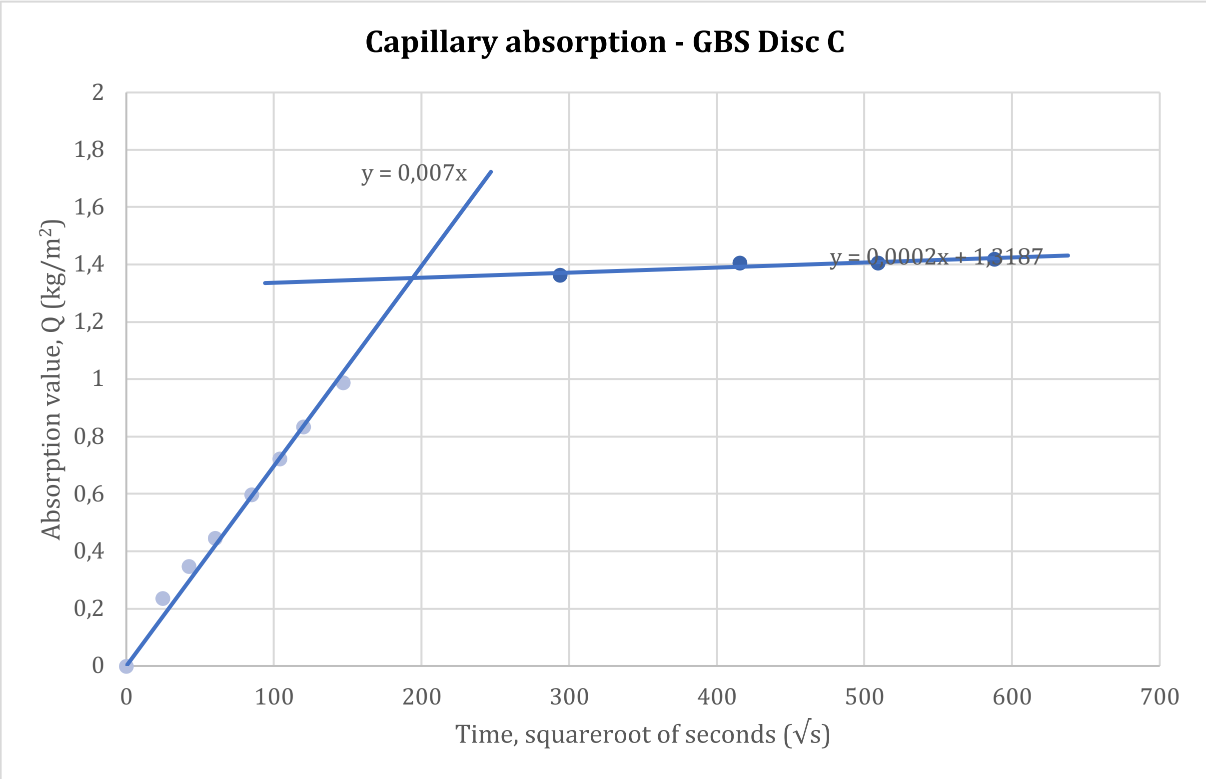

Attachment 14: Capillary absorption trend lines for GBS Disc C

Regression output Phase 1	
Multiple R	0,9972882
R-squared	0,9945837
Adjusted R-squared	0,9936809
Standard Err.	3,9817153
Observations	8

Regression output Phase 2	
Multiple R	0,9268802
R-squared	0,8591068
Adjusted R-squared	0,7886602
Standard Err.	0,01108
Observations	4

Calculations		
	h	0,02
x	√t	192,75
y	Q_cap	1.35
	k	0,007
	m	92881406

Attachment 15: Regression analysis GBS Disc C

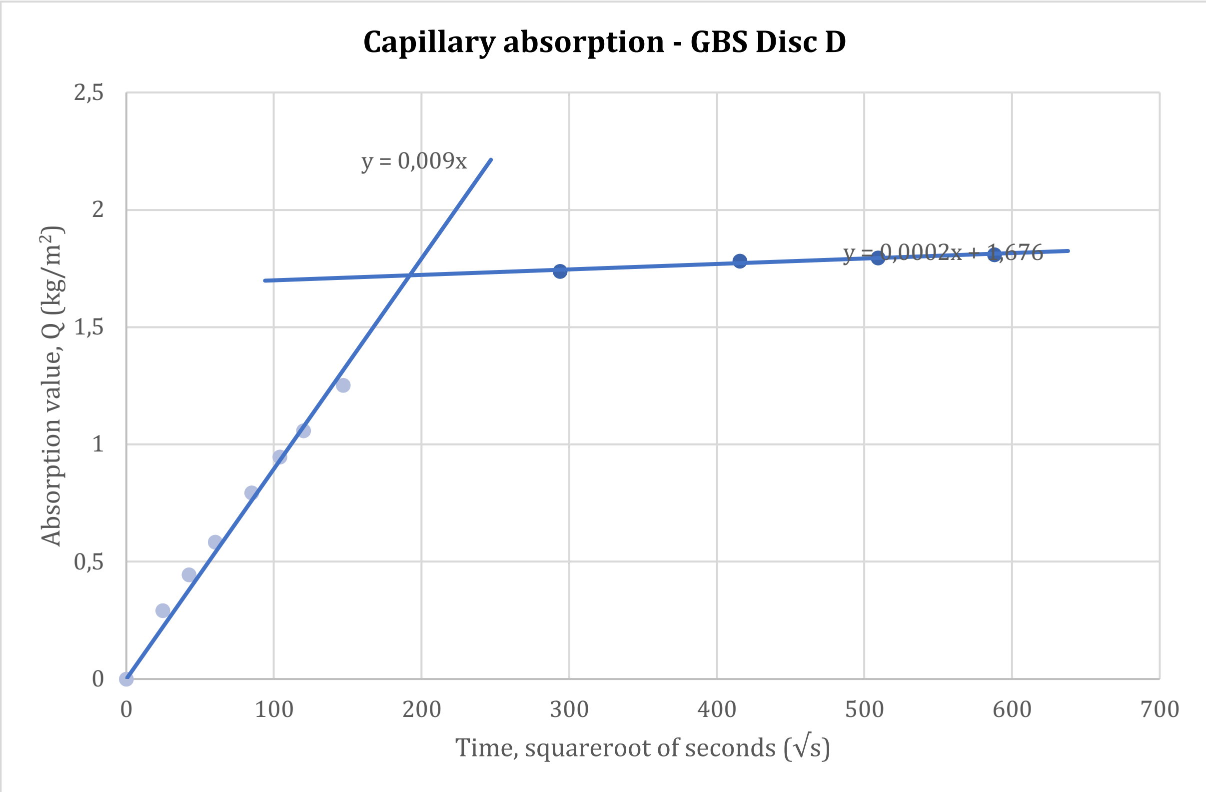

Attachment 16: Capillary absorption trend lines for GBS Disc D

Regression output Phase 1	
Multiple R	0,9967538
R-squared	0,993518
Adjusted R-squared	0,9924377
Standard Err.	4,3558209
Observations	8

Regression output Phase 2	
Multiple R	0,9793605
R-squared	0,9591471
Adjusted R-squared	0,9387206
Standard Err.	31.321006
Observations	4

Calculations		
	h	0,02
x	√t	190,45
y	Q_cap	1.71
	k	0,009
	m	90682335

Attachment 17: Regression analysis GBS Disc D

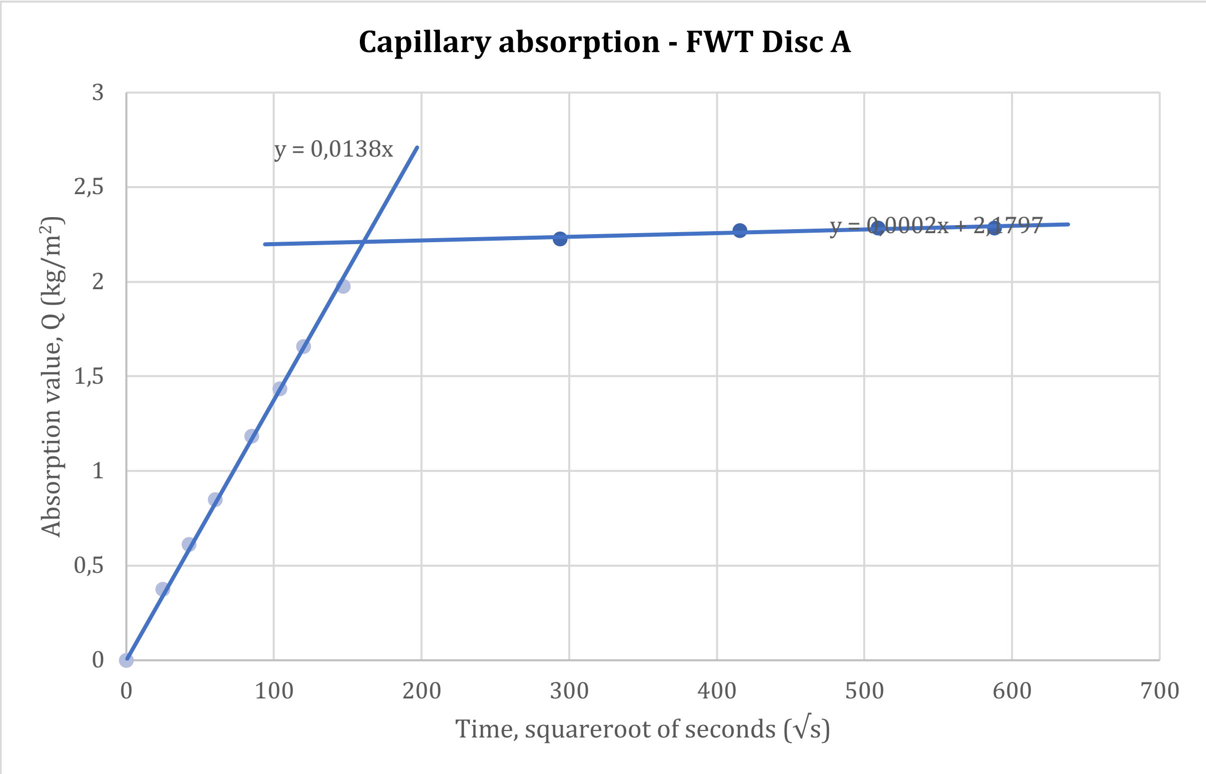

Attachment 18: Capillary absorption trend lines for FWT Disc A

Regression output Phase 1	
Multiple R	0,999578
R-squared	0,999157
Adjusted R-squared	0,999017
Standard Err.	0,021112
Observations	8

Regression output Phase 2	
Multiple R	0,928057
R-squared	0,86129
Adjusted R-squared	0,791935
Standard Err.	0,012028
Observations	4

Calculations		
	h	0,02
x	√t	160,27
y	Q_cap	2,21
	k	0,0138
	m	64217832,1

Attachment 19: Regression analysis FWT Disc A

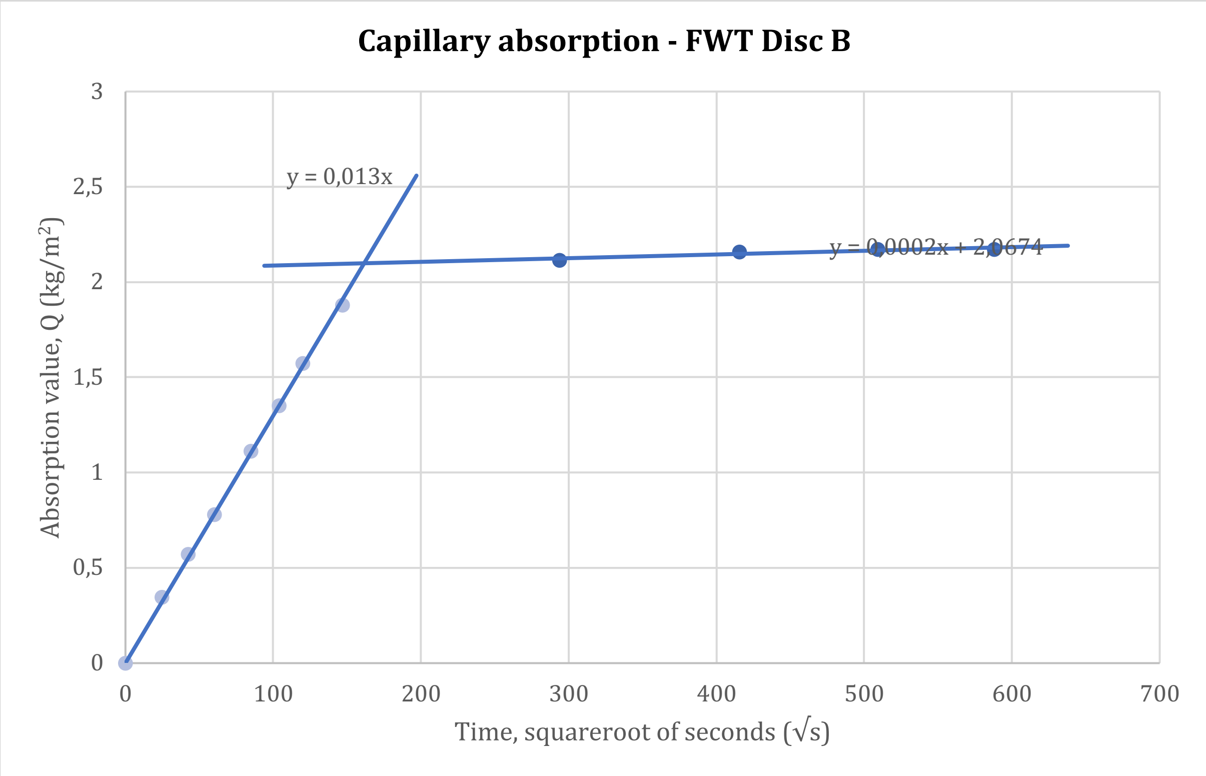

Attachment 20: Capillary absorption trend lines for FWT Disc B

Regression output Phase 1	
Multiple R	0,999728
R-squared	0,999456
Adjusted R-squared	0,999365
Standard Err.	0,016156
Observations	8

Regression output Phase 2	
Multiple R	0,928057
R-squared	0,86129
Adjusted R-squared	0,791935
Standard Err.	0,012023
Observations	4

Calculations		
	h	0,02
x	√t	161.52
y	Q_cap	2,10
	k	0,013
	m	65218242,8

Attachment 21: Regression analysis FWT Disc B

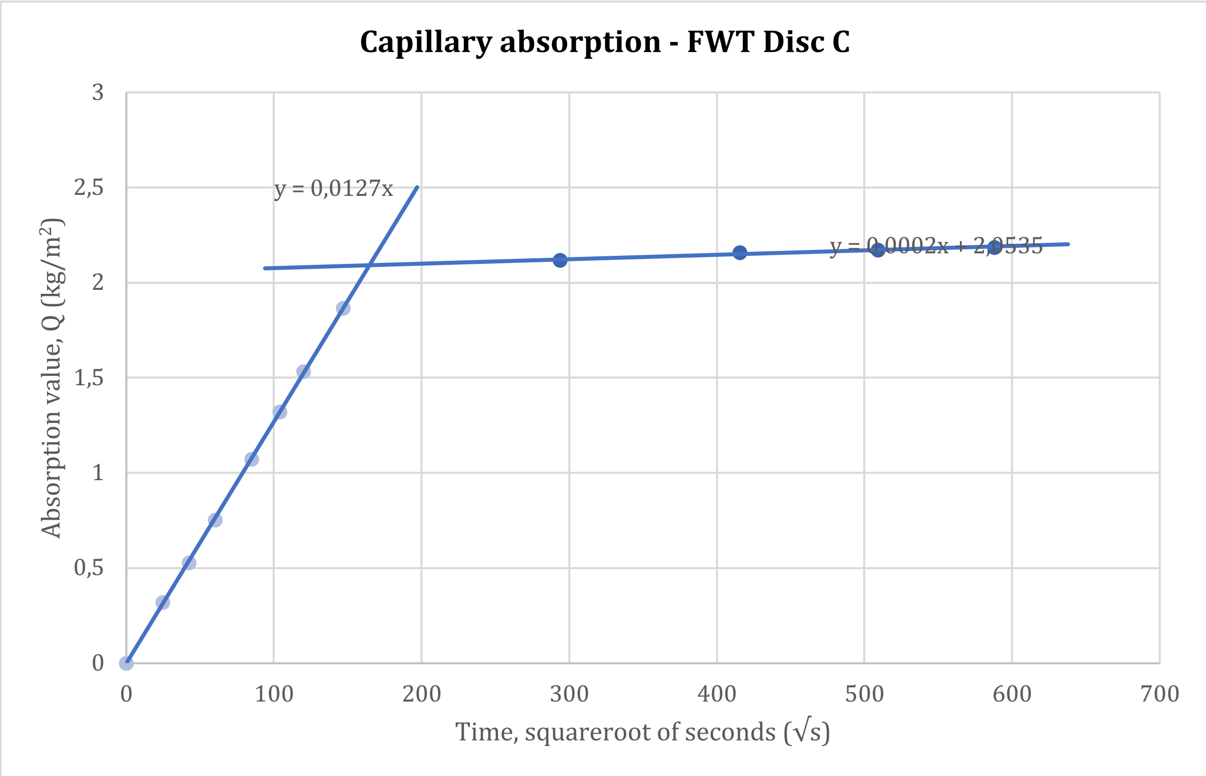

Attachment 22: Capillary absorption trend lines for FWT Disc C

Regression output Phase 1	
Multiple R	0,999935
R-squared	0,999871
Adjusted R-squared	0,999849
Standard Err.	0,007827
Observations	8

Regression output Phase 2	
Multiple R	0,979361
R-squared	0,959147
Adjusted R-squared	0,938721
Standard Err.	0,007448
Observations	4

Calculations		
	h	0,02
x	√t	164,28
y	Q_cap	2,09
	k	0,0127
	m	67469796

Attachment 23: Regression analysis FWT Disc C

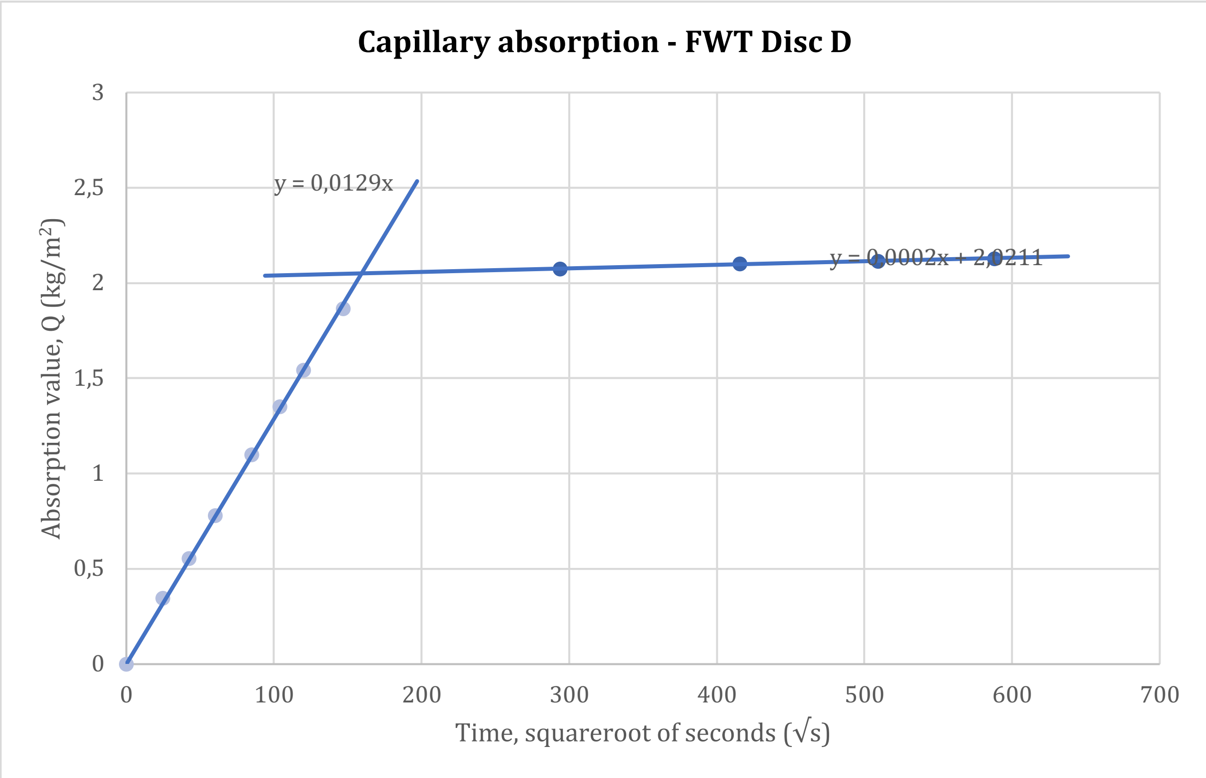

Attachment 24: Capillary absorption trend lines for FWT Disc D

Regression output Phase 1	
Multiple R	0,999784
R-squared	0,999567
Adjusted R-squared	0,999495
Standard Err.	0,014267
Observations	8

Regression output Phase 2	
Multiple R	0,995507
R-squared	0,991034
Adjusted R-squared	0,986551
Standard Err.	0,002757
Observations	4

Calculations		
	h	0,02
x	√t	159,14
y	Q_cap	2,05
	k	0,0129
	m	63315227,4

Attachment 25: Regression analysis FWT Disc D

NTNU
Norwegian University of
Science and Technology